

AD A051067

12

ELECTROMAGNETICS LABORATORY
TECHNICAL REPORT NO. 77-24

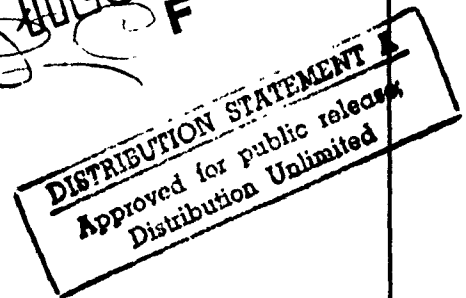
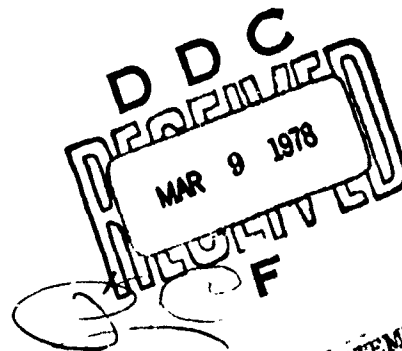
December 1977

AD NO. 100
FILE COPY

MUTUAL ADMITTANCE BETWEEN SLOTS ON A
CYLINDER OR CONE

S. W. Lee

R. Mittra



ELECTROMAGNETICS LABORATORY
DEPARTMENT OF ELECTRICAL ENGINEERING
ENGINEERING EXPERIMENT STATION
UNIVERSITY OF ILLINOIS AT URBANA-CHAMPAIGN
URBANA, ILLINOIS 61801

Supported by
Contract No. N00019-77-C-0127
Department of the Navy
Navy Air Systems Command
Washington, D.C. 20361

unclassified

SECURITY CLASSIFICATION OF THIS PAGE (When Data Entered)

REPORT DOCUMENTATION PAGE		READ INSTRUCTIONS BEFORE COMPLETING FORM
1. REPORT NUMBER	2. GOVT ACCESSION NO.	3. RECIPIENT'S CATALOG NUMBER
4. TITLE (and Subtitle)		5. TYPE OF REPORT & PERIOD COVERED
MUTUAL ADMITTANCE BETWEEN SLOTS ON A CYLINDER OR CONE		Final Report 16 Nov 76 - 15 Nov 77
6. AUTHOR(s)		7. PERFORMING ORG. REPORT NUMBER
S. W./Lee R./Mittra		ITEM-77-24, UILU-ENG-77-2267
8. PERFORMING ORGANIZATION NAME AND ADDRESS		9. CONTRACT OR GRANT NUMBER(s)
Electromagnetics Laboratory Department of Engineering, University of Illinois Urbana, IL 61801		19-77-C-0127
10. CONTROLLING OFFICE NAME AND ADDRESS		11. PROGRAM ELEMENT, PROJECT, TASK AREA & WORK UNIT NUMBERS
Department of the Navy Naval Air Systems Command Washington, D. C. 20361		PR-RJ002
12. MONITORING AGENCY NAME & ADDRESS (if different from Controlling Office)		13. REPORT DATE
		December 1977
		14. NUMBER OF PAGES
		192
		15. SECURITY CLASS. (of this report)
		unclassified
		16. DECLASSIFICATION/DOWNGRADING SCHEDULE
17. DISTRIBUTION STATEMENT (of this Report)		
Distribution unlimited. (Reduction in whole or in part is permitted for any purpose of the United States Government.)		
18. DISTRIBUTION STATEMENT (of the abstract entered in Block 20, if different from Report)		
19. SUPPLEMENTARY NOTES		
20. KEY WORDS (Continue on reverse side if necessary and identify by block number)		
GTD slot ray techniques high-frequency diffraction conformal array mutual coupling		
21. ABSTRACT (Continue on reverse side if necessary and identify by block number)		
In the present contract, we studied the mutual admittance between two thin slots on a conducting cylinder or a cone by ray techniques. Our main contribution in the development of an approximate asymptotic Green's function for the surface function, expressed in terms of Fock functions, is simple to evaluate, and gives excellent numerical results when compared with known exact solutions and/or experimental data. This report contains a brief administrative summary plus three attachments which give the technical details.		

DDC
MAR 9 1978
RESISTIVE

DD FORM 1 JAN 73 1473 EDITION OF 1 NOV 68 IS OBSOLETE

unclassified

SECURITY CLASSIFICATION OF THIS PAGE (When Data Entered)

108 102

✓

Electromagnetics Laboratory Report No. 77-24

MUTUAL ADMITTANCE BETWEEN SLOTS ON A
CYLINDER OR CONE

by

S. W. Lee
R. Mittra

Technical Report

December 1977

Supported by
Contract No. N00019-77-C-0127
Department of the Navy
Naval Air Systems Command
Washington, D.C. 20361
Mr. James Willis, AIR-310B
Contract Manager

ACCESSION for	
NTIS	Write Section <input checked="" type="checkbox"/>
DDC	Brief Section <input type="checkbox"/>
UNANNOUNCED	<input type="checkbox"/>
JUSTIFICATION	
BY	
DISTRIBUTION/AVAILABILITY CODES	
Dist	SPECIAL
A	

Electromagnetics Laboratory
Department of Electrical Engineering
Engineering Experiment Station
University of Illinois at Urbana-Champaign
Urbana, Illinois 61801

Distribution is unlimited. (Reproduction in whole or in part is permitted for any purpose of the United States Government.)

ACKNOWLEDGEMENT

We appreciate the many valuable discussions with R. C. Hansen,
W. H. Kummer, and J. Willis.

TABLE OF CONTENTS

	Page
I. INTRODUCTION.	1
II. PERSONNEL	2
III. TECHNICAL RESULTS	3
IV. PUBLICATIONS AND PRESENTATIONS.	4
ATTACHMENT A: MUTUAL ADMITTANCE BETWEEN SLOTS ON A CYLINDER	5
ATTACHMENT B: SIMPLE APPROXIMATE FORMULA FOR MUTUAL ADMITTANCE BETWEEN SLOTS ON A CYLINDER	107
ATTACHMENT C: MUTUAL ADMITTANCE OF SLOTS ON A CONE: SOLUTION BY RAY TECHNIQUE	147

I. INTRODUCTION

The contract N00019-77-C-0127 was awarded to the University of Illinois by the Naval Air Systems Command for "Mutual Admittance Between Slots on a Cylinder or Cone" for a one-year period, 16 November 1976 to 15 November 1977. Mr. J. Willis of AIR-310B is the contract monitor.

This is the final report for the contract, covering personnel (section II), technical results (section III and attachments), publications and presentations (section IV).

The attachments have their own pagination. The report is page numbered in lower left-hand and right-hand corners.

II. PERSONNEL

S. W. Lee, Professor of Electrical Engineering, University of Illinois,
principal investigator

R. Mittra, Professor of Electrical Engineering, University of Illinois,
principal investigator

J. Boersma, Professor of Mathematics, Technological University of Eindhoven,
The Netherlands, and visiting professor, University of Illinois

V. Krichevsky, Associate Professor of Electrical Engineering, University of
Illinois

S. Safavi-Naini, Research Assistant, University of Illinois

L. Grun, Research Assistant, University of Illinois

P. Chang, Computer Programmer, University of Illinois

C. L. Law, Computer Programmer, University of Illinois

III. TECHNICAL RESULTS

In the design of a slot array on a conformed surface, a most important parameter is the mutual admittance Y_{12} between two slots. In the present contract, we have studied the following problems about Y_{12} :

(a) When the conformal surface is a conducting cylinder, a GTD solution of Y_{12} has been successfully developed. It applies to cylinders with radius greater than one wavelength, and gives excellent numerical results (error is within 0.25 dB in magnitude and several degrees in phase). Details are given in Attachment A.

(b) For the slot array on a cylinder, a simple approximate solution of Y_{12} is derived. It is generally valid when the separation between the slots is greater than two wavelengths (Attachment B).

(c) The GTD solution described in (a) has been generalized, so that it now can be used to calculate Y_{12} between slots on a general convex conducting surface. In particular, it was applied to slots on a cone, and the numerical results of Y_{12} are in good agreement with the experimental results (Attachment C).

IV. PUBLICATIONS AND PRESENTATIONS

- (1) S. W. Lee, S. Safavi-Naini, and R. Mittra, "Mutual Admittance Between Slots on a Cylinder," University of Illinois, Electromagnetics Lab. Tech. Rept. 77-8, Urbana, Illinois, March 1977.
- (2) S. W. Lee and S. Safavi-Naini, "Simple Approximate Formula for Mutual Admittance Between Slots on a Cylinder," University of Illinois, Electromagnetics Lab. Tech. Rept. 77-13, Urbana, Illinois, July 1977.
- (3) S. W. Lee and R. Mittra, "Mutual Admittance Between Slots on a Cylinder or a Cone," Final Report, Contract N00019-77-C-0127 (including the above two reports as attachments), December 1977.
- (4) S. W. Lee and S. Safavi-Naini, "Approximate Asymptotic Solution of Surface Field Due to a Magnetic Dipole on a Cylinder," to appear in IEEE Trans. Antenna Propagat., 1978.
- (5) S. W. Lee and S. Safavi-Naini, "An Unexpected Result About Surface Rays," Digest of International Symposium on Antennas and Propagat., pp. 52-55, Stanford, CA, 20-22 June 1977.
- (6) S. W. Lee, S. Safavi-Naini, and R. Mittra, "Mutual Admittance Between Slots on a Cylinder," paper presented at Program Review of Naval Air Systems Command, Hughes Aircraft Company, Culver City, CA, 29 March 1977.

ATTACHMENT A

Report 77-8

MUTUAL ADMITTANCE BETWEEN SLOTS ON A CYLINDER

ELECTROMAGNETICS LABORATORY
TECHNICAL REPORT NO. 77-8

March 1977

MUTUAL ADMITTANCE BETWEEN SLOTS ON A CYLINDER

S. W. Lee
S. Safavi-Naini
R. Mittra



ELECTROMAGNETICS LABORATORY
DEPARTMENT OF ELECTRICAL ENGINEERING
ENGINEERING EXPERIMENT STATION
UNIVERSITY OF ILLINOIS AT URBANA-CHAMPAIGN
URBANA, ILLINOIS 61801

Supported by
Contract No. N00019-77-C-0127
Department of the Navy
Naval Air Systems Command
Washington, D.C. 20361

SECURITY CLASSIFICATION OF THIS PAGE (When Data Entered)

REPORT DOCUMENTATION PAGE		READ INSTRUCTIONS BEFORE COMPLETING FORM
1. REPORT NUMBER	2. GOVT ACCESSION NO.	3. RECIPIENT'S CATALOG NUMBER
4. TITLE (and Subtitle) Mutual Admittance Between Slots On a Cylinder		5. TYPE OF REPORT & PERIOD COVERED Technical
7. AUTHOR(s) S. W. Lee, S. Safavi-Naini, R. Mittra		6. PERFORMING ORG. REPORT NUMBER EM 77-8; UILU-Eng-77-2549
9. PERFORMING ORGANIZATION NAME AND ADDRESS Electromagnetics Laboratory Department of Electrical Engineering University of Illinois, Urbana, Illinois 61801		8. CONTRACT OR GRANT NUMBER(s) NC0019-77-C-0127
11. CONTROLLING OFFICE NAME AND ADDRESS Department of the Navy Naval Air Systems Command Washington, D. C. 20361		10. PROGRAM ELEMENT, PROJECT, TASK AREA & WORK UNIT NUMBERS PR - RJ002
14. MONITORING AGENCY NAME & ADDRESS (if different from Controlling Office)		12. REPORT DATE March 1977
		13. NUMBER OF PAGES 93
		15. SECURITY CLASS. (of this report) Unclassified
		15a. DECLASSIFICATION/DOWNGRADING SCHEDULE
16. DISTRIBUTION STATEMENT (of this Report) Distribution Unlimited. (Reproduction in whole or in part is permitted for any purpose of the United States Government.)		
17. DISTRIBUTION STATEMENT (of the abstract entered in Block 20, if different from Report)		
18. SUPPLEMENTARY NOTES		
19. KEY WORDS (Continue on reverse side if necessary and identify by block number) Mutual Admittance Conformal Array GTD Surface Rays		
20. ABSTRACT (Continue on reverse side if necessary and identify by block number) In the design of conformal slot array on the surface of a conducting cylinder, the calculation of the mutual admittance Y_{12} is a crucial step, which has been studied extensively in recent years. In this paper, we summarize, in a handbook format, all of the final formulas of Y_{12} , and present some typical numerical data.		

Electromagnetics Laboratory Report No. 77-8

MUTUAL ADMITTANCE BETWEEN SLOTS ON A CYLINDER

by

S. W. Lee
S. Safavi-Naini
R. Mittra

Technical Report

March 1977

Supported by
Contract No. N00019-77-C-0127
Department of the Navy
Naval Air Systems Command
Washington, D. C. 20361

Electromagnetics Laboratory
Department of Electrical Engineering
Engineering Experiment Station
University of Illinois at Urbana-Champaign
Urbana, Illinois 61801

Distribution is unlimited. (Reproduction in whole or in part is permitted for any purpose of the United States Government.)

TABLE OF CONTENTS

	Page
1. INTRODUCTION	1
2. STATEMENT OF PROBLEM	1
3. EXACT HUGHES (GSP) MODAL SOLUTION.	5
4. EXACT UI MODAL SOLUTION.	6
5. ASYMPTOTIC SOLUTION.	7
6. EXACT PLANAR SOLUTION.	10
7. APPROXIMATE SOLUTION	10
8. CONCLUDING REMARKS	11
REFERENCES	12
APPENDIX A: NUMERICAL RESULTS.	14
DATA SET A OF MUTUAL ADMITTANCE.	15
DATA SET B OF MUTUAL ADMITTANCE.	23
DATA SET C OF MUTUAL ADMITTANCE.	28
DATA SET D OF MUTUAL ADMITTANCE.	33
DATA SET E OF MUTUAL ADMITTANCE.	40
DATA SET F OF MUTUAL ADMITTANCE.	54
APPENDIX B: COMPUTER PROGRAM LISTING	67
ASYMPTOTIC SOLUTIONS OF Y_{12}	68
UI EXACT MODAL SOLUTION OF Y_{12}	74

LIST OF FIGURES

Figure		Page
1	Two identical slots on the surface of a cylinder . .	2
A-1.	Mutual admittance Y_{12} between two circumferential slots as a function of ϕ_0	19
A-2.	Mutual admittance Y_{12} between two circumferential slots as a function of z_0	20
A-3.	$ Y_{12} $ on a cylinder (UI modal solution) and that on a plane as a function of z_0	21
A-4.	Y_{12} on a cylinder as a function of the radius R of the cylinder.	22
C-1.	$ Y_{12} $ on a cylinder (UI modal solution) and that on a plane as a function of z_0	32
E-1.	Mutual admittance Y_{12} between two circumferential slots as a function of ϕ_0	49
E-2.	Mutual admittance Y_{12} between two circumferential slots as a function of ϕ_0	50
E-3.	Mutual admittance Y_{12} between two circumferential slots as a function of ϕ_0	51
E-4.	Mutual admittance Y_{12} between two circumferential slots as a function of z_0	52
E-5.	Mutual admittance Y_{12} between two circumferential slots as a function of z_0	53
F-1.	Mutual admittance Y_{12} between two axial slots as a function of ϕ_0	64
F-2.	Mutual admittance Y_{12} between two axial slots as a function of ϕ_0	65
F-3.	Mutual admittance Y_{12} between two axial slots as a function of z_0	66

LIST OF TABLES

TABLE	Page
A-1 Y_{12} OF SLOT A FOR $\phi_0 = 0$	16
A-2 Y_{12} OF SLOT A FOR $z_0 = 2''$	17
A-3 Y_{12} OF SLOT A FOR $z_0 = 0$	17
A-4 UI SOLUTIONS OF Y_{12} OF SLOT A FOR $\phi_0 = 0$	18
B-1 UI SOLUTIONS OF Y_{12} OF SLOT B FOR $\phi_0 = 0$	24
B-2 UI SOLUTIONS OF Y_{12} OF SLOT B FOR $z_0 = 2''$	25
B-3 UI SOLUTIONS OF Y_{12} OF SLOT B FOR $z_0 = 8''$	26
B-4 COMPARISON OF HUGHES AND UI SOLUTIONS	27
C-1 Y_{12} OF SLOT C FOR $\phi_0 = 0^\circ$	29
C-2 Y_{12} OF SLOT C FOR $z_0 = 1.5''$	30
C-3 Y_{12} OF SLOT C FOR $\phi_0 = 0$ and $z_0 = 8''$	31
D-1 UI SOLUTIONS OF Y_{12} OF SLOT D FOR $\phi_0 = 0$ and $R = 2\lambda$.	34
D-2 UI ASYMPTOTIC SOLUTIONS OF Y_{12} OF SLOT D FOR $\phi_0 = 0$.	35
D-3 UI ASYMPTOTIC SOLUTIONS OF Y_{12} OF SLOT D FOR $\phi_0 = 0$.	36
D-4 UI ASYMPTOTIC SOLUTIONS OF Y_{12} OF SLOT D FOR $z_0 = 0$.	37
D-5 UI ASYMPTOTIC SOLUTIONS OF Y_{12} OF SLOT D FOR $z_0 = 1\lambda$.	38
D-6 UI ASYMPTOTIC SOLUTIONS OF Y_{12} OF SLOT D FOR $z_0 = 5\lambda$.	39
E-1 UI ASYMPTOTIC SOLUTIONS OF Y_{12} OF SLOT E FOR $z_0 = 0$.	41
E-2 UI ASYMPTOTIC SOLUTIONS OF Y_{12} FOR $z_0 = 0.5\lambda$	42
E-3 UI ASYMPTOTIC SOLUTIONS OF Y_{12} FOR $z_0 = 1\lambda$	43
E-4 UI ASYMPTOTIC SOLUTIONS OF Y_{12} FOR $z_0 = 2\lambda$	44
E-5 UI ASYMPTOTIC SOLUTIONS OF Y_{12} FOR $z_0 = 4\lambda$	45
E-6 UI ASYMPTOTIC SOLUTIONS OF Y_{12} FOR $z_0 = 8\lambda$	46
E-7 COMPARISON OF UI ASYMPTOTIC AND UI MODAL SOLUTIONS. .	47
E-8 COMPARISON OF UI ASYMPTOTIC AND UI MODAL SOLUTIONS. .	48

TABLE	Page
F-1 UI ASYMPTOTIC SOLUTIONS OF Y_{12} FOR $z_0 = 0$	55
F-2 UI ASYMPTOTIC SOLUTIONS OF Y_{12} FOR $z_0 = 0.5\lambda$	56
F-3 UI ASYMPTOTIC SOLUTIONS OF Y_{12} FOR $z_0 = 1\lambda$	57
F-4 UI ASYMPTOTIC SOLUTIONS OF Y_{12} FOR $z_0 = 2\lambda$	58
F-5 UI ASYMPTOTIC SOLUTIONS OF Y_{12} FOR $z_0 = 4\lambda$	59
F-6 UI ASYMPTOTIC SOLUTIONS OF Y_{12} FOR $z_0 = 8\lambda$	60
F-7 COMPARISON OF UI ASYMPTOTIC AND UI MODAL SOLUTIONS. .	61
F-8 COMPARISON OF UI ASYMPTOTIC AND UI MODAL SOLUTIONS. .	62
F-9 COMPARISON OF ASYMPTOTIC SOLUTIONS.	63

1. INTRODUCTION

In the design of a conformal slot array on the surface of a conducting cylinder, the calculation of the mutual admittance Y_{12} is a crucial step, which has been studied extensively in recent years. In this paper, we summarize, in a handbook format, all of the final formulas of Y_{12} , and present some typical numerical data.

2. STATEMENT OF PROBLEM

Referring to Figure 1, two identical slots, circumferential or axial, are located on the surface of an infinitely long cylinder. The geometrical parameters are

$$R = \text{radius of the cylinder} \quad (2.1)$$

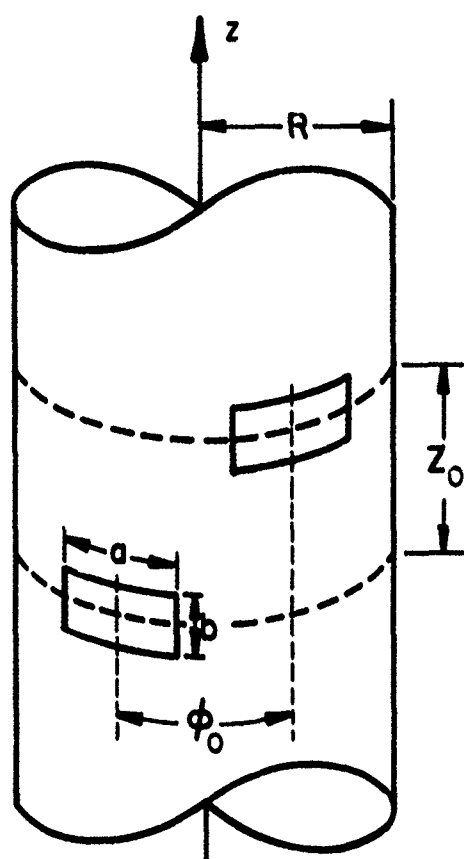
$$(a, b) = \text{dimensions of the slot along } (\phi, z) \text{ directions (a is the arc length along the cylinder)} \quad (2.2)$$

$$(z_0, R\phi_0) = \text{center-to-center distances between slots} \quad (2.3)$$

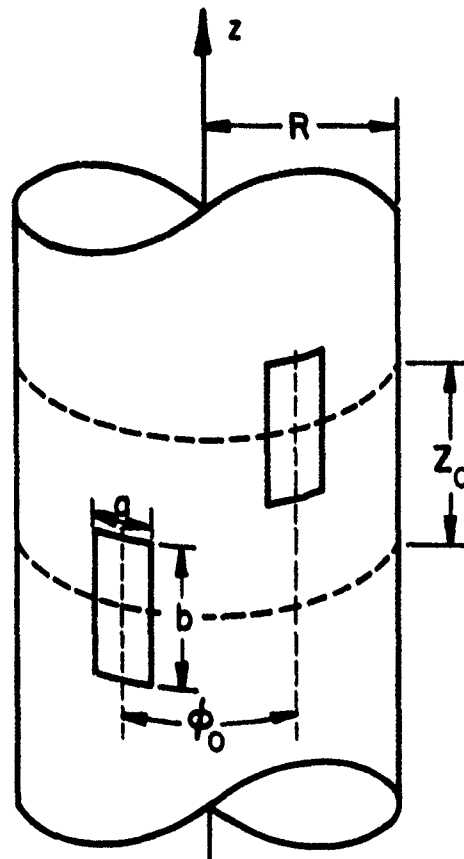
$$s_0 = \sqrt{z_0^2 + (R\phi_0)^2} \quad (2.4)$$

$$\theta_0 = \tan^{-1}(z_0/R\phi_0) \quad (2.5)$$

The problem is to determine the mutual admittance between these two slots when kR is large.



(a) CIRCUMFERENTIAL SLOTS



(b) AXIAL SLOTS

Figure 1. Two identical slots on the surface of a cylinder.

First let us define mutual admittance. Throughout this work we always assume that

$$(i) \text{ the slots are thin, and} \quad (2.6a)$$

$$(ii) \text{ their length is roughly a half-wavelength.} \quad (2.6b)$$

Then the aperture field in each slot can be adequately approximated by a simple cosine distribution, which is the so-called "one-mode" approximation. For example, if slot 1 is a circumferential (lower slot in Figure 1a), its aperture field under the "one-mode" approximation is given by (exp + j ω t time convention)

$$\vec{E} = V_1 \vec{e}_1, \quad \vec{H} = I_1 \vec{h}_1 \quad (2.7a)$$

where

$$\vec{e}_1 = \hat{z} \sqrt{\frac{2}{ab}} \cos \frac{\pi}{a} y, \quad \vec{h}_1 = \hat{x} \times \vec{e}_1 \quad (2.7b)$$

$$y = R\phi. \quad (2.7c)$$

(V_1, I_1) are respectively the modal (voltage, current) of slot 1. The mutual admittance Y_{12} is defined by

$$Y_{12} = Y_{21} = \frac{I_{21}}{V_1} \quad (2.8)$$

where I_{21} is the induced current in slot 2 when slot 1 is excited by a voltage V_1 and slot 2 is short-circuited. An alternative expression for Y_{12} is

$$Y_{12} = \frac{1}{V_1 V_2} \iint_{\Lambda_2} \vec{E}_2 \times \vec{h}_1 \cdot d\vec{s}_2 \quad (2.9)$$

where

Λ_2 = aperture of slot 2

\vec{h}_1 = magnetic field when slot 1 is excited with voltage V_1 , and slot 2 is covered by a perfect conductor

\vec{E}_2 = electric field when slot 2 is excited with voltage V_2 , and slot 1 is covered by a perfect conductor.

Because $\vec{H}_1 = I_{21} \vec{h}_2$ and $\vec{E}_2 = V_2 \vec{e}_2$, it is a simple matter to verify that (2.8) and (2.9) are equivalent [1].

There is an alternative definition of mutual admittance. Instead of (2.7), a modal voltage \bar{V}_1 (with a bar) may be defined through the expression for the aperture field of slot 1 as follows:

$$\vec{E} = \hat{z} \frac{1}{b} \bar{V}_1 \cos \frac{\pi}{a} y \quad (2.10a)$$

or equivalently

$$\bar{V}_1 = \int_{-b/2}^{b/2} (\hat{z} \cdot \vec{E})_{y=0} dz \quad (2.10b)$$

Then a different mutual admittance \bar{Y}_{12} is defined by (2.9) after replacing (V_1, V_2) by (\bar{V}_1, \bar{V}_2) . It can be easily shown that

$$\bar{Y}_{12} = \frac{a}{2b} Y_{12} \quad (2.11)$$

Two remarks are in order: (i) In the limiting case that $b \rightarrow 0$, Y_{12} goes to zero as b , whereas \bar{Y}_{12} approaches a constant independent of b .

(ii) For the special case $a = \lambda/2$ and $R \rightarrow \infty$, it is \bar{Y}_{12} that is identical to the mutual impedance Z_{12} between two corresponding dipoles calculated by the classical Carter's method [2], [3], [4]. (iii) When the slots are excited by waveguides (transmission lines), one often uses Y_{12} (\bar{Y}_{12}). From here on, we will concentrate on Y_{12} instead of \bar{Y}_{12} .

The mutual admittance defined in (2.8) and (2.9) includes the self admittance Y_{11} as a special case which occurs when two slots coincide. (All the formulas of Y_{12} given in this paper, except for the one in Section 4, can be used for calculating Y_{11} by setting $\phi_0 \rightarrow 0$ and $z_0 \rightarrow 0$.)

3. EXACT HUGHES (GSP) MODAL SOLUTION

Once the one-mode approximation in (2.7) is accepted, Y_{12} can be determined exactly in terms of cylindrical modal functions, as has been done by Stewart, Golden, and Pridmore-Brown [5], [6]. The final result reads:

Circumferential slots

$$Y_{12} = \int_{-\infty}^{\infty} dk_z \sum_{m=-\infty}^{\infty} \psi(m, k_z) G(m, k_z) e^{-j(m\phi_0 + k_z z_0)} \quad (3.1)$$

where

$$\psi(m, k_z) = \frac{ab}{8\pi^2 R} \frac{\sin^2(k_z b/2)}{(k_z b/2)^2} \cdot \left\{ \frac{\sin(m\phi_a + \pi/2)}{(m\phi_a + \pi/2)} + \frac{\sin(m\phi_a - \pi/2)}{(m\phi_a - \pi/2)} \right\}^2 \quad (3.2)$$

$$\phi_a = (a/2R)$$

$$G(m, k_z) = Y_0 \left[\frac{jk}{k_t} \frac{H_m^{(2)'}(k_t R)}{H_m^{(2)}(k_t R)} + \left(\frac{mk_z}{k_t^2 R} \right)^2 \frac{k_t}{jk} \frac{H_m^{(2)}(k_t R)}{H_m^{(2)'}(k_t R)} \right] \quad (3.3)$$

$$k_t = \begin{cases} \sqrt{k^2 - k_z^2} & , \text{ if } k \geq k_z \\ -j \sqrt{k_z^2 - k^2} & , \text{ if } k \leq k_z \end{cases} \quad (3.4)$$

Axial slots

$$Y_{12} = \int_{-\infty}^{\infty} dk_z \sum_{m=-\infty}^{\infty} \phi(m, k_z) F(m, k_z) e^{-j(m\phi_0 + k_z z_0)} \quad (3.5)$$

where

$$\phi(m, k_z) = \frac{ab}{8R} \left(\frac{\sin(m\phi_a)}{(m\phi_a)} \cdot \frac{\cos(k_z b/2)}{(k_z b/2)^2 - (\pi/2)^2} \right)^2 \quad (3.6)$$

$$F(m, k_z) = Y_0 \frac{k_t}{jk} \frac{H_m^{(2)}(k_t R)}{H_m^{(2)'}(k_t R)} \quad (3.7)$$

This solution is suitable for numerical calculation if (i) $z_0 < b$ for circumferential slots, and $z_0 < a$ for axial slots, (ii) kR is less than 20, and (iii) the medium is slightly lossy so that k has a small (negative) imaginary part. Based on this solution, extensive numerical results have been reported by Hughes Aircraft Company at Culver City [7], [8], [9].

4. EXACT UI MODAL SOLUTION

Under the one-mode approximation, another exact modal solution is given in [10]. This solution is derived from the Hughes (SGP) solution in Section 3 by a deformation of integration contour and an application of the Duncan transform [11]. The final result reads

Circumferential slots

$$Y_{12} = G + jB \quad (4.1a)$$

$$G = \int_0^k \sum_{m=0}^{\infty} \frac{\cos m\phi_0}{\epsilon_m} \cos k_z z_0 \psi(m, k_z) R(m, k_z) dk_z \quad (4.1b)$$

$$B = \sum_{m=0}^{\infty} \frac{\cos m\phi_0}{\epsilon_m} \left\{ - \int_0^k R(m, k_z) \psi(m, k_z) \sin k_z z_0 dk_z + \int_0^{\infty} R(m, j\eta) \psi(m, j\eta) e^{-\eta z_0} d\eta \right\} \quad (4.1c)$$

where

$$R(m, k_z) = \frac{2}{\pi k_t R} \cdot \frac{k}{k_t} \cdot \left[\frac{1}{N_m^2(k_t R)} + \left(\frac{\ln k_z}{k_t k R} \right)^2 \frac{1}{N_m^2(k_t R)} \right] \quad (4.2)$$

$$N_m^2(\chi) = J_m^2(\chi) + Y_m^2(\chi) \quad (4.3)$$

$$N_m^2(\chi) = J_m'^2(\chi) + Y_m'^2(\chi) \quad (4.4)$$

$$\epsilon_m = \begin{cases} 2, & m = 0 \\ 1, & m \neq 0 \end{cases} \quad (4.5)$$

$\psi(m, k_z)$ is defined in (3.2) and k_t in (3.4) (4.6)

Axial slots

$$Y_{12} = \frac{8Y_0}{\pi kR} \sum_{m=0}^{\infty} \frac{\cos m\phi_0}{\epsilon_m} \left(\int_0^k \phi(m, k_z) e^{-jk_z z_0} \frac{dk_z}{N_m^2(k_t R)} \right. \\ \left. + j \int_0^{\infty} \phi(m, j\eta) e^{-\eta z_0} \frac{d\eta}{N_m^2(R\sqrt{\eta^2 + k^2})} \right) \quad (4.7)$$

where $\phi(m, k_z)$ is defined in (3.6)

This solution is valid only if $z_0 > b$ for circumferential slots and $z_0 > a$ for axial slots. It is suitable for numerical calculation if kR is less than 20.

5. ASYMPTOTIC SOLUTION

The two modal solutions given in Sections 3 and 4 are based on fields in the Fourier transform domain. An alternative calculation of Y_{12} involves the field in the spatial domain, namely,

Circumferential slots

$$Y_{12} = \frac{-2}{ab} \int_{A_1} dy_1 dz_1 \int_{A_2} dy_2 dz_2 [\cos \frac{\pi}{a} y_1] [\cos \frac{\pi}{a} (y_2 - R\phi_0)] g_{\phi}(s, \theta) \quad (5.1)$$

Axial slots

$$Y_{12} = \frac{-2}{ab} \int_{A_1} dy_1 dz_1 \int_{A_2} dy_2 dz_2 [\cos \frac{\pi}{b} z_1] [\cos \frac{\pi}{b} (z_2 - z_0)] g_z(s, \theta) \quad (5.2)$$

where (y_n, z_n) = a typical point in the aperture of slot n ($n = 1$ or 2).

(5.3)

A_n = aperture of slot n

(5.4)

$$s = \sqrt{(y_2 - y_1)^2 + (z_2 - z_1)^2} \quad (5.5)$$

$$\theta = \tan^{-1}[(z_2 - z_1)/(y_2 - y_1)] \quad (5.6)$$

Several versions of the Green's functions g_ϕ and g_z have been approximately determined under the condition that $kR \gg 1$. They are listed as follows:

OSU Asymptotic solution [12] [13]

$$g_\phi \sim G(s) [v(\xi) \sin^2 \theta + (\frac{1}{ks}) u(\xi) \cos^2 \theta] \quad (5.7)$$

$$g_z \sim G(s) [v(\xi) \cos^2 \theta + (\frac{1}{ks}) u(\xi) \sin^2 \theta] \quad (5.8)$$

PINY Asymptotic solution [9] [14]

$$g_\phi \sim G(s) \left[v(\xi) [\sin^2 \theta + \frac{1}{ks} (1 - 3 \sin^2 \theta)] + \frac{1}{ks} \sec^2 \theta [u(\xi) - v_1(\xi) \sin^2 \theta] \right] \quad (5.9)$$

$$g_z \sim G(s) v(\xi) [\cos^2 \theta + \frac{1}{ks} (2 - 3 \cos^2 \theta)] \quad (5.10)$$

UI Asymptotic solution [15]

$$g_\phi \sim G(s) \left[v(\xi) [\sin^2 \theta + \frac{1}{ks} \cos 2\theta] + (\frac{1}{ks}) u(\xi) [\cos^2 \theta (1 - \frac{2j}{ks}) + (\frac{1}{ks}) \sin^2 \theta] + j(\sqrt{2} kR / \cos^2 \theta)^{-2/3} [v'(\xi) \sin^2 \theta + (\tan^4 \theta + \frac{1}{ks}) u'(\xi) \cos^2 \theta] \right] \quad (5.11)$$

$$g_z = G(s) \left[v(\xi) [\cos^2 \theta - \frac{1}{ks} \cos 2\theta] + (\frac{1}{ks}) u(\xi) [\sin^2 \theta (1 - \frac{2j}{ks}) + (\frac{1}{ks}) \cos^2 \theta] + j(\sqrt{2} kR / \cos^2 \theta)^{-2/3} [v'(\xi) \cos^2 \theta + (1 + \frac{1}{ks}) u'(\xi) \sin^2 \theta] \right] \quad (5.12)$$

where

$$G(s) = \frac{k^2 Y_0}{2\pi j} \frac{e^{-jks}}{ks}, \quad Y_0 = (120\pi)^{-1} \quad (5.13)$$

$$\xi = (k \cos^4 \theta / 2R^2)^{1/3} s \quad (5.14)$$

The Fock functions, u , v , etc., can be calculated from the following two representations:

For $0 \leq \xi \leq 0.7$

$$v(\xi) \sim 1 - \frac{\sqrt{\pi}}{4} e^{j\pi/4} \xi^{3/2} + \frac{7j}{60} \xi^3 + \frac{7\sqrt{\pi}}{512} e^{-j\pi/4} \xi^{9/2} - 4.141 \times 10^{-3} \xi^6 \quad (5.15)$$

$$u(\xi) \sim 1 - \frac{\sqrt{\pi}}{2} e^{j\pi/4} \xi^{3/2} + \frac{5j}{12} \xi^3 + \frac{5\sqrt{\pi}}{64} e^{-j\pi/4} \xi^{9/2} - 3.701 \times 10^{-2} \xi^6 \quad (5.16)$$

$$v_1(\xi) \sim 1 + \frac{\sqrt{\pi}}{2} e^{j\pi/4} \xi^{3/2} - \frac{7j}{12} \xi^3 - \frac{7\sqrt{\pi}}{64} e^{-j\pi/4} \xi^{9/2} + 4.555 \times 10^{-2} \xi^6 \quad (5.17)$$

$$v'(\xi) \sim \frac{3\sqrt{\pi}}{8} e^{-j3\pi/4} \xi^{1/2} + \frac{7j}{20} \xi^2 + \frac{63\sqrt{\pi}}{1024} e^{-j\pi/4} \xi^{7/2} - 2.485 \times 10^{-2} \xi^5 \quad (5.18)$$

$$u'(\xi) \sim \frac{3}{4} \sqrt{\pi} e^{-j3\pi/4} \xi^{1/2} + \frac{5j}{4} \xi^2 + \frac{45\sqrt{\pi}}{128} e^{-j\pi/4} \xi^{7/2} - 2.221 \times 10^{-1} \xi^5 \quad (5.19)$$

For $0.7 \leq \xi \leq \infty$

$$v(\xi) \approx e^{-j\pi/4} \sqrt{\pi} \xi^{1/2} \sum_{n=1}^{10} (t'_n)^{-1} e^{-j\xi t'_n} \quad (5.20)$$

$$u(\xi) \approx e^{j\pi/4} 2\sqrt{\pi} \xi^{3/2} \sum_{n=1}^{10} e^{-j\xi t_n} \quad (5.21)$$

$$v_1(\xi) \approx e^{j\pi/4} 2\sqrt{\pi} \xi^{3/2} \sum_{n=1}^{10} e^{-j\xi t'_n} \quad (5.22)$$

$$v'(\xi) \approx \frac{1}{2} e^{-j\pi/4} \sqrt{\pi} \xi^{-1/2} \sum_{n=1}^{10} (1 - j2\xi t'_n) (t'_n)^{-1} e^{-j\xi t'_n} \quad (5.23)$$

$$u'(\xi) \approx e^{j\pi/4} 3\sqrt{\pi} \xi^{1/2} \sum_{n=1}^{10} \left(1 - j \frac{2}{3} \xi t_n\right) e^{-j\xi t_n} \quad (5.24)$$

where $t_n = |t_n| \exp(-j\pi/3)$, $t'_n = |t'_n| \exp(-j\pi/3)$, and

n	$ t_n $	$ t'_n $
1	2.33811	1.01879
2	4.08795	3.24820
3	5.52056	4.82010
4	6.78671	6.16331
5	7.99413	7.37218

n	$ t_n $	$ t'_n $
6	9.02265	8.48849
7	10.04017	9.53545
8	11.00852	10.52766
9	11.93602	11.47506
10	12.82878	12.38479

It has been verified through several hundred numerical examples that the UI asymptotic solution given above is in excellent agreement (within a quarter db in magnitude and a few degrees in phase) with the exact model solution for all slot separations (ϕ_0, z_0) provided that $kR \geq 5$.

In using the asymptotic solutions for calculating the self admittance Y_{11} , care must be exercised in avoiding the singularity in the Green's function which occurs at $s = 0$. A most convenient way to avoid this apparent difficulty is to (i) use a large number of points for the two surface integrals in (5.1) and (5.2), and (ii) shift slightly the integration nets for this two surface integrals.

6. EXACT PLANAR SOLUTION

In the limit $kR \rightarrow \infty$ the Green's function of the UI solution in (5.11) and (5.12) is reduced to

$$g_\phi = G(s) \left[\sin^2 \theta + \frac{1}{ks} (2 - 3 \sin^2 \theta) \left(1 - \frac{1}{ks}\right) \right] \quad (6.1)$$

$$g_z = G(s) \left[\cos^2 \theta + \frac{1}{ks} (2 - 3 \cos^2 \theta) \left(1 - \frac{1}{ks}\right) \right] \quad (6.2)$$

When (6.1) and (6.2) are used in (5.1) and (5.2), we obtain the exact solution (under the "one-mode" approximation of course) for two slots on an infinitely large, conducting plane.

7. APPROXIMATE SOLUTION

Based on the UI asymptotic solution, a simple approximate solution, is reported in [10], i.e.,

Circumferential slots

$$Y_{12} \approx - \frac{8ab}{\pi^2} [S(b \sin \theta) C(a \sin \theta)]^2 \bar{g}_\phi \quad (7.1)$$

Axial slots

$$Y_{12} \approx - \frac{8ab}{\pi^2} [S(a \cos \theta) C(b \sin \theta)]^2 \bar{g}_z \quad (7.2)$$

where

$$S(x) = \frac{\sin (kx/2)}{(kx/2)} , \quad C(x) = \frac{\cos (kx/2)}{1 - (kx/\pi)^2} . \quad (7.3)$$

The (simplified) Green's functions \bar{g}_ϕ and \bar{g}_z are given by

$$\begin{aligned} \bar{g}_\phi = G(s) & \left[v(\xi) \left(\sin^2 \theta + \frac{1}{ks} \cos 2\theta \right) + \frac{1}{ks} u(\xi) \cos^2 \theta \right. \\ & \left. + ju'(\xi) (\sqrt{2} kR \cos \theta)^{-2/3} \sin^4 \theta \right] \end{aligned} \quad (7.4)$$

$$\bar{g}_z = G(s) \left[v(\xi) \left(\cos^2 \theta - \frac{1}{ks} \cos 2\theta \right) + \frac{1}{ks} u(\xi) \sin^2 \theta \right]. \quad (7.5)$$

This solution gives an accurate numerical result (within several percent in magnitude and less than 5° in phase) provided that $kR \geq 10$ and the slot separation is greater than two wavelengths.

8. CONCLUDING REMARKS

Based on extensive numerical data, we conclude that Y_{12} (including Y_{11} as a special case) can be best calculated by

- (i) Hughes modal solution if $kR \leq 5$ and z_0 is less than the axial dimension of the slot,
- (ii) UI modal solution if $kR \leq 5$ and z_0 is greater than the axial dimension of the slot, and
- (iii) UI asymptotic solution if $kR \geq 5$ for all slot separations.

If several percents of error are acceptable, the approximate solution can be used if $kR \geq 10$ and the slot separation is greater than two wavelengths.

REFERENCES

- [1] J. H. Richmond, "A reaction theorem and its application to antenna impedance calculation," IEEE Trans. Antennas Propagat., vol. AP-9, pp. 515-520, 1961.
- [2] E. C. Jordan and K. Balmain, Electromagnetic Waves and Radiating Systems, 2nd Ed. Englewood Cliffs, New Jersey: Prentice-Hall, 1968, Chapter 14.
- [3] R. C. Hansen, "Formulation of echelon dipole mutual impedance for computer," IEEE Trans. Antennas Propagat., vol. AP-20, pp. 780-781, 1972.
- [4] R. C. Hansen, "Mutual coupling of slots on a flat ground plane," Rept. No. TR648-1 on Contract N00019-76-0276, R. C. Hansen, Inc., Tarzana, California, 1976.
- [5] G. E. Stewart and K. E. Golden, "Mutual admittance for axial rectangular slots in a large conducting cylinder," IEEE Trans. Antennas Propagat., vol. AP-19, pp. 120-122, 1971.
- [6] K. E. Golden, G. E. Stewart, and D. C. Pridmore-Brown, "Approximation techniques for the mutual admittance of slot antennas on metallic cones," IEEE Trans. Antennas Propagat., vol. AP-22, pp. 43-48, 1974.
- [7] P. C. Bargeliot, A. T. Villeneuve, and W. H. Kummer, "Phased array antennas scanned near endfire," Final Report (January 1975-March 1976), Contract N00019-75-0160, Hughes Aircraft Company, Culver City, California, 1976.
- [8] P. C. Bargeliot, A. T. Villeneuve, and W. H. Kummer, "Conformal phased array breadboard," Quarterly Progress Reports, Contract N00019-76-C-0495, Hughes Aircraft Company, Culver City, California, 1976.
- [9] Z. W. Chang, L. B. Felsen, and A. Hessel, "Surface ray methods for mutual coupling in conformal arrays on cylinder and conical surface," Polytechnic Institute of New York, Final Report (September 1975-February 1976), 1976; prepared under Contract N00123-76-C-0236.
- [10] S. W. Lee and S. Safavi-Naini, "Approximate closed-form solution for mutual admittance of slots on cylinder," University of Illinois at Urbana-Champaign, Electromagnetics Laboratory, Report No. 77 - 1977.
- [11] R. H. Duncan, "Theory of the infinite cylindrical antenna including the feedpoint singularity in antenna current," J. Res. Natl. Bur. Std.-D. Radio Propagat., vol. 66D, pp. 181-188, 1962.

- [12] Y. Hwang and R. G. Kouyoumjian, "The mutual coupling between slots on an arbitrary convex cylinder," ElectroScience Laboratory, The Ohio State University, Semi-Annual Report 2902-21, 1975; prepared under Grant NGL 36-003-138.
- [13] P. H. Pathak, "Analysis of a conformal receiving array of slots in a perfectly-conducting circular by the geometrical theory of diffraction," ElectroScience Laboratory, The Ohio State University, Technical Report ESL 3735-2, 1975; prepared under Contract N00140-74-C-6017.
- [14] Z. W. Chang, L. B. Felsen, A. Hessel, and J. Shmoys, "Surface ray method in the analysis of conformal arrays," in Digest of 1976 AP-S International Symposium, University of Massachusetts at Amherst, October 1976, pp. 366-369.
- [15] S. W. Lee and S. Safavi-Naini, "Asymptotic solution of surface field due to a magnetic dipole on a cylinder," University of Illinois at Urbana-Champaign, Electromagnetics Laboratory Report No. 76-11, 1976.

APPENDIX A: NUMERICAL RESULTS

By using the formulas of Y_{12} presented in the text, we have analyzed the following 6 slots:

Slot	Type	Dimension	Suggested by
A	Circumf.	0.9" x 0.4" (f = 9 GHz)	Aerospace Hughes
B	Circumf.	0.5 λ x 0.01 λ (R in inch)	Hansen
C	Axial	0.4" x 0.9" (f = 9 GHz)	Aerospace Hughes
D	Circumf.	0.5 λ x 0.01 λ (R in λ)	Hansen
E	Circumf.	0.5 λ x 0.2 λ	Hansen
F	Axial	0.5 λ x 0.2 λ	

In all tables, Y_{12} is listed in (db, phase in degree) format where $\text{db} = 20 \log_{10} (Y_{12} \text{ in mho})$. In all figures, the normalized phase of Y_{12} is equal to $\text{Arg}(Y_{12} \exp jks_0)$.

DATA SET A OF MUTUAL ADMITTANCE

- (1) The mutual admittance Y_{12} between two circumferential slots on an infinitely long cylinder is calculated from the

- * (Exact) Hughes modal solution
- * (Exact) UI modal solution
- * UI asymptotic solution
- * OSU asymptotic solution
- * PINY asymptotic solution.

The parameters are

- * Frequency: $f = 9 \text{ GHz}$, $k = 4.7878 \text{ (inch)}^{-1}$, $\lambda = 1.3123''$
- * Cylinder: $R = 1.991''$ unless specified otherwise
- * Slot A: Circumferential
 - $a = 0.9'' = 0.6858\lambda$
 - $b = 0.4'' = 0.3048\lambda$
 - $|Y_{11}| = 1.70747 \times 10^{-3} \text{ mho} = -55.35 \text{ db}$
 - $Y_g = 1.8155 \times 10^{-3} \text{ mho}$
- * Center-to-center distance between two slots is $(R\phi_0, z_0)$.

- (2) Y_{12} is listed in (db value, phase in degree), where

$$\text{db value} = 20 \log_{10} (|Y_{12}| \text{ in mho}).$$

- (3) Data are presented in

TABLE A-1: $\phi_0 = 0$ and various z_0

A-2: $z_0 = 2''$ and various ϕ_0

A-3: $z_0 = 0$ and various ϕ_0

A-4: $\phi_0 = 0$ and various z_0 .

Figure A-1: Mutual admittance Y_{12} between two circumferential slots as a function of ϕ_0 .

A-2 Mutual admittance Y_{12} between two circumferential slots as a function of z_0 .

A-3: $|Y_{12}|$ on a cylinder (UI modal solution) and that on a plane as a function of z_0 .

A-4: Y_{12} on a cylinder as a function of the radius R of the cylinder.

TABLE A-1

 Y_{12} OF SLOT A FOR $\phi_0 = 0$

z_0	Modal		Asymptotic			Exact Planar $R=\infty$
	Hughes	UI	UI	OSU	PINY	
0.5"	-62.62 db -72°	-62.62 -72°	-62.54 -72°	-64.22 -43°	-61.7 -68°	-63.69 -67°
2"	-71.87 -117°	-71.78 -117°	-71.66 -116°	-73.67 -100°	-70.96 -118°	-73.53 106°
8"	-82.3 33°	-81.84 34°	-81.83 37°	-85.46 55°	-80.80 34°	-85.4 54°
16"		-86.48 -4°	-86.6 -1°	-91.41 20°	-85.26 -4°	-91.40 19°
40"		-91.95 -115°	-92.46 -110°	-99.34 -83°	-90.83 -112°	-99.33 -83°

TABLE A-2

 Y_{12} OF SLOT A FOR $z_o = 2''$

ϕ_o	Modal		Asymptotic		
	Hughes	UI	UI	OSU	PINY
0°	-71.87 db	-71.78	-71.66	-73.67	-70.96
	-117 $^\circ$	-117 $^\circ$	-116 $^\circ$	-100 $^\circ$	-118 $^\circ$
30°	-77.60	-77.42	-77.69	-79.25	-76.6
	175 $^\circ$	175 $^\circ$	177 $^\circ$	170 $^\circ$	172 $^\circ$
60°	-89.98	-90.00	-90.17	-91.11	-88.41
	-4 $^\circ$	-3 $^\circ$	-1 $^\circ$	6 $^\circ$	-10 $^\circ$
90°	-103.15	-102.52	-103.10	-103.83	-101.69
	116 $^\circ$	120 $^\circ$	116 $^\circ$	119 $^\circ$	106 $^\circ$

TABLE A-3

 Y_{12} OF SLOT A FOR $z_o = 0$

ϕ_o	Modal	Asymptotic		
	Hughes	UI	OSU	PINY
30°	-81.33 db	-81.34	-89.72	-83.14
	-77 $^\circ$	-75 $^\circ$	-62 $^\circ$	-60 $^\circ$
40°	-89.87	-90.02	-98.66	-91.11
	168 $^\circ$	170 $^\circ$	174 $^\circ$	-180 $^\circ$
50°	-96.37	-96.72	-105.95	-97.43
	58 $^\circ$	61 $^\circ$	58 $^\circ$	69 $^\circ$
60°	-101.97	-102.48	-112.59	-102.93
	-49 $^\circ$	-47 $^\circ$	-55 $^\circ$	-39 $^\circ$

TABLE A-4

UI SOLUTIONS OF Y_{12} OF SLOT A FOR $\phi_0 = 0$

z_0	Modal	Asymptotic	z_0	Modal	Asymptotic
0.5"	-62.62 db -72°	-62.54 -72°	11"	-84.06 -70°	-84.06 -68°
1"	-66.82 155°	-66.71 155°	12"	-84.61 15°	-84.65 18°
2"	-71.78 -117°	-71.66 -116°	13"	-85.12 100°	-85.20 103°
3"	-74.78 -31°	-74.67 -30°	14"	-85.63 -175°	-85.70 -172°
4"	-76.89 54°	-76.89 54°	15"	-86.09 -90°	-86.17 -86°
5"	-78.51 139°	-78.44 141°	16"	-86.48 -4°	-86.60 -1°
6"	-79.85 -136	-79.77 -134	17"	-86.85 81	-87.01 84
7"	-80.94 -51°	-80.88 -49°	18"	-87.24 166°	-87.38 170°
8"	-81.84 34°	-81.83 37°	20"	-87.91 -24°	-88.08 -19°
9"	-82.65 119°	-82.66 122°	30"	-90.33 110°	-90.68 115°
10"	-83.40 -156°	-83.40 -153°	40"	-91.95 -115°	-92.46 -110°

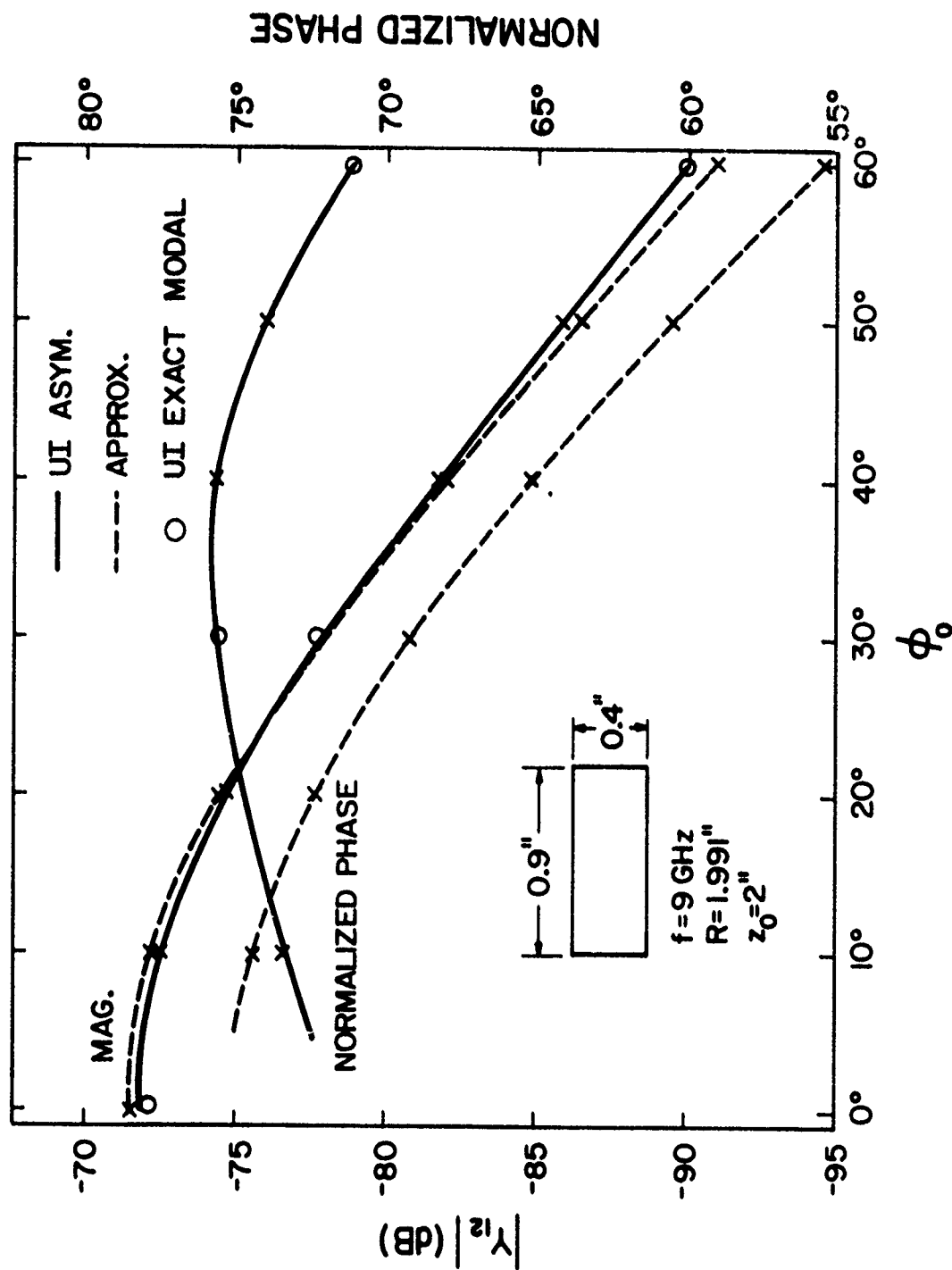


Figure A-1. Mutual admittance Y_{12} between two circumferential slots as a function ϕ_0 .

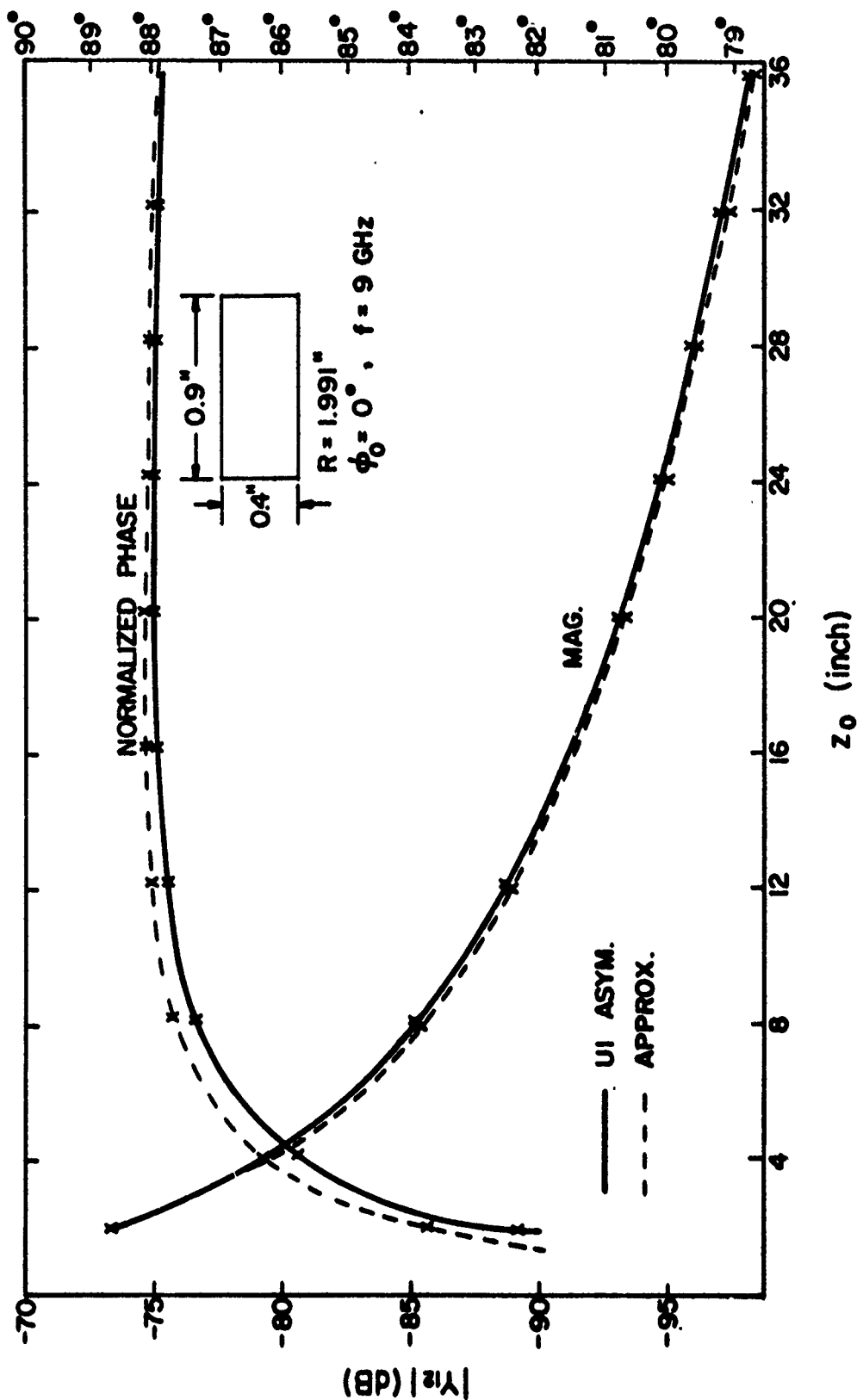


Figure A-2. Mutual admittance Y_{12} between two circumferential slots as a function of z_0 .

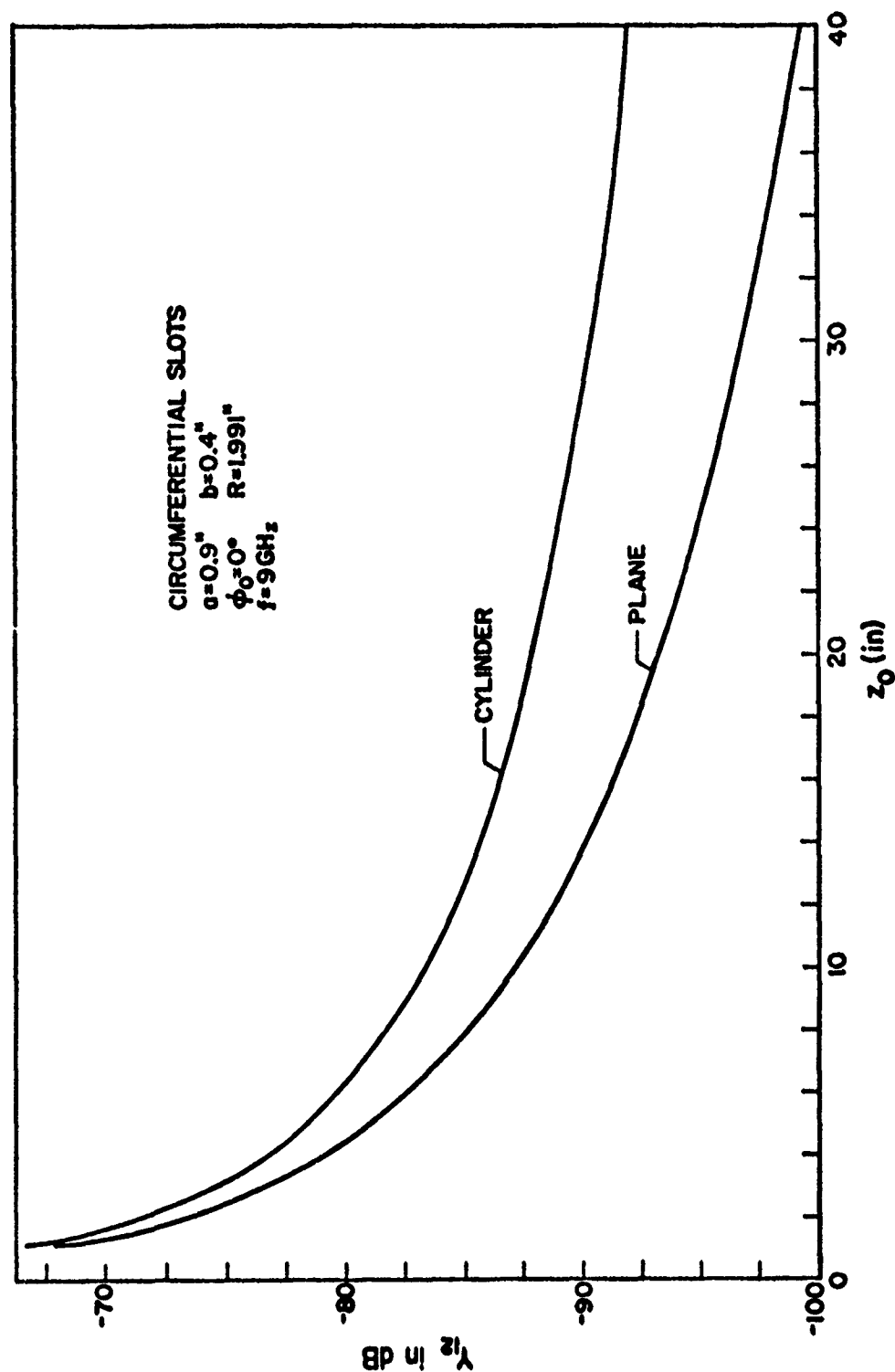


Figure A-3: $|Y_{12}|$ on a cylinder (UI modal solution) and that on a plane as a function of z_0 .

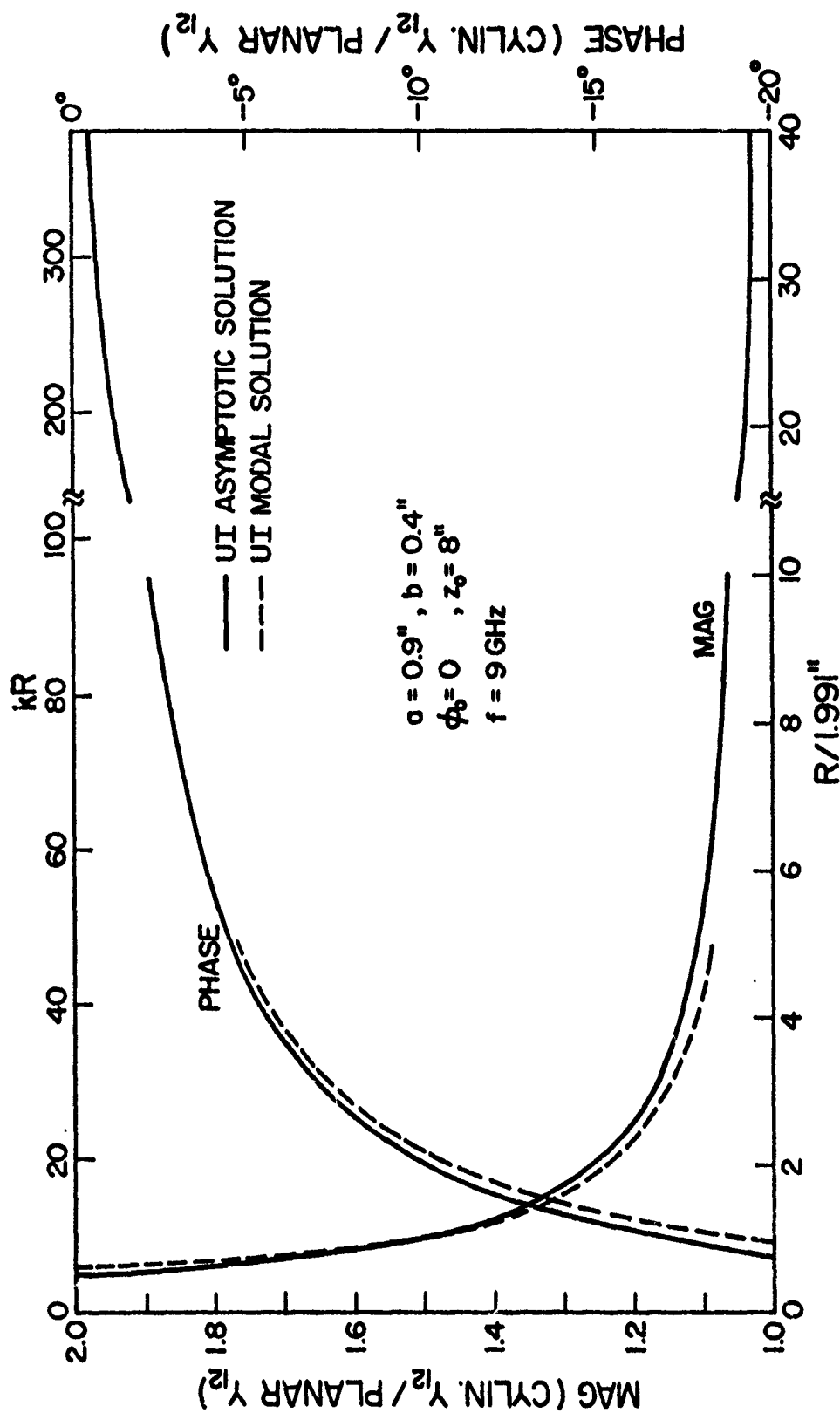


Figure A-4: Y_{12} on a cylinder as a function of the radius R of the cylinder. Y_{12} is normalized by Y_{12} on a plane which is $5.37 \times 10^{-5} \exp(j53.55^\circ)$ mho.

DATA SET B OF MUTUAL ADMITTANCE

- (1) The mutual admittance Y_{12} between two circumferential slots on an infinitely long cylinder is calculated from the

- * (Exact) UI modal solution
- * UI asymptotic solution.

The parameters are

- * Frequency: $f = 9 \text{ GHz}$, $k = 4.787787 \text{ (inch)}^{-1}$, $\lambda = 1.3123''$
- * Cylinder: $R = 1.991''$, $3.777''$, $6''$
- * Slot B: Circumferential
 - $a = 0.656168'' = 0.50\lambda$
 - $b = 0.013123'' = 0.01\lambda$
- * Center-to-center distance between two slots is $(R\phi_0, z_0)$.

- (2) Y_{12} is listed in (db value, phase in degree), where

$$\text{db value} = 20 \log_{10} (|Y_{12}| \text{ in mho}).$$

- (3) Data are presented in

TABLE B-1: $\phi_0 = 0$ and various z_0

B-2: $z_0 = 2''$ and various ϕ_0

B-3: $z_0 = 8''$ and various ϕ_0 .

B-4: Comparison of Hughes and UI solutions

TABLE B-1

UI SOLUTIONS OF Y_{12} OF SLOT B FOR $\phi_0 = 0$

z_0	R = 1.991"		R = 3.777"		R = 6"		Exact Planar R= ∞
	Modal	Asymp	Modal	Asymp	Modal	Asymp	
0.5"	-92.00 db -79°	-92.03 -78°	-92.48 -77°	-92.52 -78°	-92.70 -76°	-92.74 -76°	-93.11 -74°
1"	-96.31 152°	-96.28 153°	-96.97 156°	-96.92 159°	-97.24 157°	-97.19 157°	-97.61 155°
2"	-101.33 -117°	-101.32 -116°	-102.20 -113°	-102.17 -113°	-102.56 -111°	-102.54 -111°	-103.20 -109°
4"	-106.50 54°	-106.51 56°	-107.70 60°	-107.66 61°	-108.23 63°	-108.77 63°	-109.10 67°
8"	-111.48 36°	-111.56 37°	-113.13 42°	-113.11 43°	-113.85 46°	-113.81 46°	-115.08 53°
16"	-116.13 -4°	-116.35 -1°	-118.37 5°	-118.38 6°	-119.36 10°	-119.33 10°	-121.10 20°

TABLE B-2

UI SOLUTIONS OF Y_{12} OF SLOT B FOR $z_o = 2''$

ϕ_o	R = 1.991"		R = 3.777"		R = 6.0"	
	Modal	Asymp	Modal	Asymp	Modal	Asymp
10°	-102.01 db -125°	-102.04 -125°	-104.18 -140°	-104.22 -140°	-106.89 -177°	-106.94 -177°
20°	-103.94 -149°	-104.11 -148°	-109.18 142°	-109.36 143°	-115.80 11°	-115.93 12°
30°	-106.86 172°	-107.20 173°	-115.53 27°	-115.75 28°	-124.77 140°	-124.95 141°
45°	-112.51 92°	-112.98 93°	-125.07 169°	-125.40 170°	-136.67 106°	-136.82 105°
60°	-119.01 -11°	-119.28 -9°	-134.48 -81°	-134.38 -77°	-148.07 51°	-147.24 44°
90°	-131.40 110°	-131.83 106°	-148.22 132°	-150.57 113°	-155.92 -170°	-165.47 -102°

TABLE B-3

UI SOLUTIONS OF Y_{12} OF SLOT B FOR $z_o = 8''$

ϕ_o	R = 1.991"		R = 3.777"		R = 6.0"	
	Modal	Asymp	Modal	Asymp	Modal	Asymp
10°	-111.63 db 32°	-111.74 34°	-113.45 34°	-113.47 34°	-114.44 26°	-114.46 26°
20°	-112.08 24°	-112.29 26°	-114.40 9°	-114.54 9°	-116.18 -34°	-116.32 -34°
30°	-112.83 11°	-113.18 13°	-115.94 -32°	-116.26 -32°	-118.94 -130°	-119.21 -129°
45°	-114.41 -17°	-115.12 -16°	-119.29 -122°	-119.82 -121°	-124.43 27°	-124.85 29°
60°	-116.70 -56°	-117.70 -55°	-123.69 118°	-124.22 121°	-131.31 127°	-131.37 130°
90°	-122.98 -161°	-124.10 159°	-134.62 169°	-134.27 172°	-146.21 -132°	-145.33 146°

TABLE B-4
COMPARISON OF HUGHES AND UI SOLUTIONS

		R = 1.991"			R = 3.777"			R = 6"		
ϕ_o	z_o	Hughes Modal	UI		Hughes Modal	UI		Hughes Modal	UI	
			Modal	Asymp		Modal	Asymp		Modal	Asymp
0°	0.5"	-92.3 db -79°	-92 -79°	-92.03 -78°	-92.83 -77°	-92.48 -77°	-92.52 -78°	-92.87 -76°	-92.70 -76°	-92.74 -76°
	1"	-96.5 153°	-96.31 152°	-96.28 153°	-97.18 157°	-96.97 156°	-96.92 159°	-97.34 156°	-97.24 157°	-97.19 157°
	8"	-112.02 33°	-111.5 36°	-111.56 37°	-113.65 40°	-113.13 42°	-113.11 43°	-114.42 44°	-113.85 46°	-113.81 46°
	16"	-117.08 -6°	-116.13 -4°	-116.35 -1°	-119.27 3°	-118.37 5°	-118.38 6°		-119.36 10°	-119.33 10°
45°	2"	-112.73 91°	-112.51 92°	-112.98 93°	-125.43 168°	-125.07 169°	-125.40 170°	-137.17 104°	-136.7 106°	-136.82 105°

DATA SET C OF MUTUAL ADMITTANCE

- (1) The mutual admittance Y_{12} between two axial slots on an infinitely long cylinder is calculated from the

* (Exact) UI modal solution

* UI asymptotic solution

The parameters are

* Frequency: $f = 9 \text{ GHz}$, $k = 4.7877 \text{ (inch)}^{-1}$, $\lambda = 1.3123''$

* Cylinder: $R = 1.991''$, and other values

* Slot C: Axial

$$a = 0.4'' = 0.3048\lambda$$

$$b = 0.9'' = 0.6858\lambda$$

* Center-to-center distance between two slots is $(R\phi_0, z_0)$.

- (2) Y_{12} is listed in (db value, phase in degree), where db value = $20 \log_{10} (|Y_{12}| \text{ in mho})$

- (3) Data are presented in

TABLE C-1: $\phi_0 = 0$, $R = 1.991''$, and various z_0 .

C-2: $z_0 = 1.5''$, $R = 1.991''$, and various ϕ_0 .

C-3: $\phi_0 = 0$, $z_0 = 8''$, and various R .

Figure C-1: $|Y_{12}|$ on a cylinder (UI modal solution) and that on a plane as a function of z_0 .

TABLE C-1

Y₁₂ OF SLOT C FOR $\phi_0 = 0^\circ$

z ₀	Modal	Asymp	z ₀	Modal	Asymp
1"	-77.38 ^{db} -59°	-77.28 -59°	12"	-123.86 134°	-123.55 130°
2"	-92.00 8°	-91.86 6°	14"	-127.50 -51°	-126.23 -59°
3"	-99.48 89°	-99.25 86°	16"	-128.96 115°	-128.55 112°
4"	-104.68 172°	-104.36 170°	18"	-131.64 -68°	-130.60 -76°
5"	-108.88 -103°	-108.28 -106°	20"	-133.39 102°	-132.43 95°
6"	-111.94 -17°	-111.48 -21°	24"	-136.07 81°	-135.59 77°
7"	-114.61 68°	-114.17 64°	28"	-138.79 72°	-138.27 60°
8"	-116.93 151°	-116.5 149°	32"	-141.24 59°	-140.59 42°
9"	-119.28 -122°	-118.55 -126°	36"	-143.68 39°	-142.63 25°

TABLE C-2

 Y_{12} OF SLOT C FOR $z_0 = 1.5''$

ϕ_0	Modal	Asymptotic
0°	-86.58 db 151°	-86.31 149°
30°	-86.41 -26°	-85.15 -38°
60°	-87.43 84°	-85.77 72°
90°	-93.02 169°	-91.04 156°

TABLE C-3

 Y_{12} OF SLOT C FOR $\phi_o = 0$ and $z_o = 8''$

R	Modal	Asymptotic
0.995"	-118.07 ^{db} 150°	-116.55 148°
1.991"	-116.93 151°	-116.50 149°
3.982"	-116.91 150°	-116.47 149°
5.973"	-116.90 154°	-116.46 149°
7.964"	-116.89 154°	-116.45 149°
11.946"	-116.84 153°	-116.45 149°
15.928"	-116.82 153°	-116.45 149°
19.910"		-116.44 149°

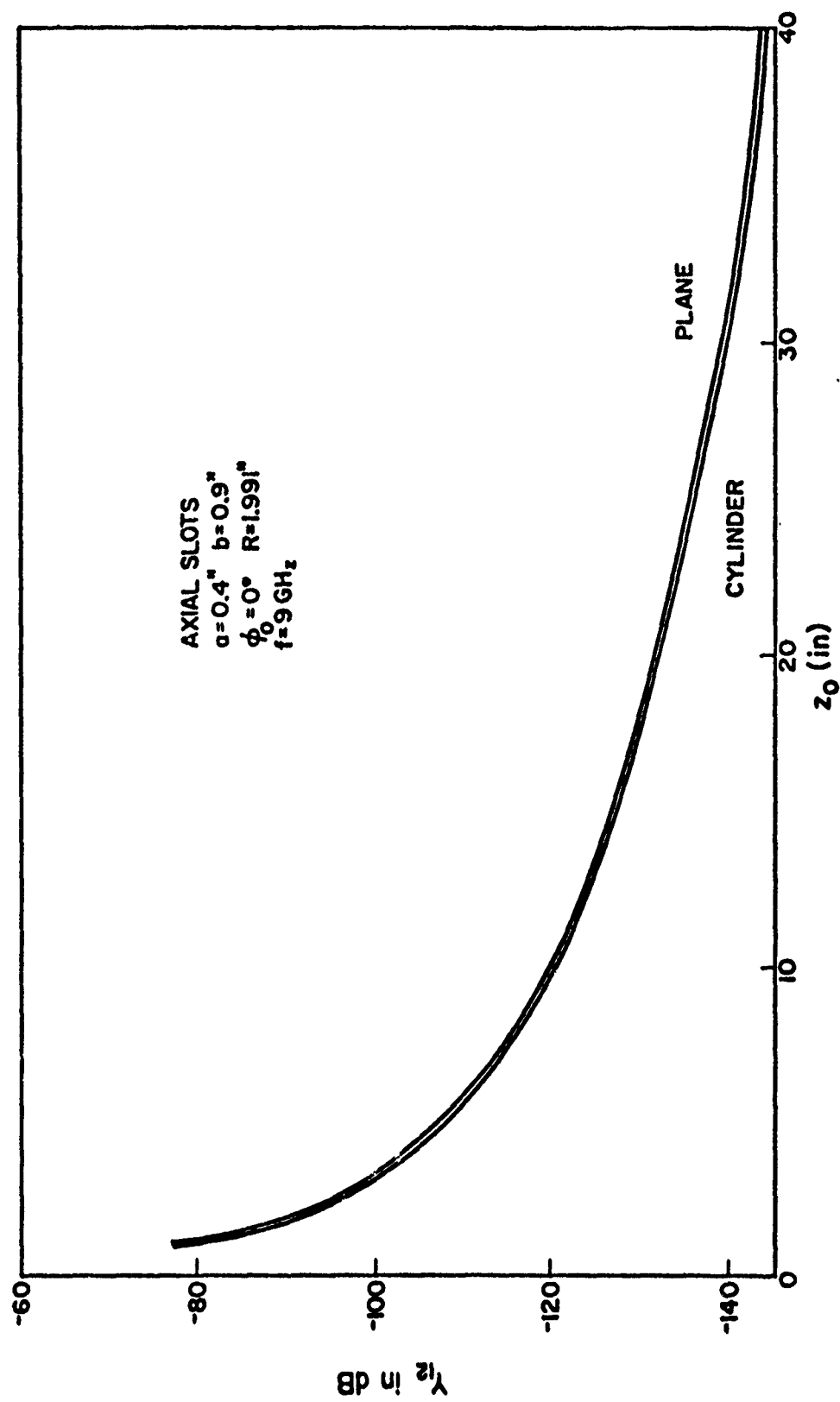


Figure C-1: $|Y_{12}|$ on a cylinder (UI modal solution) and that on a plane as a function of z_0 .

DATA SET D OF MUTUAL ADMITTANCE

- (1) The mutual admittance Y_{12} between two circumferential slots on an infinitely long cylinder from the

- * (Exact) UI modal solution
- * UI asymptotic solution

The parameters are

- * Cylinder: $R = 1\lambda, 2\lambda, 4\lambda, 10\lambda, \infty$ (planar)
- * Slot D: Circumferential

$$a = 0.5\lambda$$

$$b = 0.01\lambda$$

- * Center-to-center distance between two slots is $(R\phi_o, z_o)$

- (2) Y_{12} is listed in (db value, phase in degree), where

$$\text{db value} = 20 \log_{10} (|Y_{12}| \text{ in mho})$$

- (3) Data are presented in

TABLE D-1: $\phi_o = 0, R = 2\lambda$ and various z_o

D-2: $\phi_o = 0$ and various R and z_o

D-3: $\phi_o = 0$ and various R and z_o

D-4: $z_o = 0$ and various R and ϕ_o

D-5: $z_o = 1\lambda$ and various R and ϕ_o

D-6: $z_o = 5\lambda$ and various R and ϕ_o

TABLE D-1

UI SOLUTIONS OF Y_{12} OF SLOT D FOR $\phi_0 = 0$ and $R = 2\lambda$

z_0	Modal	Asymptotic
1λ	-98.60 db 71°	-98.56 71°
2λ	-103.87 74°	-103.84 75°
3λ	-106.98 75°	-106.96 75°
4λ	-109.17 74°	-109.16 75°
5λ	-110.84 73°	-110.85 75°
6λ	-112.19 73°	-112.21 74°
7λ	-113.32 72°	-113.35 74°
8λ	-114.28 72°	-114.33 73°
9λ	-115.12 71°	-115.18 73°
10λ		-115.94 72°

TABLE D-2

UI ASYMPTOTIC SOLUTIONS OF Y_{12} OF SLOT D FOR $\phi_0 = 0$

z_0	$R = 1\lambda$	$R = 2\lambda$	$R = 4\lambda$	$R = 10\lambda$	Planar ($R = \infty$)
0	81.51 db 90°	81.51 90°	81.51 90°	81.51 90°	
1λ	-97.49 67°	-98.56 71°	-99.15 74°	-99.51 76°	-99.76 77°
2λ	-102.39 69°	-103.84 75°	-104.63 79°	-105.13 81°	-105.47 83°
3λ	-105.26 69°	-106.96 75°	-107.92 80°	-108.52 83°	-108.93 86°
4λ	-107.25 68°	-109.16 75°	-110.25 80°	-110.94 84°	-111.40 87°
5λ	-108.76 67°	-110.85 75°	-112.05 80°	-112.81 84°	-113.33 87°
6λ	-109.97 67°	-112.21 74°	-113.51 80°	-114.34 84°	-114.91 88°
7λ	-110.98 66°	-113.35 74°	-114.74 80°	-115.63 84°	-116.25 88°
8λ	-111.85 65°	-114.33 73°	-115.80 79°	-116.75 84°	-117.40 88°
9λ	-112.60 65°	-115.18 73°	-116.72 79°	-117.73 84°	-118.43 89°
10λ	-113.27 64°	-115.94 72°	-117.55 79°	-118.61 84°	-119.34 89°

TABLE D-3

UI ASYMPTOTIC SOLUTIONS OF Y_{12} OF SLOT D FOR $\phi_o = 0$

z_o	$R = 1\lambda$	$R = 2\lambda$	$R = 4\lambda$	$R = 10\lambda$	Planar ($R = \infty$)
0.5λ	-93.01 db -119°	-93.83 -116°	-94.27 -115°	-94.55 -114°	-94.74 -113°
1.5λ	-100.34 -111°	-101.62 -106°	-102.32 -103°	-102.76 -100°	-103.05 -99°
2.5λ	-103.98 -111°	-105.56 -104°	-106.44 -100°	-106.99 -98°	-107.37 -95°

TABLE D-4

UI ASYMPTOTIC SOLUTIONS OF Y_{12} OF SLOT D FOR $z_o = 0$

ϕ_o	$R = 1\lambda$	$R = 2\lambda$	$R = 4\lambda$	$R = 10\lambda$
10°	-7.62 db 90°	-43.02 90°	-106.09 59°	-124.64 92°
20°	-43.02 90°	-107.10 62°	-121.97 29°	-140.01 20°
30°	-98.90 19°	-117.45 155.34°	-131.85 122°	-150.99 52°
45°	-112.59 106°	-128.38 52°	-143.53 84°	-164.60 165°
60°	-121.31 143°	-137.31 102°		-175.95 74°

TABLE D-5

UI ASYMPTOTIC SOLUTIONS OF Y_{12} OF SLOT D FOR $z_o = 1\lambda$

ϕ_o	$R = 1\lambda$	$R = 2\lambda$	$R = 4\lambda$	$R = 10\lambda$
10°	-98.12 db 62°	-100.56 54°	-105.46 9°	-120.20 107°
20°	-99.93 48°	-105.62 4°	-116.60 -160°	-136.65 -115°
30°	-102.69 26°	-111.94 -75°	-126.33 -18°	-148.10 -17°
45°	-107.99 -24°	-121.35 134°	-138.27 -21°	-162.12 111°
60°	113.88 -89°	-129.91 -40°	-148.52 -40°	-174.13 -123°

TABLE D-6

UI ASYMPTOTIC SOLUTIONS OF Y_{12} OF SLOT D FOR $z_o = 5\lambda$

ϕ_o	$R = 1\lambda$	$R = 2\lambda$	$R = 4\lambda$	$R = 10\lambda$
10°	-108.90 db 66°	-111.13 70°	-112.73 61°	-115.49 -25°
20°	-109.31 61°	-111.98 54°	-114.67 6°	-121.98 39°
30°	-109.98 53°	-113.34 29°	-117.66 -83°	-129.87 -24°
45°	-111.47 37°	-116.23 -26°	-123.42 91°	-141.86 -72°
60°	-113.50 14°	-119.88 -99°	-130.02 -145°	-153.21 159°

DATA SET E OF MUTUAL ADMITTANCE

- (1) The mutual admittance Y_{12} between two circumferential slots on an infinitely long cylinder is calculated from the

* UI asymptotic solution

The parameters are

*Cylinder: $R = 1\lambda, 2\lambda, 4\lambda, 10\lambda$

*Slot E: Circumferential

$a = 0.5\lambda$

$b = 0.2\lambda$

*Center-to-center distance between two slots is $(R\phi_o, z_o)$

- (2) Y_{12} is listed in (db value, phase in degree), where

db value = $20 \log_{10} (|Y_{12}| \text{ in mho})$

- (3) Data are presented in

TABLE E-1: $z_o = 0$, various ϕ_o and R

E-2: $z_o = 0.5\lambda$, various ϕ_o and R

E-3: $z_o = 1\lambda$, various ϕ_o and R

E-4: $z_o = 2\lambda$, various ϕ_o and R

E-5: $z_o = 4\lambda$, various ϕ_o and R

E-6: $z_o = 8\lambda$, various ϕ_o and R

E-7: Comparison of UI asymptotic and UI modal solutions

E-8: Comparison of UI asymptotic and UI modal solutions

Figure E-1: Mutual admittance Y_{12} between two circumferential slots as a function of ϕ_o .

E-2: Mutual admittance Y_{12} between two circumferential slots as a function of ϕ_o .

E-3: Mutual admittance Y_{12} between two circumferential slots as a function of ϕ_o .

E-4: Mutual admittance Y_{12} between two circumferential slots as a function of z_o .

E-5: Mutual admittance Y_{12} between two circumferential slots as a function of z_o .

TABLE E-1

UI ASYMPTOTIC SOLUTIONS OF Y_{12} OF SLOT E FOR $z_o = 0$

ϕ_o	$R = 1\lambda$	$R = 2\lambda$	$R = 4\lambda$	$R = 10\lambda$
30°	-73.94 7 $^\circ$	-91.47 153 $^\circ$	-105.83 121 $^\circ$	-124.96 52 $^\circ$
45°	-86.67 -110 $^\circ$	-102.35 -54 $^\circ$	-117.50 83 $^\circ$	-138.57 165 $^\circ$
60°	-95.31 140 $^\circ$	-111.28 101 $^\circ$	-127.44 49 $^\circ$	-149.93 77 $^\circ$

TABLE E-2

UI ASYMPTOTIC SOLUTIONS OF Y_{12} FOR $z_o = 0.5\lambda$

ϕ_o	$R = 1\lambda$	$R = 2\lambda$	$R = 4\lambda$	$R = 10\lambda$
0°	-67.67 ^{db} -117 ^o	-68.46 -114 ^o	-68.89 -112 ^o	-69.16 -111 ^o
10°	-69.00 -122 ^o	-72.97 -132 ^o	-81.72 170 ^o	-98.38 -146 ^o
20°	-72.67 -137 ^o	-82.21 164 ^o	-95.39 -39 ^o	-113.59 -49 ^o
30°	-77.77 -165 ^o	-90.67 64 ^o	-105.02 75 ^o	-124.52 32 ^o
45°	-85.89 130 ^o	-100.98 -116 ^o	-116.60 50 ^o	-138.17 150 ^o
60°	-93.37 47 ^o	-109.75 51 ^o	-126.60 20 ^o	-149.69 -90 ^o

TABLE E-3

UI ASYMPTOTIC SOLUTIONS OF Y_{12} FOR $z_o = 1\lambda$

ϕ_o	$R = 1\lambda$	$R = 2\lambda$	$R = 4\lambda$	$R = 10\lambda$
0°	-72.28 db 68 $^\circ$	-73.34 73 $^\circ$	-73.92 76 $^\circ$	-74.28 78 $^\circ$
10°	-72.91 64 $^\circ$	-75.33 55 $^\circ$	-80.15 9 $^\circ$	-94.52 105 $^\circ$
20°	-74.71 49 $^\circ$	-80.31 3 $^\circ$	-91.02 -161 $^\circ$	-110.75 -116 $^\circ$
30°	-77.44 26 $^\circ$	-86.49 -76 $^\circ$	-100.56 -20 $^\circ$	-122.14 -18 $^\circ$
45°	-82.65 -24 $^\circ$	-95.69 132 $^\circ$	-112.38 -22 $^\circ$	-136.13 111 $^\circ$
60°	-88.42 -90 $^\circ$	-104.13 -42 $^\circ$	-122.57 -41 $^\circ$	-148.13 -124 $^\circ$

TABLE E-4

UI ASYMPTOTIC SOLUTIONS OF Y_{12} FOR $z_o = 2\lambda$

ϕ_o	$R = 1\lambda$	$R = 2\lambda$	$R = 4\lambda$	$R = 10\lambda$
0°	-77.24 db 70 $^\circ$	-78.67 76 $^\circ$	-79.46 80 $^\circ$	-79.96 82 $^\circ$
10°	-77.52 67 $^\circ$	-79.44 65 $^\circ$	-81.77 37 $^\circ$	-89.55 -148 $^\circ$
20°	-78.37 57 $^\circ$	-81.60 31 $^\circ$	-87.38 -79 $^\circ$	-103.31 76 $^\circ$
30°	-79.73 42 $^\circ$	-84.81 -21 $^\circ$	-94.18 112 $^\circ$	-114.68 -144 $^\circ$
45°	-82.59 9 $^\circ$	-90.76 -130 $^\circ$	-104.37 162 $^\circ$	-128.88 15 $^\circ$
60°	-86.17 -35 $^\circ$	-97.24 94 $^\circ$	-113.88 177 $^\circ$	-141.23 153 $^\circ$

TABLE E-5

UI ASYMPTOTIC SOLUTIONS OF Y_{12} FOR $z_o = 4\lambda$

ϕ_o	$R = 1\lambda$	$R = 2\lambda$	$R = 4\lambda$	$R = 10\lambda$
0°	-82.10 db 68 ^o	-84.01 75 ^o	-85.10 81 ^o	-85.78 84 ^o
10°	-82.26 67 ^o	-82.26 67 ^o	-85.97 57 ^o	-89.37 -49 ^o
20°	-82.73 61 ^o	-82.73 61 ^o	-88.41 -10 ^o	-97.35 -37 ^o
30°	-83.51 52 ^o	-83.51 52 ^o	-92.03 -116 ^o	-106.24 -149 ^o
45°	-85.21 32 ^o	-85.21 32 ^o	-98.74 26 ^o	-118.99 -108 ^o
60°	-87.48 5 ^o	-87.48 5 ^o	-106.08 117 ^o	-130.69 -58 ^o

TABLE E-6

UI ASYMPTOTIC SOLUTIONS OF Y_{12} FOR $z_o = 8\lambda$

ϕ_o	$R = 1\lambda$	$R = 2\lambda$	$R = 4\lambda$	$R = 10\lambda$
0°	-86.70 db 66 $^\circ$	-89.18 73 $^\circ$	-90.65 80 $^\circ$	-91.60 85 $^\circ$
10°	-86.81 64 $^\circ$	-89.38 70 $^\circ$	-91.06 67 $^\circ$	-92.96 14 $^\circ$
20°	-87.12 61 $^\circ$	-89.97 60 $^\circ$	-92.26 31 $^\circ$	-96.69 171 $^\circ$
30°	-87.63 56 $^\circ$	-90.93 43 $^\circ$	-94.18 -28 $^\circ$	-101.98 -140 $^\circ$
45°	-88.77 44 $^\circ$	-93.03 5 $^\circ$	-98.14 -156 $^\circ$	-111.31 -35 $^\circ$
60°	-90.35 27 $^\circ$	-95.78 -45 $^\circ$	-102.98 34 $^\circ$	-121.14 -47 $^\circ$

TABLE E-7

COMPARISON OF UI ASYMPTOTIC AND UI MODAL SOLUTIONS

z_o	ϕ_o	$R = 1\lambda$		$R = 2\lambda$	
		Modal	Asym.	Modal	Asym
1λ	0°	-72.54 db 67 ⁰	-72.28 68 ⁰	-73.64 73 ⁰	-73.34 73 ⁰
	10°	-73.12 63 ⁰	-79.91 64 ⁰	-75.54 55 ⁰	-75.33 55 ⁰
	20°	-74.78 48 ⁰	-74.71 49 ⁰	-80.33 3 ⁰	-80.31 3 ⁰
	30°	-77.34 25 ⁰	-77.44 26 ⁰	-86.37 -77	-86.49 76 ⁰
	45°	-82.3 -26 ⁰	-82.65 -24 ⁰	-95.62 130 ⁰	-95.69 132 ⁰
	60°	-88.05 -91 ⁰	-88.42 -90 ⁰	-103.77 -41 ⁰	-104.13 -42 ⁰

TABLE E-8

COMPARISON OF UI ASYMPTOTIC AND UI MODAL SOLUTIONS

ϕ_0	z_0	R = 1λ		R = 2λ		Planar (Exact)
		Modal	Asym.	Modal	Asym.	
0°	0.5λ	-67.87 db -117°	-67.67 -117°	-68.69 -114°	-68.46 -114°	-69.35 -110°
	1λ	-72.54 67°	-72.28 68°	-73.64 73°	-73.34 73°	-74.52 79°
	2λ	-77.46 68°	-77.24 70°	-78.98 75°	-78.67 76°	-80.29 84°
	4λ	-82.22 66°	-82.10 68°	-84.3 75°	-84.01 75°	-86.25 87°
	8λ	-86.65 62°	-86.7 66°	-89.41 72°	-89.18 73°	-92.25 89°

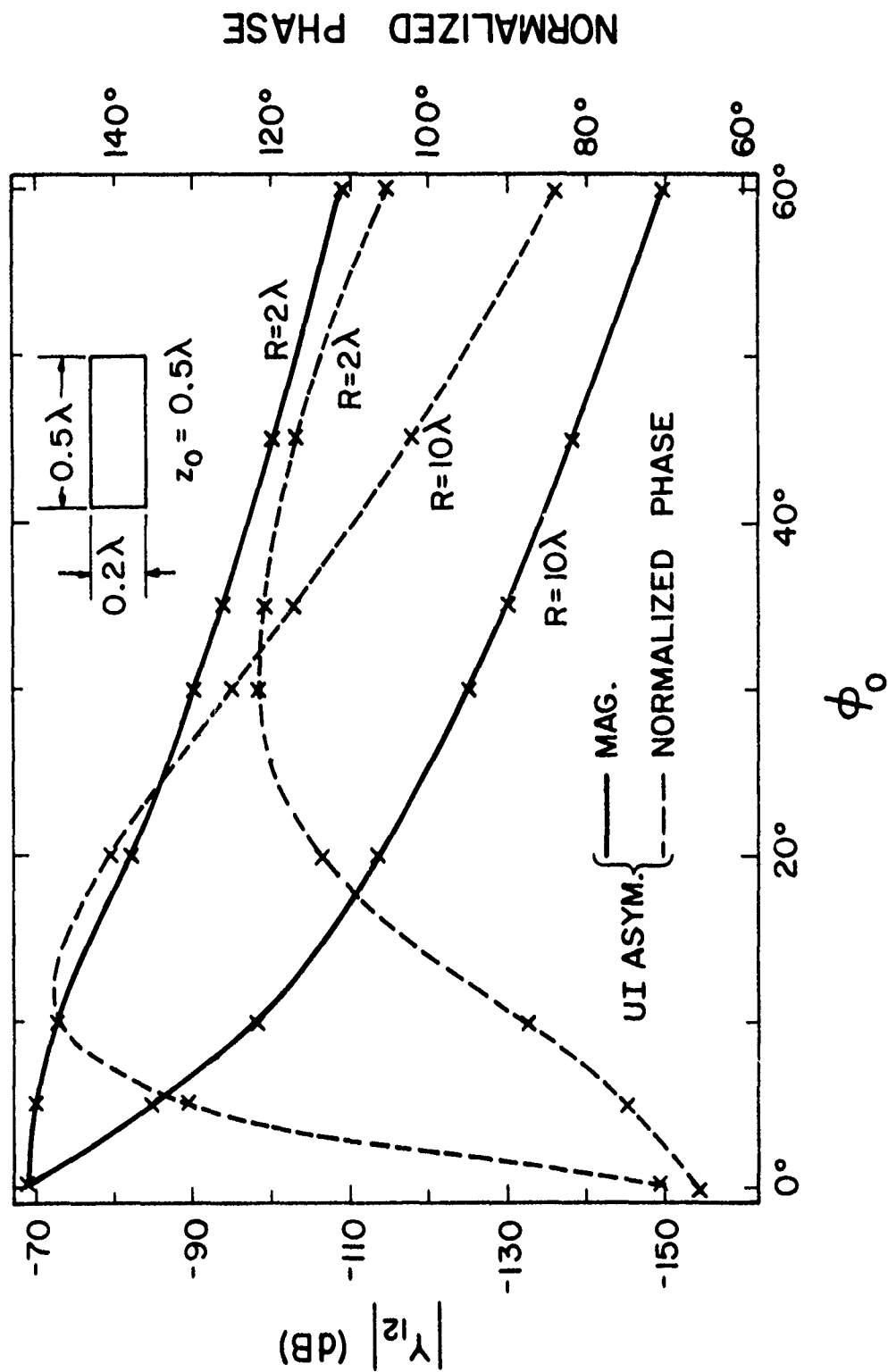


Figure E-1. Mutual admittance Y_{12} between two circumferential slots as a function of ϕ_0 .

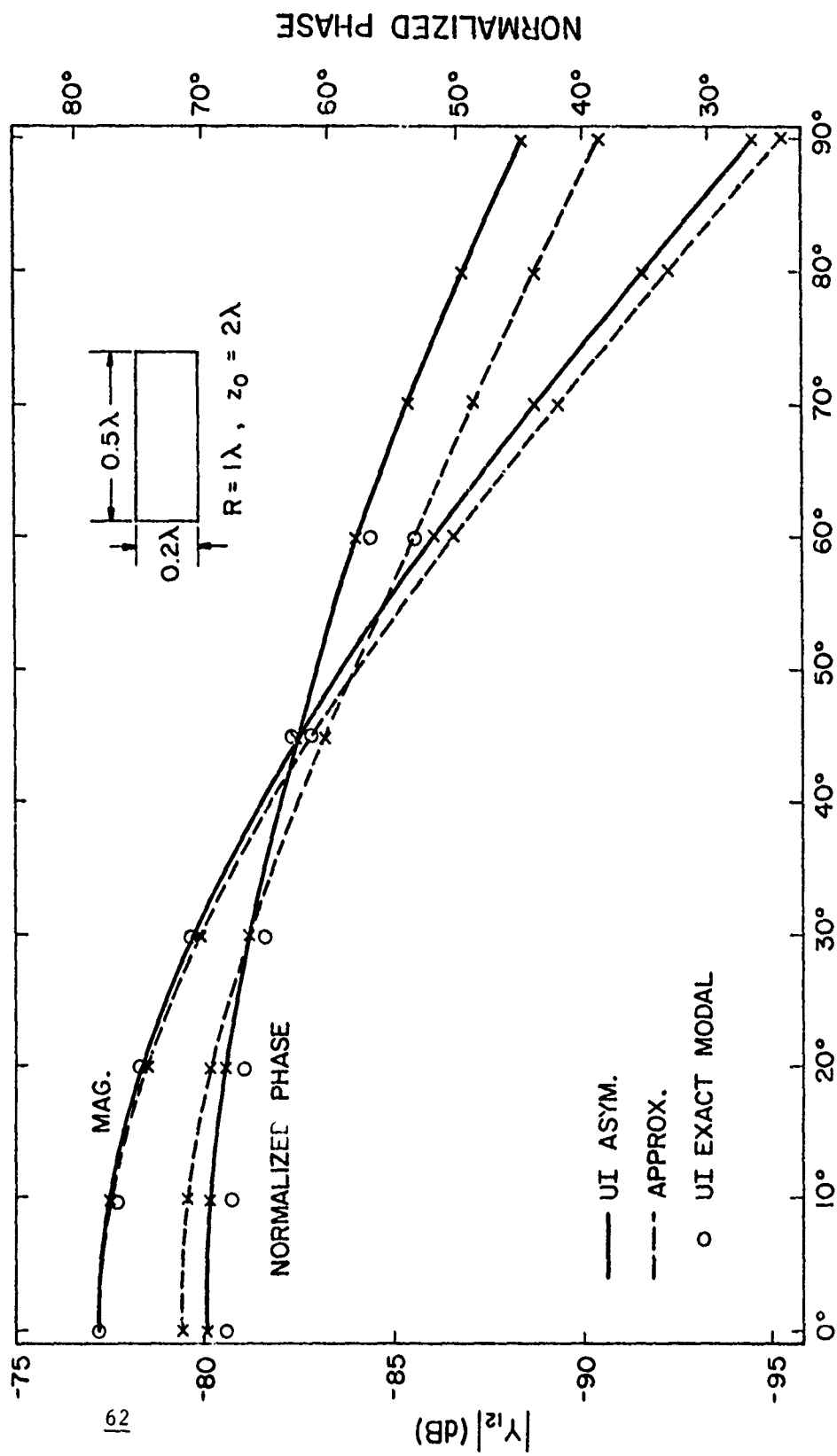


Figure E-2. Mutual admittance Y_{12} between two circumferential slots as a function of ϕ_0 .

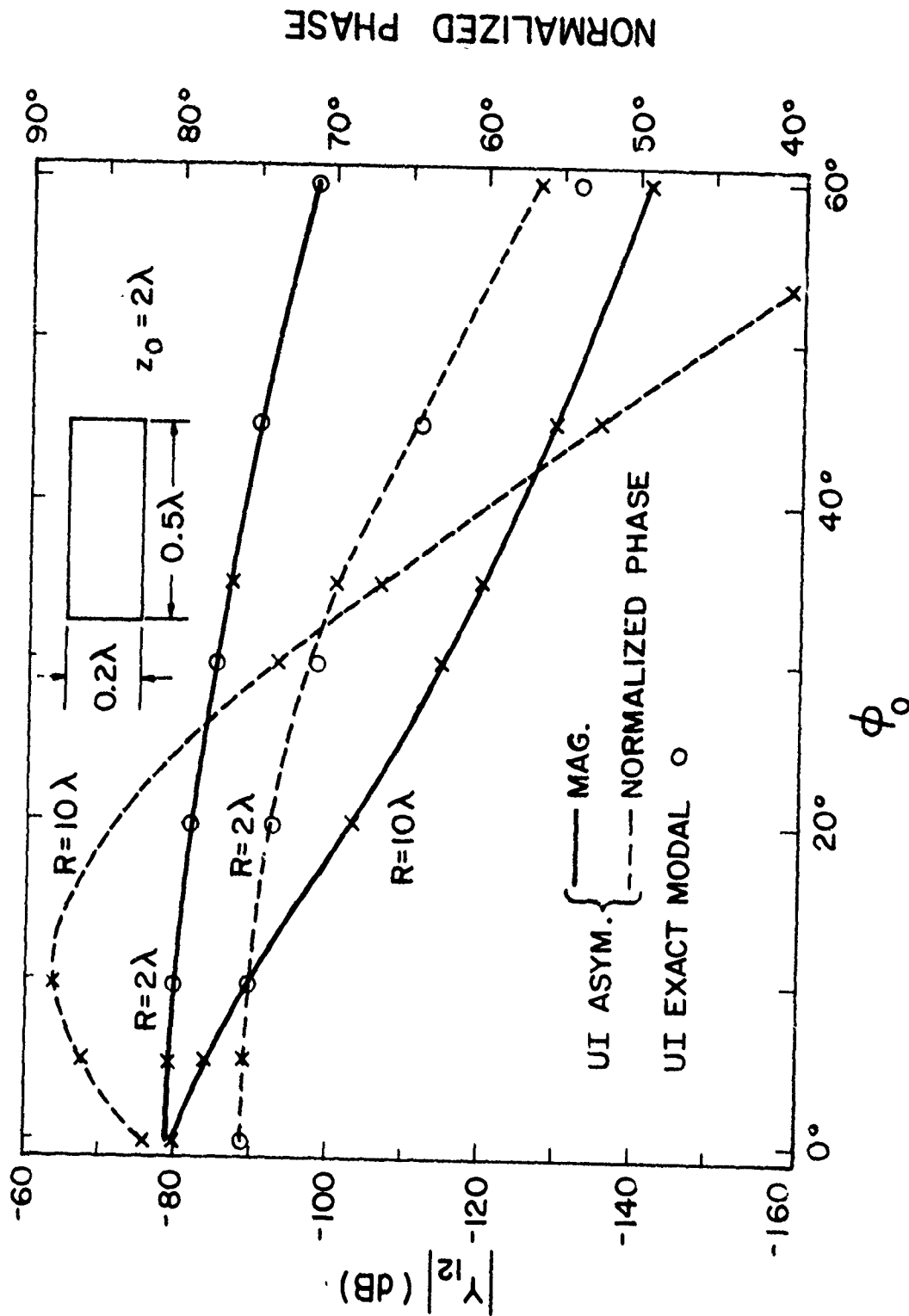


Figure E-3. Mutual admittance Y_{12} between two circumferential slots as a function of ϕ_0 .

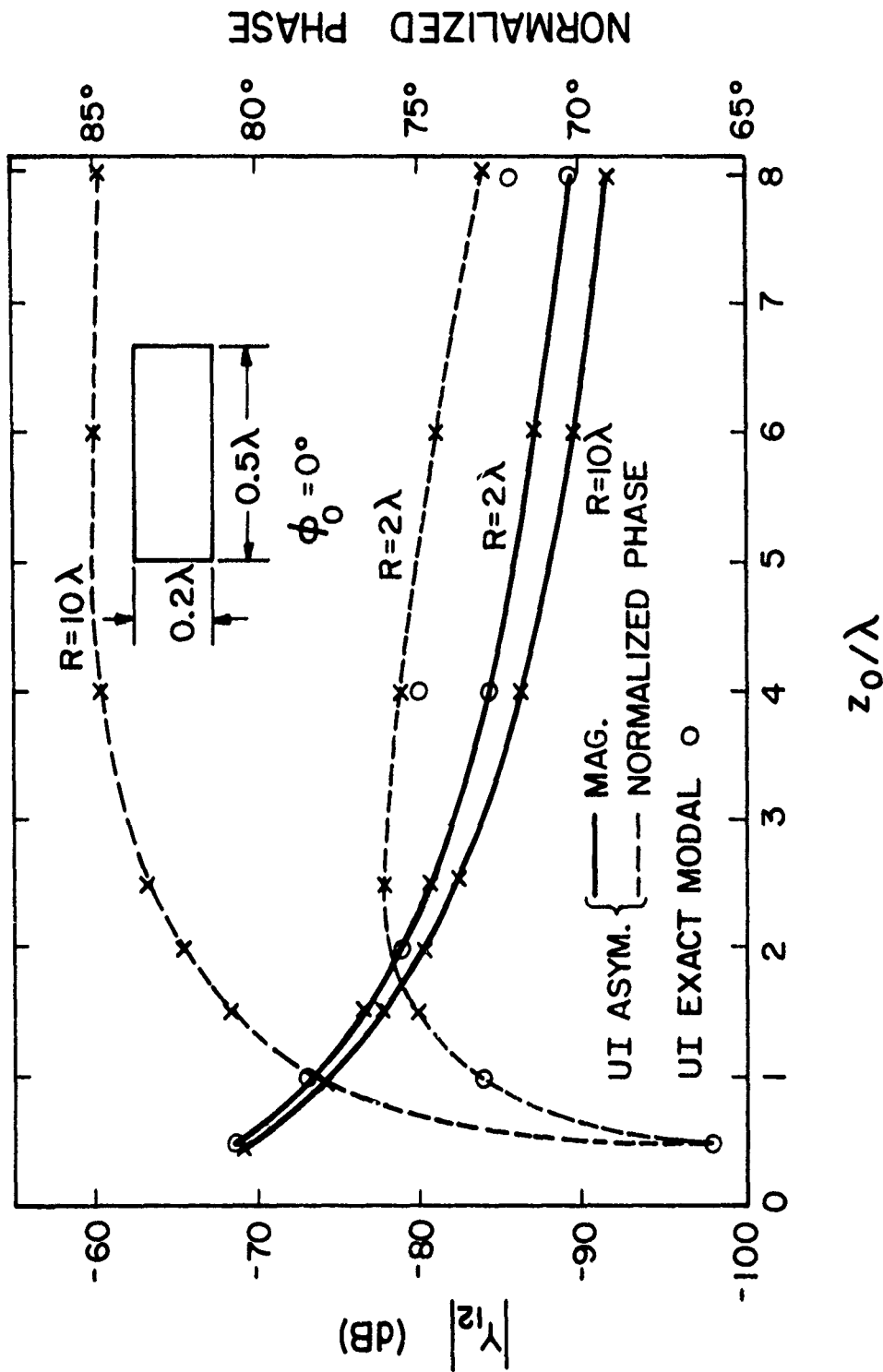


Figure E-4. Mutual admittance Y_{12} between two circumferential slots as a function of z_0 .

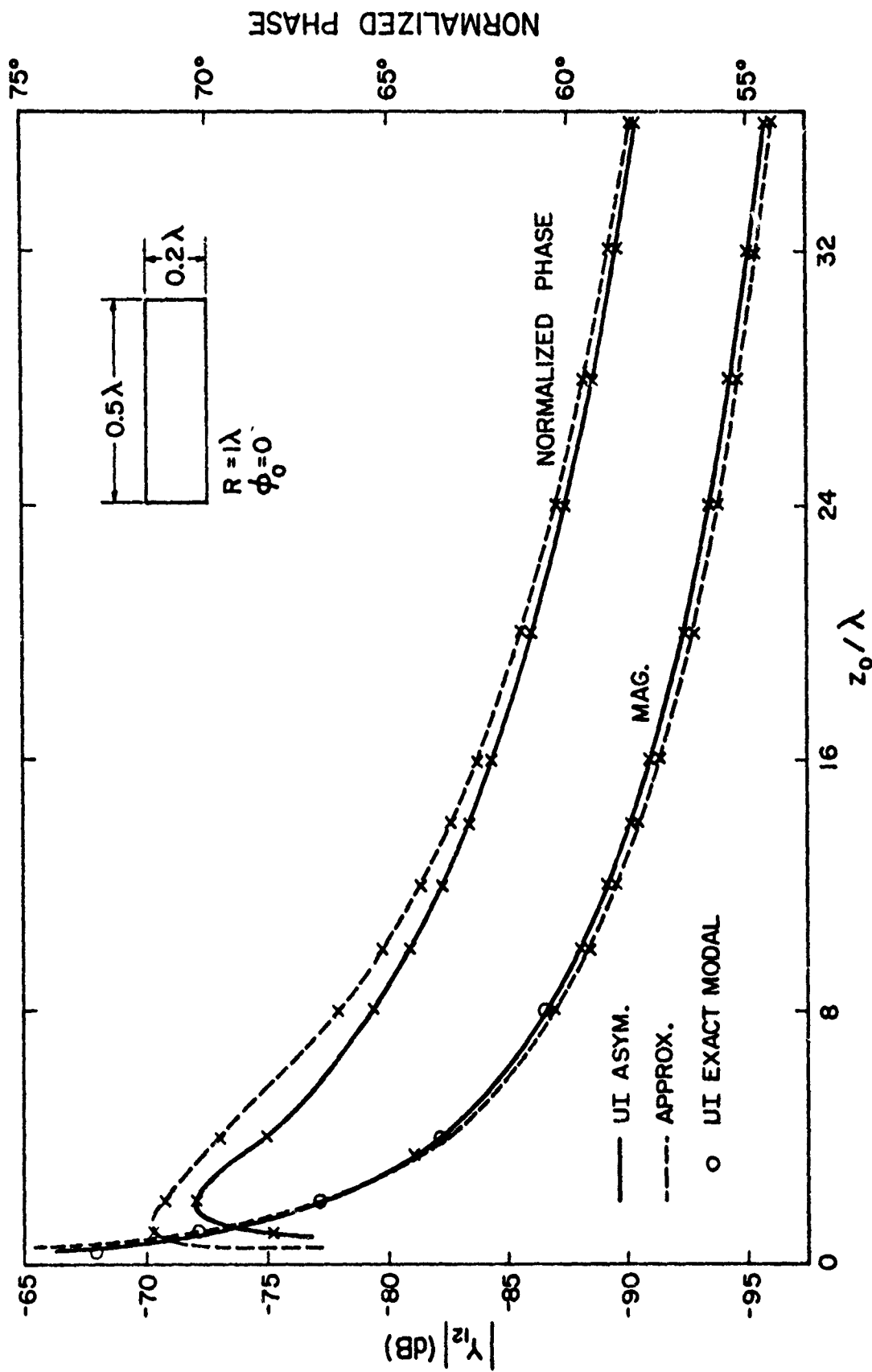


Figure E-5. Mutual admittance Y_{12} between two circumferential slots as a function of z_0 .

DATA SET F OF MUTUAL ADMITTANCE

- (1) The mutual admittance Y_{12} between two axial slots on an infinitely long cylinder is calculated from the

*UI asymptotic solution

The parameters are

*Cylinder: $R = 1\lambda, 2\lambda, 4\lambda, 10\lambda$

*Slot F: Axial

$$a = 0.2\lambda$$

$$b = 0.5\lambda$$

*Center-to-center distance between two slots is $(R\phi_0, z_0)$

- (2) Y_{12} is listed in (db value, phase in degree), where

$$\text{db value} = 20 \log_{10} (|Y_{12}| \text{ in mho}).$$

- (3) Data are presented in

TABLE F-1: $z_0 = 0$, various ϕ_0 and R

F-2: $z_0 = 0.5\lambda$, various ϕ_0 and R

F-3: $z_0 = 1\lambda$, various ϕ_0 and R

F-4: $z_0 = 2\lambda$, various ϕ_0 and R

F-5: $z_0 = 4\lambda$, various ϕ_0 and R

F-6: $z_0 = 8\lambda$, various ϕ_0 and R

F-7: Comparison of UI asymptotic and UI modal solutions

F-8: Comparison of UI asymptotic and UI modal solutions

F-9: Comparison of asymptotic solutions

Figure F-1: Mutual admittance Y_{12} between two axial slots as a function of ϕ_0 .

F-2: Mutual admittance Y_{12} between two axial slots as a function of ϕ_0 .

F-3: Mutual admittance Y_{12} between two axial slots as a function of ϕ_0 .

TABLE F-1

UI ASYMPTOTIC SOLUTIONS OF Y_{12} FOR $z_0 = 0$

ϕ_0	$R = 1\lambda$	$R = 2\lambda$	$R = 4\lambda$	$R = 10\lambda$
10°	-63.59 -120	-67.11 -660	-72.13 1780	-80.11 1670
20°	-67.13 -690	-72.57 1730	-78.93 -750	-88.04 -1100
30°	-70.46 -1310	-76.90 440	-83.98 260	-94.11 -320
45°	-74.93 1300	-82.36 -1540	-90.41 -60	-102.17 820
60°	-78.97 280	-87.25 60	-96.29 -390	-109.73 -1640

TABLE F-2

UI ASYMPTOTIC SOLUTIONS OF Y_{12} FOR $z_0 = 0.5\lambda$

ϕ_0	$R = 1\lambda$	$R = 2\lambda$	$R = 4\lambda$	$R = 10\lambda$
0°	-70.14 25° db	-70.11 25°	-70.10 25°	-70.09 26°
10°	-74.24 20°	-76.61 94°	-77.20 139°	-81.28 144°
20°	-76.84 101°	-77.58 133°	-80.64 102°	-88.34 123°
30°	-77.48 112°	-79.63 10°	-84.79 6°	-94.24 41°
45°	-79.13 90°	-83.71 179°	-90.78 19°	-102.22 77°
60°	-81.68 6°	-88.04 14°	-96.49 50°	-109.76 168°

TABLE F-3

UI ASYMPTOTIC SOLUTIONS OF Y_{12} FOR $z_o = 1\lambda$

ϕ_o	$R = 1\lambda$	$R = 2\lambda$	$R = 4\lambda$	$R = 10\lambda$
0°	-86.65 db -173 $^\circ$	-86.63 -172 $^\circ$	-86.61 -172 $^\circ$	-86.60 -172 $^\circ$
10°	-87.35 172 $^\circ$	-87.92 134 $^\circ$	-86.18 33 $^\circ$	-84.30 78 $^\circ$
20°	-88.37 128 $^\circ$	-86.51 26 $^\circ$	-84.78 -180 $^\circ$	-89.22 -160 $^\circ$
30°	-88.07 70 $^\circ$	-85.53 -81 $^\circ$	-86.95 -51 $^\circ$	-94.63 -66 $^\circ$
45°	-87.12 -15 $^\circ$	-87.09 109 $^\circ$	-91.80 -60 $^\circ$	-102.39 60 $^\circ$
60°	-87.51 -99 $^\circ$	-90.13 -72 $^\circ$	-97.06 -81 $^\circ$	-109.84 179 $^\circ$

TABLE F-4

UI ASYMPTOTIC SOLUTIONS OF Y_{12} FOR $z_o = 2\lambda$

ϕ_o	$R = 1\lambda$	$R = 2\lambda$	$R = 4\lambda$	$R = 10\lambda$
0°	-99.37 ₀ db -177 ₀	-99.34 ₀ -176 ₀	-99.33 ₀ -176 ₀	-99.33 ₀ -176 ₀
10°	-99.72 ₀ 176 ₀	-100.00 ₀ 157 ₀	-98.96 ₀ 93 ₀	-92.20 ₀ -144 ₀
20°	-100.48 ₀ 152 ₀	-99.39 ₀ 85 ₀	-94.33 ₀ -67 ₀	-92.24 ₀ 62 ₀
30°	-100.83 ₀ 115 ₀	-97.05 ₀ 4 ₀	-93.13 ₀ 109 ₀	-96.09 ₀ -163 ₀
45°	-99.82 ₀ 49 ₀	-95.40 ₀ -126 ₀	-95.21 ₀ 150 ₀	-103.04 ₀ -7 ₀
60°	-98.70 ₀ -15 ₀	-96.10 ₀ 89 ₀	-99.12 ₀ 161 ₀	-110.19 ₀ 129 ₀

TABLE F-5

UI ASYMPTOTIC SOLUTIONS OF Y_{12} FOR $z_o = 4\lambda$

ϕ_o	$R = 1\lambda$	$R = 2\lambda$	$R = 4\lambda$	$R = 10\lambda$
0°	-111.56 db -178 $^\circ$	-111.54 -178 $^\circ$	-111.53 -178 $^\circ$	-111.52 -178 $^\circ$
10°	-111.78 177 $^\circ$	-111.97 168 $^\circ$	-111.81 132 $^\circ$	-105.41 -27 $^\circ$
20°	-112.38 164 $^\circ$	-112.36 126 $^\circ$	-108.23 21 $^\circ$	-100.03 -35 $^\circ$
30°	-113.06 143 $^\circ$	-111.16 67 $^\circ$	-104.80 -104 $^\circ$	-100.65 -154 $^\circ$
45°	-113.38 97 $^\circ$	-108.48 -24 $^\circ$	-103.49 28 $^\circ$	-105.31 100 $^\circ$
60°	-112.64 47 $^\circ$	-107.29 -123 $^\circ$	-104.94 114 $^\circ$	-111.46 -67 $^\circ$

TABLE F-6

UI ASYMPTOTIC SOLUTIONS OF Y_{12} FOR $z_o = 8\lambda$

ϕ_o	$R = 1\lambda$	$R = 2\lambda$	$R = 4\lambda$	$R = 10\lambda$
0°	-123.63 db -179 ₀	-123.61 -179 ₀	-123.61 -179 ₀	-123.60 -179 ₀
10°	-123.78 -178 ₀	-123.92 173 ₀	-124.05 155 ₀	-120.63 54 ₀
20°	-124.23 171 ₀	-124.56 150 ₀	-122.90 83 ₀	-113.13 -178 ₀
30°	-124.87 159 ₀	-124.73 113 ₀	-119.69 -2 ₀	-110.52 -137 ₀
45°	-125.87 131 ₀	-123.26 46 ₀	-116.53 -145 ₀	-111.57 -36 ₀
60°	-126.32 94 ₀	-121.57 -21 ₀	-115.88 38 ₀	-115.46 -50 ₀

TABLE F-7

COMPARISON OF UI ASYMPTOTIC AND UI MODAL SOLUTIONS

z_o	ϕ_o	$R = 1\lambda$		$R = 2\lambda$	
		Modal	Asym.	Modal	Asym.
1λ	0°	-87.06 db -171 $^\circ$	-86.65 -173 $^\circ$	-86.83 -172 $^\circ$	-86.63 -172 $^\circ$
	10°	-87.69 176 $^\circ$	-87.35 172 $^\circ$	-88.23 139 $^\circ$	-87.92 134 $^\circ$
	20°	-88.91 139 $^\circ$	-88.37 128 $^\circ$	-87.64 35 $^\circ$	-86.51 26 $^\circ$
	30°	-89.40 85 $^\circ$	-88.07 70 $^\circ$	-87.01 -72 $^\circ$	-85.77 -81 $^\circ$
	45°	-89.19 2 $^\circ$	-87.32 -15 $^\circ$	-88.67 119 $^\circ$	-87.30 109 $^\circ$
	60°	-89.84 -83 $^\circ$	-87.72 -99 $^\circ$	-91.86 -61 $^\circ$	-90.36 -72 $^\circ$

TABLE F-8

COMPARISON OF UI ASYMPTOTIC AND UI MODAL SOLUTIONS

ϕ_0	z_0	R = 1λ		R = 2λ		Plan. (Exact)
		Modal	Asym.	Modal	Asym.	
0°	0.5λ	--	-70.14_{25}° db	--	-70.11_{25}°	-70.08_{26}°
	1λ	-87.06_{-171}°	-86.65_{-173}°	-86.83_{-172}°	-86.63_{-172}°	-86.6_{-172}°
	2λ	-99.97_{-174}°	-99.37_{-177}°	-99.61_{-176}°	-99.34_{-176}°	-99.32_{-176}°
	4λ	-112.43_{-175}°	-111.56_{-178}°	-111.93_{-177}°	-111.54_{-178}°	-111.52_{-178}°
	8λ	-124.33_{-174}°	-123.63_{-179}°	-124.12_{-177}°	-123.61_{-179}°	-123.60_{-179}°

TABLE F-9
COMPARISON OF ASYMPTOTIC SOLUTIONS

z_0	ϕ_0	$R = 2\lambda$			$R = 10\lambda$		
		UI Asym.	PINY	OSU	UI Asym.	PINY	OSU
2λ	0°	-99.34 db	-99.42	-105.44	-99.33	-99.41	-105.42
		-176°	-172°	-172°	-176°	-172°	-172°
	10°	-100.00	-99.93	-105.37	-92.2	-92.51	-92.53
		157°	164°	152°	-144°	-142°	-143°
	20°	-99.39	-99.71	-101.89	-92.24	-92.46	-92.45
		85°	98°	78°	62°	64°	65°
	30°	-97.05	-97.85	-98.23	-96.09	-96.30	-96.30
		4°	17°	4°	-163°	-161°	-160°
	45°	-95.40	-96.16	-96.09	-103.04	-103.25	-103.25
		-126°	-115°	-120°	-7°	-5°	-4°
	60°	-96.10	-96.68	-96.6	-110.19	-110.41	-110.41
		89°	97°	96°	129°	131°	131°

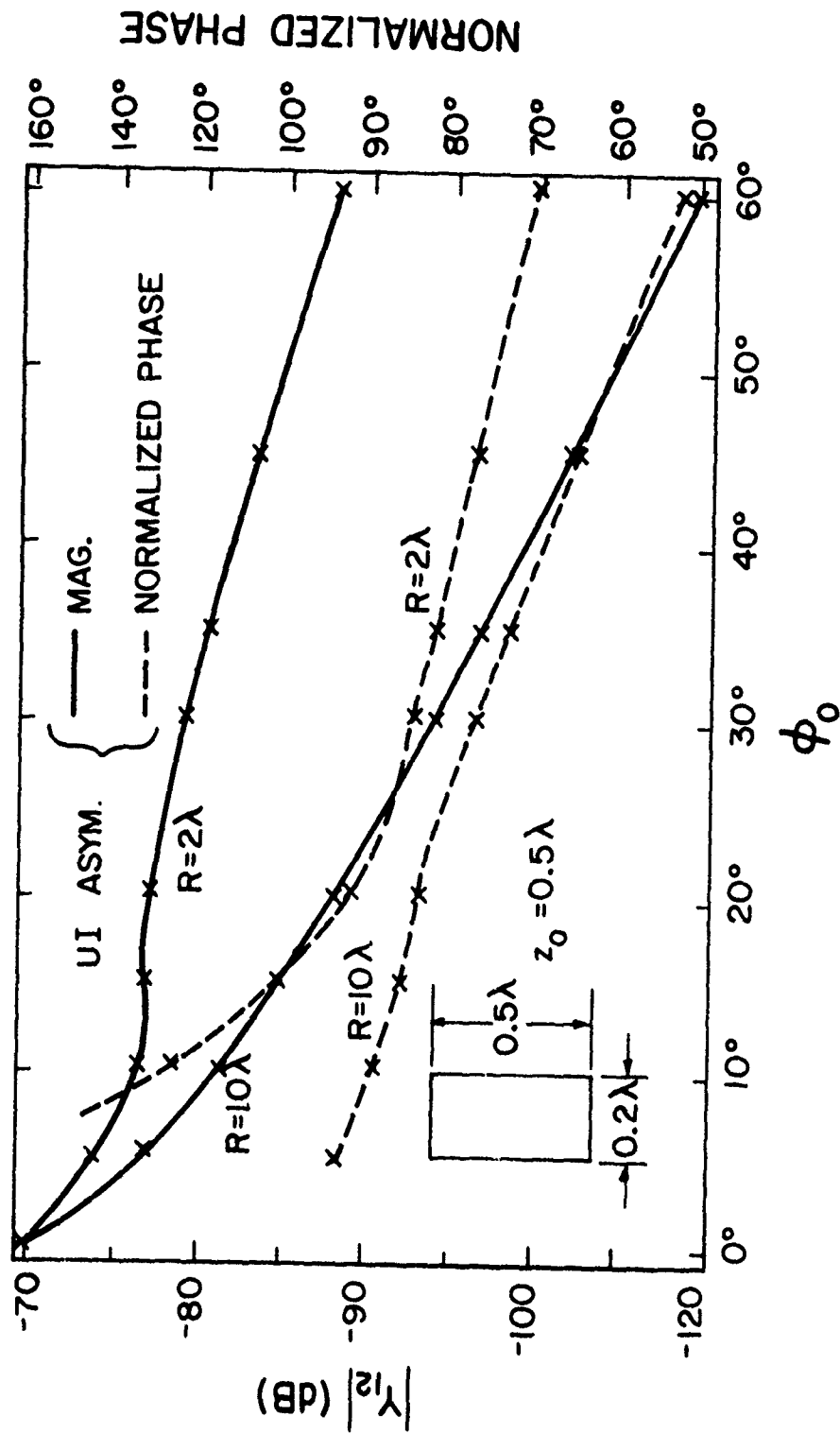


Figure F-1: Mutual admittance Y_{12} between two axial slots as a function of ϕ_0 .

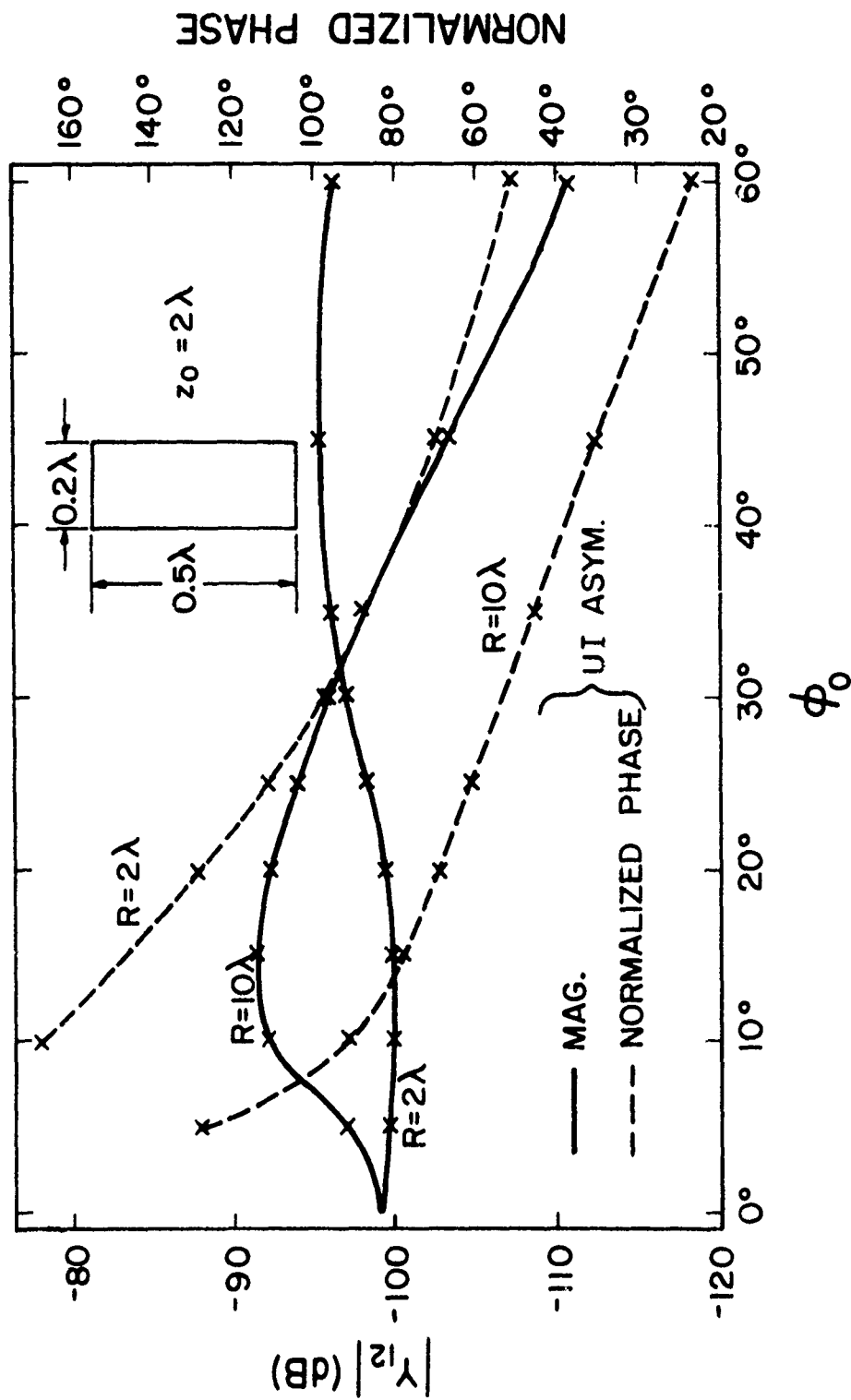


Figure F-2: Mutual admittance Y_{12} between two axial slots as a function of ϕ_0 .

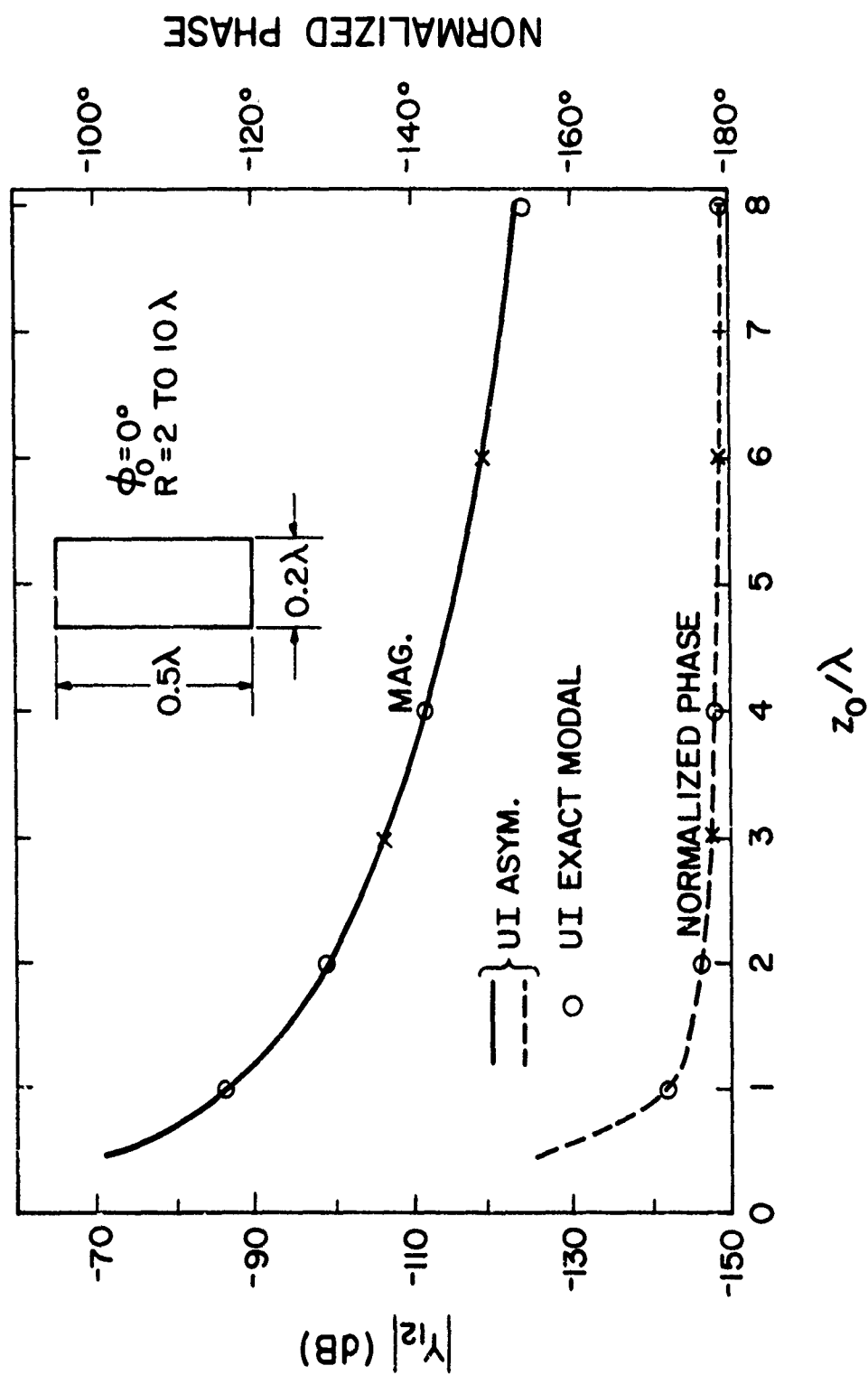


Figure F-3: Mutual admittance Y_{12} between two axial slots as a function of z_0 .

APPENDIX B: COMPUTER PROGRAM LISTING

This appendix contains the program listing of all solutions, except the exact Hughes modal solution, discussed in the text.

BEST AVAILABLE COPY

PROGRAM CYORPL (INPUT, TAPE 6, OUTPUT, TAPE 7=OUTPUT, TAPE 5=INPUT)

```
*****
*
*   MUTUAL ADMITTANCE OF SLOTS ON A CYLINDER OR PLANE
*   =====
*
*
*   BY:   S. W. LEE
*         S. SAFAVI-NAINI
*         P. CHANG
*         C. L. LAW
*
*
*   DATE:   8/10/77
*
*
*   UNIVERSITY OF ILLINOIS
*
*****
```

C THIS IS A MODIFIED VERSION OF THE PROGRAMS SOLVING MUTUAL
C ADMITTANCE OF SLOTS ON A CYLINDER OR ON A PLANE.
C THIS PROGRAM IS MODIFIED TO RUN UNDER CDC CYBER 170 SERIES
C COMPUTER SYSTEMS.

C THE ORIGINAL VERSION WAS REPORTED IN "ELECTROMAGNETICS
C LABORATORY TECHNICAL REPORT NO. 77-8" DATE: MARCH 1977.

C THIS PROGRAM CONTAINS THE FOLLOWING SUBPROGRAMS:

C (1) PLANAR
C 1A) EXACT (PLANAR)
C 1B) APPROXIMATE (APROX1 & APROX2)

C (2) CYLINDRICAL
C 2A) UI ASYMPTOTIC (CYLIND)
C 2B) UI EXACT MODAL (PROG1 & PROG2)
C 2C) OSU ASYMPTOTIC (CYLIND)
C 2D) PINY ASYMPTOTIC (CYLIND)
C 2E) APPROXIMATE (APROX1 & APROX2)
C 2F) UI(2) ASYMPTOTIC (CYLIND)

C EACH SUBPROGRAM IS A SUBROUTINE TO THE MAIN PROGRAM.

CC

C

BEST AVAILABLE COPY

```

C THE INPUT FORMAT IS AS FOLLOW :
C
C
C --(1)/(2)
C --1A/1B/2A/2B/2C/2D/2E/2F
C --AXIAL/CIRCUMFERENTIAL
C --FREQUENCY
C --SLOT DIMENSION (A,B)
C
C IF USING APPROXIMATE OR UI EXACT MODAL JUMP TO
C THE NEXT SECTION
C --INTEGRATION GRID (IPA,IPB)
C
C IF USING OTHER THAN UI EXACT MODAL JUMP TO THE NEXT SECTION
C (UI EXACT MODAL IS USING TRAPEZOIDAL RULE FOR INTEGRATION.
C NCYCLE=NO. OF SUBSECTIONS BETWEEN ANY TWO SUCCESSIVE ZEROS
C OF INTEGRAND
C MMAX IS THE MAXIMUM NO. OF TERMS WHICH HAS BEEN USED IN
C CALCULATION OF INFINITE SERIES)
C --NCYCLE,MMAX
C
C THE NORMALIZATION FACTOR (Y11)
C --NORMALIZATION FACTOR
C
C INPUT Z0
C --TOTAL NO. OF ELEMENTS IN Z0 (MMAX.=20)
C --Z0(1)
C --Z0(2)
C --
C
C IF USING PLANAR "(1)" INPUT THE FOLLOWING ,IF NOT
C JUMP TO THE NEXT SECTION
C --TOTAL NO. OF ELEMENTS IN Y0 (MAX.=20)
C --Y0(1)
C --Y0(2)
C --
C
C IF USING CYLINDER "(2)" INPUT THE FOLLOWING;
C --TOTAL NO. OF ELEMENTS IN PHI (MAX.=20)
C --PHI(1)
C --PHI(2)
C --
C --TOTAL NO. OF ELEMENTS IN RADIUS (MAX.=20)
C --RADIUS(1)
C --RADIUS(2)
C --
C
CCCCCCCCCCCCCCCCCCCCCCCCCCCCCCCCCCCCCCCCCCCCCCCCCCCCCCCCCCCC
IMPLICIT COMPLEX (C,H,Z),REAL(A-B,D-G,P-Y)
REAL PHI(20),RADIUS(20),Z(20),YP(20)
REAL TN(10),TNPI(10)
INTEGER PINY,OSU,UI,TEST

```

##FORMAT##

* A10
* 2A10
* A10
* G15.0
* 2G15.0

* 2I5

* 2I5

* G15.0

* I2
* G15.0
* G15.0
* G15.0

* I2
* G15.0
* G15.0
* G15.0

* I2
* G15.0
* G15.0
* G15.0
* I2
* G15.0
* G15.0
* G15.0

BEST AVAILABLE COPY

```

LOGICAL CUM,AXIAL
REAL MAG,Z0
REAL CONF,CONF1,CONF2,K0,Z0
COMMON FI,TZ1,TZ2,TY1,TY2,R,THETHA
COMMON/DATA1/TN,TNFI,RH0,C1,C2,F2,IOP,CC,RADN,DEG
COMMON/DATA4/AC02,SN2,TN2,R2,ACON1,ACON2,C01,C10
COMMON/DATA2/A0,B0,Z0,Y0
COMMON/DATA3/K0,NCYCLE,PHIO,Z0,Y11,MMAX,A,B
DATA TN/2.33811,4.08795,5.52154,6.78671,7.99417,
$          9.02265,10.04017,11.00852,11.93602,12.82878/
DATA TNFI/1.01879,3.24820,4.82010,6.16331,7.37218,
$          8.48849,9.53545,10.52766,11.47506,12.38479/
DATA UI/0/,OSU/0/,PINY/0/,TYPE1/10HEXACT /,
$      PRO2/10HCYLINDRICA/,PRO1/10HPLANAR /,
$      TYPE2/10HAPPROXIMAT/,TYPE3/10HUI EXACT M/,
$      TYPE4/10HUI ASYMPTO/,TYPE5/10HOSU ASYMPT/,
$      TYPE6/10HPINY ASYMP/,TYPE7/10HUI(2) ASYM/,
$      CONF1/10HAXIAL /,CONF2/10HCIRCUMFERE/
DATA IPAA/1/,IPBB/1/
PI=4*ATAN(1.E0)
RADN=PI/180. $      DEG=180./PI
ACON1=187./64. $      ACON2=2./3.
C01=(0.,1.) $      C10=(1.,0.)
WRITE(6,555)
READ(5,9099)PRO
9099  FORMAT(A10)
      IF(PRO.EQ.PRO1)GOTO 8082
      IF(PRO.EQ.PRO2)GOTO 8083
      WRITE(7,8084)
      STOP
8083  IPLAN=2
      WRITE(6,566)
      GOTO8093
8082  IPLAN=1
      WRITE(6,777)
8093  READ(5,8081)TYPE,TYPEE
      READ(5,9099)CONF
      READ(5,8086)XK
      READ(5,8087)AA,BB
8087  FORMAT(2G15.0)
      IF(TYPE.EQ.TYPE1)GOTO 8097
      IF(TYPE.EQ.TYPE2)GOTO 8099
      IF(TYPE.EQ.TYPE3)GOTO 9000
      IF(TYPE.EQ.TYPE4)GOTO 8097
      IF(TYPE.EQ.TYPE5)GOTO 8097
      IF(TYPE.EQ.TYPE6)GOTO 8097
      IF(TYPE.EQ.TYPE7)GOTO 8097
      WRITE(7,8084)
      STOP
9000  READ(5,8098)NCYCLE,MMAX
      GOTO 8099
8097  READ(5,8098)IPAA,IPBB

```

BEST AVAILABLE COPY

```

8099 READ(5,8086)Y11
      ZY1=CMPLX(Y11,0.E0)
      READ(5,8091)NDZ
      DO 8092 I=1,NDZ
8092  READ(5,8086)Z(I)
      IF(IPLAN.LT.2)GOTO 2230
      READ(5,8091)NDPHI
      DO 8095 I=1,NDPHI
8095  READ(5,8086)PHI(I)
      READ(5,8091)NDR
      DO 8094 I=1,NDR
8094  READ(5,8086)RADIUS(I)
      GOTO 8096
2230  READ(5,8091)NDY
      DO 8089 I=1,NDY
8089  READ(5,8086)YP(I)
8096  IF(CONF1.EQ.CONF)GOTO 9092
      AXIAL=.FALSE.
      CUM=.TRUE.
      GOTO 9093
9092  AXIAL=.TRUE.
      CUM=.FALSE.
9093  WRITE(6,555)
      WRITE(6,771)TYPE,TYPEE
771  FORMAT(//1X,20(" ")/1X,""/1X,"",3X,"METHOD OF SOLUTION : "
$      ,4X,2A10/1X,""/1X,20(" "))
      WRITE(6,772)
772  FORMAT(/1X,20(" ")/1X,"")
773  FORMAT(1X,""/1X,20(" "))
      WRITE(6,888)XK
888  FORMAT(1X,"",3X,"FREQUENCY :  K= ",E14.6)
      WRITE(6,773)
      WRITE(6,772)
      IF(IPLAN.EQ.1)GOTO 113
      WRITE(6,999)PRO2
999  FORMAT(1X,"",3X,"GOMETRY :  ",A10)
      GOTO 112
113  WRITE(6,999)PRO1
112  WRITE(6,773)
      WRITE(6,772)
      WRITE(6,111)AA,BB
111  FORMAT(1X,"",3X,"SLOT DIMENSION :  A(ALONG PH)= ",F8.5,
$      " ;  B(ALONG Z)= ",F8.5)
      WRITE(6,773)
      WRITE(6,772)
      IF(CONF.EQ.CONF1)GOTO 114
      WRITE(6,333)
333  FORMAT(1X,"",3X,"SLOT ORIENTATION :  CIRCUMFERENTIAL ")
      GOTO 115
114  WRITE(6,444)
444  FORMAT(1X,"",3X,"SLOT ORIENTATION :  AXIAL ")
115  WRITE(6,773)

```

BEST AVAILABLE COPY

```

      IF (TYPE.EQ.TYPE2)GOTO 774
      WRITE(6,772)
      IF (TYPE.EQ.TYPE3)GOTO 775
      WRITE(6,99)IPAA,IPRB
99    FORMAT(1X,"*",3X,"INTEGRATION GRID : ",I3," X",I3)
      GOTO 776
775   WRITE(6,881)NCYCLE,MMAX
881   FORMAT(1X,"*",3X,"NCYCLE= ",I5,"          ;          MMAX= ",I5)
776   WRITE(6,773)
774   WRITE(6,772)
      WRITE(6,882)Y11
882   FORMAT(1X,"*",3X,"NORMALIZATION FACTOR : Y11= ",F7.2)
      WRITE(6,773)
      WRITE(6,883)
883   FORMAT(///10X,"$$$$$ DATA OUTPUT $$$$$$/")
884   FORMAT(/2X,"PHI= ",F7.2," <DEG>          ;          ZO= ",F7.3,
$      "          ;          RADIUS= ",E14.5)
885   FORMAT(/2X,"          Y= ",F9.4,"          ;          Z= ",F7.3)
      IF (TYPE.EQ.TYPE3)GOTO 9095
      IF (TYPE.EQ.TYPE4)IOP=1
      IF (TYPE.EQ.TYPE5)IOP=2
      IF (TYPE.EQ.TYPE6)IOP=3
      IF (TYPE.EQ.TYPE7)IOP=4
      IF (CUM)GOTO 9094
      A=BB
      B=AA
      IPA=IPRB
      IPR=IPAA
      GOTO 9091
9094  A=AA
      B=BB
      IPA=IPAA
      IPR=IPRB
      GOTO 9091
9095  A=AA $ B=BB $ KO=XK
      DO 9096 I=1,NOR
      RHO=RADIUS(I)
      DO 9096 II=1,NDZ
      ZO=Z(II)
      DO 9096 III=1,NDFHI
      PHIO=PHI(III)*RADN
      WRITE(6,884)PHI(III),ZO,RHO
      IF (CONF1.EQ.CONF)GOTO 9097
      CALL PROG2(RHO,MAG,PHASE,DB,PHN)
      GOTO 9096
9097  CALL PROG1(RHO,MAG,PHASE,DB,PHN)
9096  WRITE(6,78)MAG,PHASE,DB,PHN
      STOP
8081  FORMAT(A10,A10)
8084  FORMAT(5X,"$$$ ERROR $$$ ,PLEASE CHECK YOUR INPUT AGAIN")
8086  FORMAT(G15.0)
8091  FORMAT(I2)

```

BEST AVAILABLE COPY

```

8098  FORMAT(2I5)
C
9091  ICUM=1
      IAXIAL =2
      IF(.NOT.ICUM) ICUM=2
      IF(.NOT.IAXIAL) IAXIAL=1
      DO 30 IJ=ICUM,IAXIAL
      IF(IJ.EQ.2)GOTO 5
      AO=A*XXK
      BO=B*XXK
      GO TO 6
5     SAVE=A
      A=B
      R=SAVE
      AO=A*XXK
      BO=B*XXK
      ITEMP=IPB
      IPB=IPA
      IPA=ITEMP
6     WIDTH1=AO/IPA
      WIDTH2=BO/IPB
      C1=CEXP(CMPLX(0.E0,-PI/3.))
      C2=CEXP(CMPLX(0.E0,PI/4.))
      CC=C2**3
      F2=SQRT(PI)
      Y1=-AO/2.-WIDTH1/2.
      Z1=-BO/2.-WIDTH2/2.
      IF(IPLAN.EQ.1)GOTO 7
      GOTO 8
7     NDR=1
      RADIUS(1)=1.E20
8     CONTINUE
      DO 50 IRAD=1,NDR
      RHO=XK*RADIUS(IRAD)
      DO 60 JZ=1,NDZ
      ZO=Z(JZ)*XK
      IF(IPLAN.EQ.1) NDPHI=NDY
      DO 70 IY=1,NDPHI
      IF(IPLAN.EQ.1) GO TO 13
      YO=RHO*PHI(IY)*RADN
      IF(PHI(IY).EQ.0.0) YO=0.001
      Y=YO/XK
      GO TO 14
13    Y=YF(IY)
      YO=Y*XXK
14    CONTINUE
      IF(TYPE.EQ.TYPE2)GOTO 17
      Y2=YO-AO/2.-WIDTH1/2.
      Z2=ZO-BO/2.-WIDTH2/2.
      ZSUM=0.
      DO 80 K=1,IPA
      TY1=Y1+WIDTH1*K

```

BEST AVAILABLE COPY

```

DO 90 L=1,IPB
TZ1=Z1+WIDTH2*L
DO 100 M=1,IPA
TY2=Y2+WIDTH1*M
DO 110 N=1,IPB
TZ2=Z2+WIDTH2*N
R=SQRT((TY2-TY1)**2+(TZ2-TZ1)**2)
THETHA=ATAN2((TZ2-TZ1),(TY2-TY1))
ACOS2=COS(THETHA)**2
R2=R**2
IF(IPLAN.EQ.1) GO TO 600
SN2=SIN(THETHA)**2
TN2=TAN(THETHA)**2
CALL CYLIND(IJ,ZSUM)
GO TO 110
600 CALL PLANAR(IJ,ZSUM)
110 CONTINUE
100 CONTINUE
90 CONTINUE
80 CONTINUE
ZY2=ZSUM*(WIDTH1*WIDTH2)**2*(-2.)/(A0*B0)
IF(IPLAN.EQ.1)GOTO 26
WRITE(6,884)PHI(TY),Z(JZ),RADIUS(IRAD)
GOTO 18
26 WRITE(6,885)YP(IY),Z(JZ)
GOTO 18
17 IF(IPLAN.EQ.1)GOTO 15
WRITE(6,884)PHI(IY),Z(JZ),RADIUS(IRAD)
GOTO 19
15 WRITE(6,885)YP(IY),Z(JZ)
19 IF(CONF.EQ.CONF1)GOTO 16
CALL APROX1(A0,B0,Z0,Y0,PI,ZY2)
GOTO 18
16 CALL APROX2(A0,B0,Z0,Y0,PI,ZY2)
18 MAG=CABS(ZY2)
PHASE=ATAN2(AIMAG(ZY2),REAL(ZY2))*DEG
ZEXPON=CEXP(CMPLX(0,E0,SQRT(Y0**2+Z0**2)))
ZPROD=ZY2*ZEXPON
PHN=ATAN2(AIMAG(ZPROD),REAL(ZPROD))*DEG
DB=20.*ALOG10(CABS(ZY2/ZY1))
WRITE(6,78) MAG,PHASE,DB,PHN
70 CONTINUE
60 CONTINUE
IF(IPLAN.EQ.1) GO TO 30
50 CONTINUE
30 CONTINUE
78 FORMAT(1X,"Y12= ",E13.4," <MHO> ",F7.2," <DEG> ",5X,"DB= ",E12.5,
1 " ",
1 " NORM PHASE= ",F7.2," <DEG> ")
555 FORMAT(/10X,"*****")
666 FORMAT(10X," MUTUAL ADMITTANCE OF SLOTS ON A CYLINDER ")
777 FORMAT(10X," MUTUAL ADMITTANCE OF SLOTS ON A PLANE ")
STOP

```

BEST AVAILABLE COPY

END

BEST AVAILABLE COPY

```

SUBROUTINE APROX1(A0,B0,Z0,Y0,PI,ZY2)
IMPLICIT COMPLEX (C,H,Z),REAL(A-B,D-G,P-Y)
REAL TN(10),TNPI(10)
REAL KA,Z0
COMMON /DATA1/TN,TNPI,RHO,C1,C2,F2
COMMON /CF/CVF,CUF,CVIF,CVFF,CUPF
THETHA=ATAN2(Z0,Y0)
IF (THETHA.GE.89.99*PI/180.) THETHA=89.99*PI/180.
R=SQRT(Z0**2+Y0**2)
RHOG=RHO/COS(THETHA)**2
ZGR=(0.,-1.)*CEXP(CMPLX(0.E0,-R))/(240.*PI**2*R)
KA=R*ABS((1./(2.*RHOG**2))**(1./3.))
IF (KA.LT.0.7) GO TO 20
CALL FOCK(KA)
GO TO 30
20 CALL FOCK1(KA)
30 ZT1=CVF*(SIN(THETHA)**2+(0.,1.)*COS(2*THETHA)/R)
  ZT2=(0.,1.)*CUF*COS(THETHA)**2/R
  ZT3=(0.,1.)*(1./(SQRT(2.)*RHO*COS(THETHA)))*(2./3.)
  & *SIN(THETHA)**4*CUPF
  HFHI=ZGR*(ZT1+ZT2+ZT3)
  IF (THETHA.EQ.0.) GO TO 40
  TM1=SIN(B0*SIN(THETHA)/2.)/(B0*SIN(THETHA)/2.)
  GO TO 50
40 TM1=1.
50 TM2=COS(A0*COS(THETHA)/2.)/(1.-(A0*COS(THETHA)/PI)**2)
  ZY2=-8.*A0*B0*(TM1*TM2/PI)**2*HFHI
  RETURN
END
SUBROUTINE APROX2(A0,B0,Z0,Y0,PI,ZY2)
IMPLICIT COMPLEX (C,H,Z),REAL(A-B,D-G,P-Y)
REAL TN(10),TNPI(10)
REAL KA,Z0
COMMON /DATA1/TN,TNPI,RHO,C1,C2,F2
COMMON /CF/CVF,CUF,CVIF,CVFF,CUPF
THETHA=ATAN2(Z0,Y0)
IF (THETHA.GE.89.99*PI/180.) THETHA=89.99*PI/180.
R=SQRT(Z0**2+Y0**2)
RHOG=RHO/COS(THETHA)**2
ZGR=(0.,-1.)*CEXP(CMPLX(0.E0,-R))/(240.*PI**2*R)
KA=R*ABS((1./(2.*RHOG**2))**(1./3.))
IF (KA.LT.0.7) GO TO 20
CALL FOCK(KA)
GO TO 30
20 CALL FOCK1(KA)
30 ZT1=CVF*(COS(THETHA)**2-(0.,1.)*COS(2*THETHA)/R)
  ZT2=(0.,1.)*CUF*SIN(THETHA)**2/R
  HZ=ZGR*(ZT1+ZT2)
  TM1=(SIN(A0*COS(THETHA)/2.)/(A0*COS(THETHA)/2.))**2
  TM2=(COS(B0*SIN(THETHA)/2.)/(1.-(B0*SIN(THETHA)/PI)**2))**2
  ZY2=-8.*A0*B0*TM1*TM2*HZ/PI**2
  RETURN

```

BEST AVAILABLE COPY

```

END
SUBROUTINE FMFN(X,N,FM,FN)
REAL DUM1(400),DUM2(400)
REAL FJ(400),XB,BSSY(400),FM(400),FN(400)
PI=3.14159265
XB=X
IF(X-0.1) 10,10,20
10 GAMLOG=ALOG(X/2.)+0.5772156649
X2=X*X
X3=X2*X
X4=X*X3
X5=X*X4
BSSY1=2.*(GAMLOG*(1.-X2/4.+X4/64.)+X2/4.-3.*X4/128.)/PI
BSSY2=-2./(PI*X)+2.*(GAMLOG*(X/2.-X3/16.+X5/384.)-X/4.+1.25*X3/16.
-3.33333*X5/768.)/PI
GO TO 25
20 CALL BESY(X,0,BSSY1,IER)
CALL BESY(X,1,BSSY2,IER)
25 CONTINUE
BSSY(1)=BSSY1
BSSY(2)=BSSY2
DBSSY1=-BSSY(2)
I=1
80 I=I+1
BSSY(I+1)=2.*(I-1)*BSSY(I)/X-BSSY(I-1)
BSSYI1=BSSY(I+1)
IF(ABS(BSSYI1).GE.1.E10).GO TO 100
GO TO 80
100 NMAX=I+1
IF(NMAX.GE.N) NMAX=N
N1=N-1
CALL BSLJZ(XB,FJ,NMAX+1,0,D00,7,IERR,DUM1,DUM2)
IF FJ1=-FJ(2)
FM(1)=1./(BSSY(1)**2+FJ(1)**2)
FN(1)=1./(DBSSY1**2+DFJ1**2)
DO 200 I=1,N1
IF(I.GE.NMAX) GO TO 250
DBSSY=BSSY(I)-I*BSSY(I+1)/X
DFJ=FJ(I)-I*FJ(I+1)/XB
FM(I+1)=1./(BSSY(I+1)**2+FJ(I+1)**2)
FN(I+1)=1./(DBSSY**2+DFJ**2)
200 CONTINUE
250 CONTINUE
N=NMAX
RETURN
END
SUBROUTINE 'BESY'
PURPOSE
COMPUTE THE Y BESSEL FUNCTION FOR A GIVEN ARGUMENT AND ORDER
USAGE
CALL BESY(X,N,BY,IER)

```

BEST AVAILABLE COPY

DESCRIPTION OF PARAMETERS

X -THE ARGUMENT OF THE Y BESSEL FUNCTION DESIRED
 N -THE ORDER OF THE Y BESSEL FUNCTION DESIRED
 BY -THE RESULTANT Y BESSEL FUNCTION
 IER-RESULTANT ERROR CODE WHERE
 IER=0 NO ERROR
 IER=1 N IS NEGATIVE
 IER=2 X IS NEGATIVE OR ZERO
 IER=3 BY HAS EXCEEDED MAGNITUDE OF 10**70

REMARKS

VERY SMALL VALUES OF X MAY CAUSE THE RANGE OF THE LIBRARY,
 FUNCTION ALOG TO BE EXCEEDED
 X MUST BE GREATER THAN ZERO
 N MUST BE GREATER THAN OR EQUAL TO ZERO

SUBROUTINES AND FUNCTION SUBPROGRAMS REQUIRED

NONE

METHOD

RECURRENCE RELATION AND POLYNOMIAL APPROXIMATION TECHNIQUE
 AS DESCRIBED BY A.J.M.HITCHCOCK, 'POLYNOMIAL APPROXIMATIONS
 TO BESSEL FUNCTIONS OF ORDER ZERO AND ONE AND TO RELATED
 FUNCTIONS', M.T.A.C., V.11, 1957, PP.86-88, AND G.N. WATSON,
 'A TREATISE ON THE THEORY OF BESSEL FUNCTIONS', CAMBRIDGE
 UNIVERSITY PRESS, 1958, P. 62

.....
 SUBROUTINE BESY(X,N,BY,IER)

CHECK FOR ERRORS IN N AND X

IF(N)180,10,10

10 IER=0

IF(X)190,190,20

BRANCH IF X LESS THAN OR EQUAL 4

20 IF(X-4.0)40,40,30

COMPUTE Y0 AND Y1 FOR X GREATER THAN 4

30 I1=4.0/X

I2=I1*I1

P0=((((-.0000037043*I2+.0000173565)*I2+.0000487613)*I2

+1.00017343)*I2-.001753062)*I2+.3989423

P0=((((.000032312*I2+.0000142078)*I2+.0000342468)*I2

+1.0000857791)*I2+.0004564324)*I2-.01246694

P1=((((.0000042414*I2+.0000200920)*I2+.0000580759)*I2

+1.000223203)*I2+.002921826)*I2+.3989423

BEST AVAILABLE COPY

```

Q1=((((-0.0000036594*T2+.00001622)*T2-.0000398708)*T2
1: +.0001064741)*T2-.0006390400)*T2+.03740084
A=2.0/SQRT(X)
B=A*T1
C=X-.7853982
Y0=A*P0*SIN(C)+B*Q0*COS(C)
Y1=-A*P1*COS(C)+B*Q1*SIN(C)
GO TO 90

C
C      COMPUTE Y0 AND Y1 FOR X LESS THAN OR EQUAL TO 4
C
40 XX=X/2.
   X2=XX*XX
   T=ALOG(XX)+.5772157
   SUM=0.
   TERM=T
   Y0=T
   DO 70 L=1,15
   IF(L-1)50,60,50
50 SUM=SUM+1./FLOAT(L-1)
60 FL=L
   TS=T-SUM
   TERM=(TERM*(-X2)/FL**2)*(1.-1./(FL*TS))
70 Y0=Y0+TERM
   TERM = XX*(T-.5)
   SUM=0.
   Y1=TERM
   DO 80 L=2,16
   SUM=SUM+1./FLOAT(L-1)
   FL=L
   FL1=FL-1.
   TS=T-SUM
   TERM=(TERM*(-X2)/(FL1*FL))*((TS-.5/FL)/(TS+.5/FL1))
80 Y1=Y1+TERM
   PI2=.6366198
   Y0=PI2*Y0
   Y1=-PI2/X+PI2*Y1

C
C      CHECK IF ONLY Y0 OR Y1 IS DESIRED
C
90 IF(N-1)100,100,130

C
C      RETURN EITHER Y0 OR Y1 AS REQUIRED
C
100 IF(N)110,120,110
110 BY=Y1
   GO TO 170
120 BY=Y0
   GO TO 170

C
C      PERFORM RECURRENCE OPERATIONS TO FIND YN(X)
C

```

BEST AVAILABLE COPY

```

130 YA=Y0
    YB=Y1
    K=1
140 T=FLOAT(2*K)/X
    YC=T*YB-YA
    IF(ABS(YC)-1.0E70)145,145,141
141 IER=3
    RETURN
145 K=K+1
    IF(K-N)150,160,150
150 YA=YB
    YB=YC
    GO TO 140
160 BY=YC
170 RETURN
180 IER=1
    RETURN
190 IER=2
    RETURN
    END
C   SUBROUTINE BSLJZ(X , FJ , NMAX , A , ND , IERR , FJAPRX , RR)
C
C   THIS IS ONE OF THREE ROUTINES, "BSLJZ", "BSLIZ", AND "BSCJZ",
C   BASED ON ALGORITHM 236 FROM "COMMUNICATIONS OF THE A.C.M.",
C   AUGUST 1964. THIS ONE EVALUATES THE BESSEL FUNCTIONS OF THE
C   FIRST KIND FOR REAL ORDERS AND NON-NEGATIVE REAL ARGUMENTS.
C
C   THE PARAMETERS ARE DESCRIBED AS FOLLOWS, WITH "(I)", "(O)", AND
C   "(I/O)" INDICATING, RESPECTIVELY, THAT A PARAMETER IS TO BE SET ON
C   ENTRY, WILL BE SET BY THE ROUTINE, OR BOTH :
C
C   *** ALL PARAMETERS EXCEPT "ND" , "IERR" , "NMAX" ARE ***
C   *** SINGLE PRECISION REAL NUMBERS OR ARRAYS.          ***
C
C   (I)   X           -- THE (NON-NEGATIVE) ARGUMENT TO THE BESSEL FUNCTIONS.
C   (O)   FJ           -- AN ARRAY IN WHICH THE VALUES OF THE BESSEL FUNCTIONS
C                       -- ARE STORED, AS FOLLOWS: LET  $J(X;K)$  DENOTE THE VALUE
C                       -- OF THE BESSEL FUNCTION OF ORDER K WITH ARGUMENT X.
C                       -- THEN, FOR I = 1 TO ABS(NMAX)+1,
C                       --  $FJ(I) = J(X;A + (I-1)*SIGN(NMAX))$  .
C   (I)   NMAX         -- REFER TO "FJ".
C   (I)   A            -- REFER TO "FJ". NORMALLY,  $0 \leq A < 1$ , BUT THE ALGOR-
C                       -- ITM WORKS, WITH SOME LOSS OF ACCURACY, FOR  $A \geq 1$ .
C                       -- SEE THE PROGRAM NOTES BELOW.
C   (I)   ND           -- THIS GIVES THE NUMBER OF SIGNIFICANT FIGURES OF
C                       -- ACCURACY DESIRED IN THE FUNCTION VALUES.
C   (O)   IERR         -- THIS IS AN ERROR FLAG WHICH IS SET TO 0 IF THE
C                       -- INPUT PARAMETERS ARE OKAY, AND TO SOME POSITIVE
C                       -- VALUE IF ONE OF THE PARAMETERS IS INVALID. REFER
C                       -- TO THE ERROR EXITS AT THE END OF THE CODE FOR A
C                       -- DETAILED LIST OF THE VALUES OF IERR.
C   (O)   FJAPRX       -- A SCRATCH ARRAY USED BY THE ROUTINE. IT MUST HAVE

```

BEST AVAILABLE COPY

```

C          AT LEAST ABS(NMAX)+1 ENTRIES.
C (0)  RR      --  ANOTHER SCRATCH ARRAY. IT TOO MUST HAVE AT LEAST
C          ABS(NMAX)+1 ENTRIES
C
C OTHER ROUTINES CALLED: ( * INDICATES A LOCAL ROUTINE )
C *  NRS01Z -- INVERSE FUNCTION OF X*LOG(X)
C *  UNDERZ -- ROUTINE TO CONTROL UNDERFLOW INTERRUPTS ON THE IBM 360.
C  MGAMMA -- GAMMA FUNCTION FROM THE IMSL LIBRARY.
C  ALOG   -- LOGARITHM
C  ABS    -- ABSOLUTE VALUE
C  MOD    -- REMAINDER
C  AMAX1  -- MAXIMUM OF 2 REALS
C
C NOTES:
C  THE METHOD OF COMPUTATION IS A VARIANT OF THE BACKWARD
C  RECURRENCE ALGORITHM OF J.C.P. MILLER (REFERENCE 1). THE
C  PURPORTED ACCURACY IS OBTAINED BY A JUDICIOUS SELECTION
C  OF THE INITIAL VALUE "NU" OF THE RECURSION INDEX (REP-
C  RESENTED IN THE CODE BY THE VARIABLE "XNU"), TOGETHER
C  WITH AT LEAST ONE REPETITION OF THE RECURSION WITH "NU"
C  REPLACED BY "NU"+5. NEAR A ZERO OF ONE OF THE BESSEL
C  FUNCTIONS, THE ACCURACY OF THAT PARTICULAR BESSEL FUNCTION
C  MAY DETERIORATE TO LESS THAN "NU" SIGNIFICANT DIGITS. THE
C  ALGORITHM IS MOST EFFICIENT WHEN X IS SMALL OR MODERATELY
C  LARGE.
C
C  THE ABOVE PARAGRAPH IS TAKEN FROM GAUTSCHI'S PRESENTATION
C  OF ALGORITHM 236 IN C.A.C.M. THE SELECTION OF THE INITIAL
C  "NU" IS DONE WITH THE AID OF THE FUNCTION NRS01Z, ALSO
C  BY GAUTSCHI (AND CALLED "T" BY HIM). IN THIS CODE, THE
C  FOLLOWING SPECIAL CASES HAVE BEEN ADDED:
C      A. X=0 WHEN NMAX > 0 OR A=0
C      B. A=0 AND NMAX < 0
C      C. A >= 1 : THE ALGORITHM WORKS IN THIS CASE, BUT THE
C                  INITIAL CHOICE OF "NU" IS NO LONGER
C                  OPTIMAL, AND SOME ACCURACY IS LOST. SIMPLE
C                  TESTS INDICATE THAT ONLY A FEW DECIMAL
C                  PLACES ARE SACRIFICED AT WORST. A LIMIT OF
C                  "ABIG" IS PLACED ON A TO AVOID OVERFLOW IN
C                  THE GAMMA FUNCTION. TO AVOID COMPLICATIONS,
C                  NMAX IS REQUIRED TO BE NON-NEGATIVE IF A > 1.
C
C REFERENCES:
C      1. GAUTSCHI, W. "RECURSIVE COMPUTATION OF SPECIAL FUNCTIONS",
C        UNIVERSITY OF MICHIGAN ENGINEERING SUMMER CONFER-
C        ENCES, NUMERICAL ANALYSIS, 1963.
C
C *****
C      SUBROUTINE BSLJZ(X , FJ , NMAX , A , ND , IERR , FJAPRX , RR)
C      REAL NRS01Z
C      DIMENSION FJ(1) , FJAPRX(1) , RR(1)
C      LOGICAL NEVEN , AFLAG

```

BEST AVAILABLE COPY

```

DATA      ONE/1D0/      , TWO/2D0/      , HALF/.5D0/      ,
*         TEN/10D0/     , SMALL/1D-15/   , C1/.73576D0/      ,
*         C2/1.3591D0/   , C3/2.3026D0/   , C4/1.3863D0/      ,
*         ZERO/0D0/     , ABIG/55D0/     , TWOP5/2.5D0/      ,
*         ALEPH/3777 0000 0000 0000 0000B/, FOUR/4D0/      ,
*         C5/2000 4000 0000 0000 0000B/

C*****
C INITIALIZE THE ERROR PARAMETER , TURN UNDERFLOW OFF , AND CHECK
C THE PARAMETERS FOR VALIDITY AND FOR THESE SPECIAL CASES:
C   A. X=0 WITH NMAX > 0 OR A=0
C   B. A=0 AND NMAX < 0
C
C THE CODE DELIBERATELY AVOIDS TESTING MORE THEN ONE THING IN EACH
C LOGICAL "IF" BELOW BECAUSE OF I.B.M. FORTRAN INEFFICIENCY IN THIS
C REGARD.
C
C IF A>1, NMAX MUST NOT BE NEGATIVE.
C*****
      IERR = 0
      CALL UNDER2('OFF',SAVE)
      IF(A .LT. ZERO) GOTO 999
      IF(A .GT. ABIG) GOTO 998
      IF(X .LT. ZERO) GOTO 997
      IF(NMAX .GE. 0 ) GOTO 10
      IF(A .EQ. ZERO) GOTO 10
      IF(A .LE. SMALL) GOTO 996
      IF(A .GE. ONE ) GOTO 994
10      IF(X .GT. ZERO) GOTO 40
      IF(NMAX .GE. 0 ) GOTO 20
      IF(A .GT. ZERO) GOTO 995
C*****
C IF NMAX = 0, NMAXT IS SET HERE SO THAT ONLY J(X;A) IS CALCULATED.
C THE LOOP FOLLOWING STATEMENT 800 THEN CALCULATES THE REMAINING
C FUNCTIONS BY A SIMPLE RECURRENCE.
C IF A=0, NMAXT IS SET SO THAT J(X;A+N), N=0,...,-NMAX ARE
C CALCULATED; THE CODE AFTER 800 THEN REVERSES THE SIGN OF EVERY
C OTHER ONE.
C
C WE FIRST HANDLE THE CASE X=0.
C*****
20      NTEMP = IABS(NMAX) + 1
      DO 30 I = 1,NTEMP
30      FJ(I) = ZERO
      IF(A .EQ. ZERO) FJ(1) = ONE
      GOTO 1000
C*****
40      AFLAG = (A .EQ. ZERO) .AND. (NMAX .LT. 0)
      NMAXT = NMAX
      IF(NMAX .LT. 0) NMAXT = 1
      NTEMP = MAX0(NMAX+1,1)
      IF(.NOT. AFLAG) GOTO 60
      NMAXT = - NMAX

```

BEST AVAILABLE COPY

```

      NTEMP = NMAXT + 1
60    EPSLON = TEN**(-ND)/2
      DO 80 I = 1,NTEMP
80    FJAPRX(I) = ZERO
      CALL MGAMMA(ONE+A , RESULT , IER)
      SUM = (X/TWO)**A/RESULT
      D1 = C3*ND + C4
      R = ZERO
      IF(NMAXT .GT. 0) R = NMAXT * NBS01Z(HALF*D1/NMAXT)
      S = C2 * X * NBS01Z(C1*D1/X)
C*****
C THE RECURSION INDEX "NU" IS DELIBERATELY CALCULATED AS A FLOATING
C POINT NUMBER RATHER THAN AN INTEGER, AND ALL COMPARISONS WITH IT
C ARE DONE AS FLOATING POINT COMPARISONS.
C*****
      XNU = ONE + AMAX1(R,S)
      XLIMIT = XNU/2
      TWOA = A + A
      XN = ZERO
      FL = ONE
C*****
C THE OUTER ITERATION LOOP STARTS HERE.
C
C
C THE FOLLOWING LOOP IS DONE ENTIRELY IN FLOATING POINT FOR
C EFFICIENCY.
C*****
200   XN = XN + ONE
      FL = FL * (XN + A)/(XN + ONE)
      IF(XN .LT. XLIMIT) GOTO 200
      OLDFL = FL
      OLDXN = XN
C
      N = 2*XN
      XN = N
      NEVEN = .TRUE.
      R = ZERO
      S = ZERO
      TWOA = TWO/X
C*****
C IN THE FOLLOWING LOOP, THE SUCCESSIVE VALUES OF "R" ARE PARTIAL
C FRACTIONS OF A CONTINUED FRACTION.
C*****
300   DENOM = TEMP1 * (A + XN) - R
      IF(ABS(DENOM) .LE. SMALL) DENOM = DENOM + SMALL
      R = ONE/DENOM
      FLMBDA = ZERO
      IF(.NOT. NEVEN) GOTO 400
      FL = FL * (XN + TWO)/(XN + TWOA)
      FLMBDA = FL * (XN + A)
400   S = R * (FLMBDA + S)
      IF(N .LE. NMAXT) RR(N) = R

```


BEST AVAILABLE COPY

```

      N = N - 1
      XN = XN - ONE
      NEVEN = .NOT. NEVEN
      IF(N .GE. 1) GOTO 300
C*****
      FJ(1) = SUM/(ONE + S)
      IF(NMAXT .EQ. 0) GOTO 600
      DO 500 N = 1,NMAXT
500    FJ(N+1) = RR(N) * FJ(N)
C*****
C THE LATEST APPROXIMATIONS ARE CHECKED FOR IMPROVEMENT:
C*****
600    DO 800 N = 1,NTEMP
        IF(ABS(FJ(N) - FJAPRX(N)) .LE. ABS(FJ(N))*EPSLON) GOTO 800
        DO 700 M = 1,NTEMP
700      FJAPRX(M) = FJ(M)
          XN      = OLDXN
          FL      = OLDFL
          XLIM11 = XLIMIT + TWOP5
          GOTO 200
800    CONTINUE
        IF(NMAX .GE. 0) GOTO 1000
C*****
C IF NMAX<0, WE HAVE FINISHED OBTAINING J(X;A) , AND NOW
C ITERATE TO FIND ALL THE DESIRED FUNCTIONS.
C
C FIRST WE CHECK FOR THE SPECIAL CASE A=0.
C*****
        IF(.NOT. AFLAG) GOTO 850
        NMAXT = -NMAX + 1
        DO 820 N = 2,NMAXT,2
820      FJ(N) = - FJ(N)
        GOTO 1000
C*****
850      FJ(2) = TWO * A * FJ(1)/X - FJ(2)
        IF(NMAX .EQ. -1) GOTO 1000
C*****
C THE FOLLOWING CODE IS A RENDERION OF THE LOOP
C
        DO 900 N = 2,NMAXT
C
          900      FJ(N+1) = (2/X)*(A-N)*FJ(N) - FJ(N-1)
C
C WITH OVERFLOW DETECTION. AS SOON AS THE NUMBERS GET TOO BIG, THEY
C ARE SCALED DOWN (BY A POWER OF THE MACHINE BASE, SO AS TO AVOID
C LOSS OF PRECISION) AND THE CALCULATION CONTINUES. A SEPARATE LOOP
C TRANSFORMS THE SCALED VALUES TO THE CORRECT OUTPUT VALUES, SETTING
C TOO-LARGE ONES TO PLUS OR MINUS INFINITY.
C*****
        NMAXT = -NMAX + 1
        FJNOL = FJ(1)
        FJNCL = FJ(1)
        FJMP1 = FJ(1)/X
        FJLR  = ZERO

```

```

      XNM1 = TWO
C
      DO 880 N = 3,NMAXT
      FJN = TEMP1 * (A - XNM1) * FJNM1 - FJNM2
      FJNM2 = FJNM1
      FJNM1 = FJN
      FJ(N) = FJN
      XNM1 = XNM1 + ONE
      RR(N) = OVER
      IF(ABS(FJN) .LT. C5) GOTO 880
      OVER = OVER + ONE
      FJNM1 = FJNM1/C5
      FJNM2 = FJNM2/C5
880   CONTINUE
C
      IF(NMAXT .LE. 3) GOTO 1000
      OVER = ZERO
      SCALE = ONE
C
      DO 900 N = 4,NMAXT
      IF(OVER .LT. FOUR) GOTO 890
      FJ(N) = SIGN(ALEPH,FJ(N))
      GOTO 900
890   IF(RR(N) .GT. OVER) SCALE = SCALE * C5
      FJ(N) = FJ(N) * SCALE
      OVER = RR(N)
900   CONTINUE
      GOTO 1000
C*****
C ERROR EXITS FOLLOW. MEANINGS OF THE EXIT VALUES OF "IERR" ARE:
C      0 : NO ERROR
C      1 : A < 0
C      2 : A > ABIG
C      3 : X < 0
C      4 : NMAX < 0 AND 0 < A < SMALL
C      5 : X=0, NMAX < 0, AND A > 0
C      6 : NMAX < 0 AND A >= 1
C*****
994   IERR = IERR + 1
995   IERR = IERR + 1
996   IERR = IERR + 1
997   IERR = IERR + 1
998   IERR = IERR + 1
999   IERR = IERR + 1
1000  CONTINUE
C     CALL UNDERZ('S',SAVE)
      RETURN
      END
      REAL FUNCTION NBS01Z(X)
C*****
C THIS IS A NUCLEUS FOR THE THREE BESSEL FUNCTION ROUTINES
C "BSLJZ" , "BSLIZ" , "BSCJZ" BASED ON ALGORITHM 234 FROM

```

BEST AVAILABLE COPY

```

C "COMMUNICATIONS OF THE A.C.M.",
C IT EVALUATES THE INVERSE FUNCTION OF  $X \cdot \log(X)$  FOR  $X \geq 1$  TO AN
C ACCURACY OF ABOUT ONE PER CENT.
C FOR THE INTERVAL  $0 \leq X \leq 10$  A FIFTH DEGREE APPROXIMATION IS
C USED, OBTAINED BY TRUNCATING AN EXPANSION IN CHERYCHEV POLYNOMIALS.
C FOR  $X > 10$ , A DIFFERENT APPROXIMATION IS GIVEN, AS CAN BE SEEN.
C*****
      DATA      C1/.000057941D0/      , C2/-.00176148D0/      ,
      *          C3/.0208645D0/      , C4/-.129013D0/      ,
      *          C5/.85777D0/      , C6/1.10125D0/      ,
      *          ALPHA/.775D0/      , TEN/10D0/
      IF(X.GT. TEN) GO TO 10
      NBS01Z = (((C1*X + C2)*X + C3)*X + C4)*X + C5)*X + C6
      RETURN
10      TEMP1 = ALOG(X)-ALPHA
      TEMP2 = (ALPHA-ALOG(TEMP1))/(1+TEMP1)
      NBS01Z = X/((1+TEMP2)*TEMP1)
      RETURN
      END
      SUBROUTINE PROG1(RHO,ANFY,PHASEY,ANPYDB,PHASNM)
      PROGRAM TO COMPUTE THE MUTUAL ADMITTANCE BETWEEN TWO IDENTICAL
      AXIAL SLOTS ON A CYLINDER ( UI MODAL SOLUTION)
      REAL      KO,KZ,NT,I2,KZKTRO
      COMPLEX    S1,Y12,PSIEXP,YN12
      REAL      F1(400),FM(400),FN(400),AIMAG,REAL,ATAN2
      COMMON/DATA3/KO,NCYCLE,PHIO,ZO,Y11,MMA,MAX,A,B
      C
      C INPUT PARAMETERS:
      C KO= WAVE NUMBER IN FREE SPACE IN TERMS OF 1/INCH
      C NCYCLE=NO. OF SUBSECTIONS BETWEEN ANY TWO SUCCESSIVE ZEROS OF INTEGRAND
      C IN TRAPEZOIDAL RULE FOR NUMERICAL INTEGRATION
      C A*B= SLOT DIMENSION B>A <INCH>
      C RHO=RADIUS OF CYLINDER <INCH>
      C PHIO=ANGULAR SEPARATION OF THE SLOTS (CENTER TO CENTER) <RADIAN>
      C ZO= SEPARATION OF THE SLOTS IN Z-DIRECTION <INCH>
      C Y11= NORMALIZATION FACTOR
      C MMA= MAXIMUM NO. OF TERMS WHICH HAS BEEN USED IN CALCULATION OF
      C INFINITE SERIES
      PI=3.14159265
      Y0=1./(120.*PI)
      IREQ=3.E10*KO/(2.*PI*2.54)
      AKA=KO*A
      BKB=KO*B
      RK=KO*RHO
      C PHIA=HALF ANGULAR WIDTH OF THE SLOT
      PHIA=2.*ASIN(A/(2.*RHO))
      C COMPUTATION OF INFINITE SERIES
      MMA12=MMA+1
      DO 100 M=1,MMA12
      N1=M-1
      IF(M.EQ.1) GO TO 99
      F1(M)=(COS(M1*PHIO)*(SIN(M1*PHIA/2.)/(M1*PHIA/2.))**2
      GO TO 100

```

BEST AVAILABLE COPY

```

99 F1(M)=0.5
100 CONTINUE
C   INTEGRATION OF PSI(KZ)*R1(M,KZ)*EXP(-J*KZ*ZO) BETWEEN 0 AND KO
C   DELTA= NEIGHBOURHOOD OF THE SINGULAR POINT KZ=KO IN WHICH THE INTEGRAL
C   HAS BEEN CALCULATED ANALYTICALLY
      DELTA=1.E-7*KO
C   NSECT1=NO. OF SAMPLES IN THE INTERVAL (0.,KO-DELTA).
      NSECT1=(IFIX((B+ZO+RHO)*KO/PI)+2)*NCYCLE
      DKZ=(KO-DELTA)/NSECT1
      NSECT=NSECT1+1
      I1=(0.,0.)
C   I1=FIRST INTEGRAL (BETWEEN 0. AND KO)
      DO 200 I=1,NSECT
      KZ=(I-1)*DKZ
      IF(KZ.EQ.0) KZ=0.00001*KO
      CIN=1.
      IF((I.EQ.1).OR.(I.EQ.NSECT)) CIN=0.5
      KT=SQRT(KO*KO-KZ*KZ)
      TF(ABS(KZ*B/2.-PI/2.).LE.1.E-8) KZ=1.000001*KZ
      PSIEXP=(COS(KZ*B/2.)/((KZ*B/2.）**2-(PI/2.）**2))**2*CIN*DKZ
      &*CEXP((0.,-1.)*KZ*ZO)
      MMAX1=MMAX
      ROKT=RHO*KT
C   COMPUTATION OF FM(N)=1./(JN(X)**2+YN(X)**2) AND FN(N)=1./(DJN(X)**2+
C   DYN(X)**2) FOR X=ROKT AND N=0 TO MMAX1 ; WHERE MMAX1 IS A NUMBER AFTER
C   WHICH THE CONTRIBUTIONS OF FM(N) AND FN(N) TO THE INFINITE SUM
C   BECOME NEGLIGIBLE. MMAX1 IS A FUNCTION OF THE ARGUMENT X AND IS ALWAYS
C   LESS THAN OR EQUAL TO MMAX. MMAX1, FM(N) AND FN(N) ARE CALCULATED
C   BY SUBROUTINE FMFN(X,MMAX1,FM,FN).
      CALL FMFN(ROKT,MMAX1,FM,FN)
      DO 200 M=1,MMAX1
      M1=M-1
200  I1=I1+FN(M)*PSIEXP*F1(M)
C   COMPUTATION OF I2 (BETWEEN ZERO AND ETAMAX ; WHERE ETAMAX IS A NUMBER
C   AFTER WHICH THE INTEGRAND BECOMES VERY SMALL)
      I2=0.
      ETAMAX=14./(ZO-B)
C   THE INTEGRATION IS CARRIED OUT BY TRAPEZOIDAL RULE. AT FIRST THE WHOLE
C   RANGE OF INTEGRATION (0.,ETAMAX) IS DEVIDED INTO TWO SUBINTERVALS :
C   (0.,ETA1) AND (ETA1,ETAMAX) , WHERE ETA1=ETAMAX/2.. THEN THE NUMERICAL
C   COMPUTATION OF THE INTEGRAL IS PERFORMED IN THESE SUBINTERVALS WITH THE
C   NO. OF SAMPLES IN THE FIRST SUBINTERVAL TWO TIMES THAT IN THE SECOND ONE.
      ETA1=7./(ZO-B)
      NSECT1=(IFIX(SQRT(KO*KO+ETA1**2)*RHO/PI)+2)*NCYCLE
      DETA1=ETA1/NSECT1
      DETA2=2.*DETA1
      NSECT2=IFIX((ETAMAX-ETA1)/DETA2)+1
      NSECT=NSECT1+NSECT2+2
      DO 300 I=1,NSECT
      IF(I.LE.NSECT1+1) GO TO 220
      ETA=ETA1+(I-NSECT1-2)*DETA2
      DETA=DETA2

```

BEST AVAILABLE COPY

```

GO TO 240
220 ETA=(I-1)*DETA1
   IF(ETA.EQ.0.) ETA=0.0001/A
   DETA=DETA1
240 CIN=1.
   IF((I.EQ.1).OR.(I.EQ.NSECT1+1).OR.(I.EQ.NSECT1+2).OR.(I.EQ.NSECT)
      & ) CIN=0.5
   PSEX=(COSH(ETA*B/2.)/((ETA*B/2.)*2*(PI/2.)*2))*2*DETA*CIN
   %*EXP(-ETA*ZO)
   KT=SQRT(KO*KO+ETA**2)
   MMAX1=MMAX
   CALL FMFN(RHO*KT,MMAX1,FM,FN)
   DO 300 M=1,MMAX1
   M1=M-1
300 I2=I2+FN(M)*PSEX*F1(M)
   Y12=(11+(0.,1.)*I2)*A*B*YO/(PI*KO*RHO**2)
C   NORMALIZATION OF THE PHASE OF Y12
   YN12=Y12*CEXP((0.,1.)*(KO*SQRT(ZO*ZO+(RHO*PHIO)**2)))
C   COMPUTATION OF THE ACTUAL PHASE 'PHASEY' AND NORMALIZED PHASE 'PHASNM'
C   OF Y12.
   PHASEY=ATAN2(AIMAG(Y12),REAL(Y12))*180./PI
   PHASNM=ATAN2(AIMAG(YN12),REAL(YN12))*180./PI
C   COMPUTATION OF THE MAGNITUDE OF THE Y12 IN TERMS OF <MHO> AND <DB>.
   AMPY=CABS(Y12)
   AMPYDB=ALOG10(AMPY/ABS(Y11))*20.
   RPHIO=KO*RHO*PHIO
   ZOK=KO*ZO
   PHIOO=PHIO*180./PI
   RETURN
END
SUBROUTINE PROG2(RHO,AMPY,PHASEY,AMPYDB,PHASNM)
C   PROGRAM FOR COMPUTATION OF THE MUTUAL ADMITTANCE BETWEEN TWO
C   IDENTICAL CIRCUMFERENTIAL SLOTS ON A CYLINDER(U1 MODAL SOLUTION)
   REAL KO,KZ,KI,I2,KZKTRO
   COMPLEX I1,Y12,PSEX,YN12
   REAL F1(400),FM(400),FN(400),AIMAG,REAL,ATAN2
   COMMON/DATA3/KO,NCYCLE,PHIO,ZO,Y11,MMAX,A,B
C   INPUT PARAMETERS :
C   KO= WAVE NUMBER IN FREE SPACE IN TERMS OF 1/INCH
C   RHO= RADIUS OF CYLINDER INCH.
C   PHIO= ANGULAR SEPARATION OF THE SLOTS (CENTER TO CENTER) <RADIAN>
C   ZO= SEPARATION OF THE SLOTS IN Z-DIRECTION <INCH>
C   Y11= NORMALIZATION FACTOR
C   MMAX= MAXIMUM NO. OF TERMS WHICH HAS BEEN USED IN CALCULATION OF
C   INFINITE SERIES
C   NCYCLE= NO. OF SUBSECTIONS BETWEEN ANY TWO SUCCESSIVE ZEROS OF INTEGRAND
C   IN TRAPEZOIDAL RULE FOR NUMERICAL INTEGRATION
   PI=3.14159265
   YO=1./(120.*PI)
   FRLQ=3.1410*KO/(2.*PI*2.54)
   AKA=KO*A
   KKB=KO*B

```

BEST AVAILABLE COPY

```

      RK=K0*RHO
C     PHIB=HALF ANGULAR WIDTH OF THE SLOT
      PHIB=ASIN(A/(2.*RHO))
C     COMPUTATION OF INFINITE SERIES
      MMAX12=MMAX1+1
      DO 100 N=1,MMAX12
      M1=M-1
      EPM=1.
      IF(M.EQ.1) EPM=2.
      PHIB1=PHIB
      IF(ABS(PHIB*M1-PI/2.).LE.1.E-7) PHIB1=PHIB*1.001
100  FJ(M)=COS(M1*PHIB)*(-PI*COS(M1*PHIB1)/(((M1*PHIB1)**2-(PI/2.)*2
      &)))*2*(1./EPM)
C     INTEGRATION OF PSI(KZ)*R1(M,KZ)*EXP(-J*KZ*ZO) BETWEEN 0 AND K0
C     DELTA= NEIGHBOURHOOD OF THE SINGULAR POINT KZ=K0 IN WHICH THE INTEGRAL
C     HAS BEEN CALCULATED ANALYTICALLY
      DELTA=0.0001*K0
C     DELTA1= NEIGHBOURHOOD OF THE SINGULAR POINT KZ=K0 WHERE THE INTEGRAL
C     VARIES RAPIDLY AND 'NDELTA' SAMPLES HAVE BEEN USED.
      DELTA1=0.01*K0
      NDELTA=100
      DKZ2=(DELTA1-DELTA)/NDELTA
C     NSECT1= NO. OF SUBSECTIONS BETWEEN 0 AND K0-DELTA1
      NSECT1=(FIX((B+ZO+RHO)*K0/PI)+2)*NCYCLE
      DKZ1=(K0-DELTA1)/NSECT1
      NSECT=NSECT1+NDELTA+2
C     I1=FIRST INTEGRAL (BETWEEN 0. AND K0)
      I1=(0.,0.)
      DO 200 I=1,NSECT
      IF(I.LE.NSECT1+1) GO TO 120
      KZ=K0-DELTA1+(I-NSECT1-2)*DKZ2
      DKZ=DKZ2
      GO TO 140
120  KZ=(I-1)*DKZ1
      IF(KZ.EQ.0) KZ=0.00001*K0
      DKZ=DKZ1
140  CIN=1.
      IF((I.EQ.1).OR.(I.EQ.NSECT1+1).OR.(I.EQ.NSECT1+2).OR.(I.EQ.NSECT)
      &) CIN=0.5
      KT=SQRT(K0*K0-KZ*KZ)
      PSIEXP=(SIN(KZ*B/2.)/(KZ*B/2.))*2*CIN*DKZ*CEXP((0.,-1.)*KZ*ZO)
      MMAX1=MMAX
      ROKT=RHO*KT
C     COMPUTATION OF FM(N)=1./(JN(X)**2+YN(X)**2) AND FN(N)=1./(JN(X)**2+
C     YN(X)**2) FOR X=ROKT AND N=0 TO MMAX1 ; WHERE MMAX1 IS A NUMBER AFTER
C     WHICH THE CONTRIBUTIONS OF FM(N) AND FN(N) TO THE INFINITE SUM
C     BECOME NEGLIGIBLE. MMAX1 IS A FUNCTION OF THE ARGUMENT X AND IS ALWAYS
C     LESS THAN OR EQUAL TO MMAX. MMAX1, FM(N) AND FN(N) ARE CALCULATED
C     BY SUBROUTINE FMFN(X,MMAX1,FM,FN).
      CALL FMFN(ROKT,MMAX1,FM,FN)
      KZNTRO=(KZ/(KT*K0*RHO))*2
      DO 200 M=1,MMAX1

```

BEST AVAILABLE COPY

```

M1=M-1
R1=(1./KT**2)*(FM(M)+M1**2*KZKTRO*FN(M))
200 I1=I1+R1*PSIEXP*F1(M)
      I1=(2.*KO/(PI*RHO))*(I1-F1(1)*CEXP((0.,-1.)*KO*KZ0)*(PI*PI/(2.*KO))
      *(SIN(KO*B/2.)/(KO*B/2.))**2/(2.*(0.5772156649+ALOG(RHO*SQRT
      2(KO/2.)))+ALOG(DELTA)))
C     COMPUTATION OF I2 (BETWEEN ZERO AND ETAMAX ; WHERE ETAMAX IS A NUMBER
C     AFTER WHICH THE INTEGRAND BECOMES VERY SMALL)
      I2=0.
      ETAMAX=14./(Z0-B)
C     THE INTEGRATION IS CARRIED OUT BY TRAPEZOIDAL RULE. AT FIRST THE WHOLE
C     RANGE OF INTEGRATION (0.,ETAMAX) IS DEVIDED INTO TWO SUBINTERVALS :
C     (0.,ETA1) AND (ETA1,ETAMAX) , WHERE ETA1=ETAMAX/2.. THEN THE NUMERICAL
C     COMPUTATION OF THE INTEGRAL IS PERFORMED IN THESE SUBINTERVALS WITH THE
C     NO. OF SAMPLES IN THE FIRST SUBINTERVAL TWO TIMES THAT IN THE SECOND ONE.
      ETA1=7./(Z0-B)
      NSECT1=(FIX(SQRT(KO*KO+ETA1**2)*RHO/P1)+2)*NCYCLE
      DELTA1=ETA1/NSECT1
      DELTA2=2.*DELTA1
      NSECT2=FIX((ETAMAX-ETA1)/DELTA2)+1
      NSECT=NSECT1+NSECT2+2
      DO 300 I=1,NSECT
      IF (.EQ.NSECT1+1) GO TO 220
      ETA=ETA1+(I-NSECT1-2)*DELTA2
      DELTA=DELTA2
      GO TO 240
220 LTA=(I-1)*DELTA1
      IF (ETA.LQ.0.) ETA=0.0001/R
      DELTA=DELTA1
240 CIN=1.
      IF ((.EQ.1).OR.(1.EQ.NSECT1+1).OR.(1.EQ.NSECT1+2).OR.(1.EQ.NSECT)
      2) CIN=0.5
      PSEX=(SINH(ETA*B/2.)/(ETA*B/2.))**2*EXP(-ETA*KZ0)*DELTA*CIN
      KT=SQRT(KO*KO+ETA**2)
      ETKTRO=(ETA/(RHO*KO*KT))**2
      MMAX1=MMAX
      CALL FMFN(RHO*KT,MMAX1,FM,FN)
      DO 300 N=1,MMAX1
      M1=M-1
      R1=(1/(KT*KT))*(FM(M)-M1*M1*ETKTRO*FN(M))
300 I2=I2+F1(M)*R1*PSEX
      I2=I2*2.*KO/(PI*RHO)
      Y12=(I1+(0.,1.)*I2)*AB*Y0/(2.*PI*PI*RHO)
C     NORMALIZATION OF THE PHASE OF Y12
      YN12=Y12*CEXP((0.,1.)*(KO*SQRT(Z0*KZ0+(RHO*PH10)**2)))
C     COMPUTATION OF THE ACTUAL PHASE 'PHASEY' AND NORMALIZED PHASE 'PHASNM'
C     OF Y12.
      PHASEY=ATAN2(AIMAG(Y12),REAL(Y12))*180./PI
      PHASNM=ATAN2(AIMAG(YN12),REAL(YN12))*180./PI
C     COMPUTATION OF THE MAGNITUDE OF THE Y12 IN TERMS OF <MHO> AND <DB>.
      AMPY=CABS(Y12)
      AMPYDB=ALOG10(AMPY/ABS(Y11))*20.

```

BEST AVAILABLE COPY

```

RPHIK=K0*RHO*PHIO
ZOK=K0*Z0
PHIOD=PHIO*180./PI
RETURN
END

```

```

C
C THIS SUBROUTINE IS USED TO CALCULATE THE FUNCTIONS CVF,CUF,CV1F,CVFF,CUPF
C

```

```

SUBROUTINE FOCK(X)
IMPLICIT REAL(A-B,D-H,P-Y),COMPLEX (C,Z)
REAL TN(10),TNPI(10)
COMMON/CF/CVF,CUF,CV1F,CVFF,CUPF
COMMON/DATA1/TN,TNPI,RHO,C1,C2,F2,IOP,CC,RADN,DEG
F1=SQRT(X)
F3=X**1.5
CVF=0.
CUF=0.
CV1F=0.
CVFF=0.
CUPF=0.
DO 20 N=1,10
ZTN=TN(N)*C1
ZTNPI=TNPI(N)*C1
C3=CEXP(CMPLX(0.0,-X)*ZTNPI)
C4=CEXP(CMPLX(0.0,-X)*ZTN)
CVF=CVF+C3/ZTNPI
CUF=CUF+C4
CV1F=CV1F+C3
CVFF=(1.0-CMPLX(0.0,2*X)*ZTNPI)*C3/ZTNPI+CVFF
CUPF=(1.0-CMPLX(0.0,2.*X/3.)*ZTN)*C4+CUPF
20 CONTINUE
CVF=F2*F1*CVF/C2
CUF=2.*F2*F3*C2*CUF
CV1F=2.*F2*F3*C2*CV1F
CVFF=F2*CVFF/(2.*F1*C2)
CUPF=3.*F2*F1*C2*CUPF
RETURN
ENTRY FOCK1
XTHREE=X**3
F1=SQRT(X)
F3=XTHREE
Z1=F2*C2*SQRT(F3)
Z2=CMPLX(0.0,1.0/60.)*XTHREE
Z3=F2*X**4.5/(C2*64.)
F4=F3**2
CVF=1.0-Z1/4.+7*Z2+7.*Z3/8.-4.141E-3*F4
CUF=1.0-Z1/2.+25.*Z2+5.*Z3-3.701E-2*F4
CV1F=1.0+Z1/2.-35.*Z2-7.*Z3+4.555E-2*F4
CVFF=.375*F1*F2/CC+21.*Z2/X+63.*Z3/(16.*X)-2.485E-2*F4/X
CUPF=.75*F1*F2/CC+CMPLX(0.0,1.25*X**2)+22.5*Z3/X
1 -2.221E-1*F4/X

```


RETURN
END

BEST AVAILABLE COPY

C

```
SUBROUTINE PLANAR(IJ,ZSUM)
IMPLICIT COMPLEX(C,H,Z),REAL(A-B,D-G,P-Y)
REAL Z0
COMMON PI,TZ1,TZ2,TY1,TY2,R,THETHA
COMMON/DATA2/A,B,Z0,Y0
GO TO (10,20),IJ
10 XM1=((TZ2-TZ1)/R)**2
   XM2=2,-3.*XM1
   XRL=XM2/R
   XIM=XM1+XM2/R**2
   HA=CEXP(CMPLX(0.E0,-R))*CMPLX(XRL,-XIM)/(240.*R*PI**2)
   FACTOR=COS(PI*TY1/A)*COS(PI*(TY2-Y0)/A)
   ZSUM=ZSUM+FACTOR*HA
   RETURN
20 ZA1=CMPLX(1./R**2,1./R)*(2.-3.*AC02)
   ZA2=CEXP(CMPLX(0.E0,-R))*(AC02+ZA1)/R
   HA=(0.,-1.)*ZA2/(240.*PI**2)
   FACTOR=COS(PI*TZ1/B)*COS(PI*(TZ2-Z0)/B)
   ZSUM=ZSUM+FACTOR*HA
   RETURN
END
```

C

C THIS SUBROUTINE IS USED TO GET THE "CYLINDRICAL" SOLUTION

C

```
SUBROUTINE CYLIN(IJ,ZSUM)
IMPLICIT COMPLEX(C,H,Z),REAL(A-B,D-G,P-Y)
REAL Z0,KA
REAL TN(10),TNPI(10)
COMMON PI,TZ1,TZ2,TY1,TY2,R,THETHA
COMMON/CF/CVF,CUF,CV1F,CVPF,CUPF
COMMON/DATA1/TN,TNPI,RHO,C1,C2,F2,IOP,CC,RADN,DEG
COMMON/DATA2/A,B,Z0,Y0
COMMON/DATA4/AC02,SN2,TN2,R2,ACON1,ACON2,C01,C10
ZGR=(0.,-1.)*CEXP(CMPLX(0.E0,-R))/(240.*R*PI**2)
IT=0
ANGLE=ATAN2(ABS(TZ2-TZ1),ABS(TY2-TY1))*DEG
IF(ANGLE.LT.89.99) GO TO 10
IT=1
THETHA=PI*89.99/180.
ZW=C01/R*CEXP(CMPLX(0.E0,-PI/4.E0))*SQRT(PI*R/2.)/RHO
10 RHOG=RHO/AC02
   KA=R*ABS((1./((2.*RHOG**2)))*(1./3.))
   IF(1.A.LT.0./) GO TO 20
   CALL FOCK(KA)
   GO TO 30
20 CALL FOCK(KA)
```

BEST AVAILABLE COPY

```

30 IF(IT,EQ,1) GO TO 40
   ZW=C01*(1./AC02)/R*(CUF-CV1F*SN2)
40 GO TO (21,22,23,24),IOP
21 ZHB1=CMPLX(1.E0,-1./R)*CVF
   ZHB2=CUF/R**2
   ZHB3=C01/(SQRT(2.E0)*RHO)**AC02
   ZHB4=AC02**AC02*CVFF+SN2*(CUFF/AC02**(1./3.))
   HB=ZGR*(ZHB1-ZHB2+ZHB3*ZHB4)
   ZTM1=C01*CVFF/(SQRT(2.E0)*RHO)**AC02
   HT=C01*ZGR/R*(CVF+CMPLX(1.E0,-2./R)*CUF+ZTM1)
   IF(IJ,LT,2)GOTO 25
   HZ=HB*AC02+HT*SN2
   GOTO 500
25 HPHI=HB*SN2+HT*AC02
   GO TO 500
22 HB=ZGR*CVF
   HT=C01*ZGR*CUF/R
   IF(IJ,LT,2)GOTO 26
   HZ=HB*AC02+HT*SN2
   GOTO 500
26 HPHI=HB*SN2+HT*AC02
   GO TO 500
23 ZTM2=C01*(1.-3.*SN2)/R
   IF(IJ,LT,2)GOTO 27
   HZ=ZGR*CVF*(AC02+C01*(2.-3.*AC02)/R)
   GOTO 500
27 HPHI=ZGR*(CVF*(SN2+ZTM2)+ZW)
   GOTO 500
24 IF(IJ,LT,2)GOTO 28
   HZA=CVF*(AC02*C10+(2.-3.*AC02)*CMPLX(1./R2,1./R))
   HZB=C01*(CVFF/(SQRT(2.)*RHO)**AC02)
   HZC=CMPLX(-11./12.*AC02,(-11./6.-2./3.*TN2+AC01*AC02)/R)
   HZ=ZGR*(HZA+HZB*HZC)
   GOTO 500
28 HPA=CVF*CMPLX(SN2+(2.-3.*SN2)/R2,(2.-3.*SN2)/R)
   HPQ=C01*(CUF-CVFF)/AC02/R
   HPC=C01/(SQRT(2.)*RHO**AC02)**AC02
   HP1D=(CVFF/AC02**(1./3.))
   HP2D=CMPLX(4./3.*SN2-11./12.*SN2*AC02,
$       .75*AC02-7./12.*SN2+AC01*SN2*AC02)
   HP3D=C01/12./R*CVFF/AC02**(1./3.)
   HP4D=HPC*(HP1D*HP2D+HP3D)
   HPHI=ZGR*(HPA+HPQ+HP4D)
500 ZGREEN=HPHI
   IF(IJ,EQ,2)ZGREEN=HZ
   FACTOR=COS(PI*TY1/A)*COS(PI*(TY2-Y0)/A)
   IF(IJ,EQ,2)FACTOR=COS(PI*TZ1/B)*COS(PI*(TZ2-Z0)/B)
   ZSUM=ZSUM+FACTOR*ZGREEN
   RETURN
   END

```

ATTACHMENT B

Report 77-13

SIMPLE APPROXIMATE FORMULA FOR MUTUAL ADMITTANCE
BETWEEN SLOTS ON A CYLINDER

ELECTROMAGNETICS LABORATORY
TECHNICAL REPORT NO. 77-13

July 1977

SIMPLE APPROXIMATE FORMULA FOR MUTUAL ADMITTANCE
BETWEEN SLOTS ON A CYLINDER

S. W. Lee

S. Safavi-Naini



ELECTROMAGNETICS LABORATORY
DEPARTMENT OF ELECTRICAL ENGINEERING
ENGINEERING EXPERIMENT STATION
UNIVERSITY OF ILLINOIS AT URBANA-CHAMPAIGN
URBANA, ILLINOIS 61801

Supported by
Contract No. N00019-77-C-0127
Department of the Navy
Naval Air Systems Command
Washington, D.C. 20361

SECURITY CLASSIFICATION OF THIS PAGE (When Data Entered)

REPORT DOCUMENTATION PAGE		READ INSTRUCTIONS BEFORE COMPLETING FORM
1. REPORT NUMBER	2. GOVT ACCESSION NO.	3. RECIPIENT'S CATALOG NUMBER
4. TITLE (and Subtitle) SIMPLE APPROXIMATE FORMULA FOR MUTUAL ADMITTANCE BETWEEN SLOTS ON A CYLINDER		5. TYPE OF REPORT & PERIOD COVERED Technical
7. AUTHOR(s) S. W. Lee S. Safavi-Naini		6. PERFORMING ORG. REPORT NUMBER EM 77-13; UILU-ENG 77-2555
9. PERFORMING ORGANIZATION NAME AND ADDRESS Electromagnetics Laboratory Department of Engineering, University of Illinois Urbana, Illinois 61801		8. CONTRACT OR GRANT NUMBER(s) N00019-77-C-0127
11. CONTROLLING OFFICE NAME AND ADDRESS Department of the Navy Naval Air Systems Command Washington, D.C. 20361		10. PROGRAM ELEMENT, PROJECT, TASK AREA & WORK UNIT NUMBERS
14. MONITORING AGENCY NAME & ADDRESS (if different from Controlling Office)		12. REPORT DATE July 1977
		13. NUMBER OF PAGES 35
		15. SECURITY CLASS. (of this report) Unclassified
		15a. DECLASSIFICATION/DOWNGRADING SCHEDULE
16. DISTRIBUTION STATEMENT (of this Report) Distribution unlimited. (Reproduction in whole or in part is permitted for any purpose of the United States Government.)		
17. DISTRIBUTION STATEMENT (of the abstract entered in Block 20, if different from Report)		
18. SUPPLEMENTARY NOTES		
19. KEY WORDS (Continue on reverse side if necessary and identify by block number) Mutual Admittance of Slots on Cylinder GTD Conformal Array of Slots		
20. ABSTRACT (Continue on reverse side if necessary and identify by block number) Based on a newly developed asymptotic Green's function for a magnetic dipole on a conducting surface [1], this paper presents a simple, closed- form formula for the mutual admittance between two slots on a cylinder or a plane. When compared with the exact solution obtained by numerical integra- tions, this formula gives accurate results when the slots are relatively small and their separation large.		

Electromagnetics Laboratory Report No. 77-13

SIMPLE APPROXIMATE FORMULA FOR MUTUAL ADMITTANCE
BETWEEN SLOTS ON A CYLINDER

by

S. W. Lee
S. Safavi-Naini

Technical Report

July 1977

Supported by
Contract No. N00019-77-C-0127
Department of the Navy
Naval Air Systems Command
Washington, D.C. 20361

Electromagnetics Laboratory
Department of Electrical Engineering
Engineering Experiment Station
University of Illinois at Urbana-Champaign
Urbana, Illinois 61801

SIMPLE APPROXIMATE FORMULA FOR MUTUAL ADMITTANCE
BETWEEN SLOTS ON A CYLINDER*

S. W. Lee and S. Safavi-Naini[†]

ABSTRACT

Based on a newly developed asymptotic Green's function for a magnetic dipole on a conducting surface [1], this paper presents a simple, closed-form formula for the mutual admittance between two slots on a cylinder or a plane. When compared with the exact solution obtained by numerical integrations, this formula gives accurate results when the slots are relatively small and their separation large.

*This work was supported by Naval Air Systems Command under contract N00019-77-C-0127

[†]Department of Electrical Engineering, University of Illinois, Urbana, Illinois 61801

ACKNOWLEDGEMENT

The useful discussion with Dr. R. C. Hansen was greatly appreciated. This work was supported by the Department of the Navy, Naval Air Systems Command under Contract No. N00019-77-C-0127.

TABLE OF CONTENTS

	Page
1. INTRODUCTION	1
2. APPROXIMATE FORMULA FOR MUTUAL ADMITTANCE.	3
3. NUMERICAL RESULTS AND DISCUSSION	7
4. DERIVATION OF APPROXIMATE FORMULA.	9
5. EXACT MODAL SOLUTION	12
APPENDIX - FOCK FUNCTIONS	17
REFERENCES.	19

LIST OF FIGURES

Figure		Page
1	Two slots on the surface of a conducting cylinder	21
2	Mutual admittance Y_{12} between two circumferential slots as a function of z_0	22
3	Mutual admittance Y_{12} between two circumferential slots as a function of ϕ_0	23
4	The percentage error in magnitude and absolute error in phase of the approximate formula of Y_{12} of circumferential slots as a function of their relative positions	24
5	The percentage error in magnitude and absolute error in phase of the approximate formula of Y_{12} of axial slots as a function of their relative positions	25
6	Mutual admittance Y_{12} between two identical circumferential slots as a function of radius R of the cylinder. . . .	26
7	A surface ray from source point Q' to observation point Q on a cylinder of radius R	27
8	Two circumferential slots on a developed cylinder	28
9	Contours in the complex k_z -plane for the integral in (5.4).	29

LIST OF TABLES

TABLE		Page
1	MUTUAL ADMITTANCE Y_{12} BETWEEN TWO SLOTS ON A PLANE (E-PLANE COUPLING)	30
2	MUTUAL ADMITTANCE Y_{12} BETWEEN SLOTS ON A PLANE (H-PLANE COUPLING)	31

1. INTRODUCTION

This paper contains two results for the mutual admittance Y_{12} between two slots on the surface of a large conducting cylinder (including the conducting plane as a special case). The first and the main result is that an approximate, closed-form solution of Y_{12} is derived. This solution may be considered as a simplified version of the asymptotic solution of Y_{12} reported in [1], as the two surface integrals over the apertures of the slots are no longer needed in the present approximate solution. Our second result concerns the derivation of an exact solution of Y_{12} , which is given in terms of an inverse Fourier transform and an infinite summation of cylindrical modes. This solution is based on the original expression for Y_{12} described by Stewart, Golden, and Pridmore-Brown [2], [3], and is more suitable for numerical calculation for some cases.

This work is undertaken for the following reasons. The determination of Y_{12} (or its dual problem for Z_{12} between two dipoles) is not only a classical problem in electromagnetics that has attracted wide attention [1] - [10], but also an integral part in the design of modern conformal arrays [11] - [15]. In the latter application, Y_{12} must be repeatedly calculated for a large number of times. Thus, a simple closed-form solution should greatly reduce the computation effort and, furthermore, provide a better physical insight for the design problem as the "cause" and "effect" can be readily identified in a closed-form solution.

The organization of this paper is as follows. In Section 2, we first define Y_{12} , and then give the final form of its approximate solution. Discussions and numerical results are presented in Section 3. In the

last two sections (4 and 5), the derivations of both the approximate and the exact modal solutions of Y_{12} are given. Fock functions used in the text are described in the Appendix.

2. APPROXIMATE FORMULA FOR MUTUAL ADMITTANCE

Referring to Figure 1, consider two slots on the surface of an infinitely long conducting cylinder with radius R . The orientation of the slots may be either circumferential (Figure 1b where $a_n > b_n$, $n = 1, 2$), or axial (Figure 1c where $a_n < b_n$). The problem is to determine the mutual admittance between these two slots when kR is large.

First let us define mutual admittance. Throughout this work we always assume that

$$(i) \text{ the slots are thin, and} \quad (2.1a)$$

$$(ii) \text{ their length is roughly a half-wavelength.} \quad (2.1b)$$

Then the aperture field in each slot can be adequately approximated by a simple cosine distribution, which is the so-called "one-mode" approximation. For example, if slot 1 is circumferential (Figure 1b), its aperture field under the "one-mode" approximation is given by

$$\vec{E} = V_1 \vec{e}_1, \quad \vec{H} = I_1 \vec{h}_1 \quad (2.2a)$$

where

$$\vec{e}_1 = \hat{z} \sqrt{\frac{2}{a_1 b_1}} \cos \frac{\pi}{a_1} y, \quad \vec{h}_1 = \hat{x} \times \vec{e}_1 \quad (2.2b)$$

$$y = R\phi. \quad (2.2c)$$

(V_1, I_1) are respectively the modal (voltage, current) of slot 1. The mutual admittance Y_{12} is defined by

$$Y_{12} = Y_{21} = \frac{I_{21}}{V_1} \quad (2.3)$$

where I_{21} is the induced current in slot 2 when slot 1 is excited by a voltage V_1 and slot 2 is short-circuited. An alternative expression for Y_{12} is

$$Y_{12} = \frac{1}{V_1 V_2} \iint_{A_2} \vec{E}_2 \times \vec{H}_1 \cdot d\vec{s}_2 \quad (2.4)$$

where

A_2 = aperture of slot 2

\vec{H}_1 = magnetic field when slot 1 is excited with voltage V_1 , and slot 2 is covered by a perfect conductor

\vec{E}_2 = electric field when slot 2 is excited with voltage V_2 , and slot 1 is covered by a perfect conductor.

Because $\vec{H}_1 = I_{21} \vec{h}_2$ and $\vec{E}_2 = V_2 \vec{e}_2$, it is a simple matter to verify that (2.3) and (2.4) are equivalent [16].

There is an alternative definition of mutual admittance. Instead of (2.2), a modal voltage \bar{V}_1 (with a bar) may be defined through the expression for the aperture field of slot 1 as follows:

$$\vec{E} = \hat{z} \frac{1}{b} \bar{V}_1 \cos \frac{\pi}{a_1} y, \quad (2.5a)$$

or equivalently

$$\bar{V}_1 = \int_0^b (\hat{z} \cdot \vec{E})_{y=0} dz. \quad (2.5b)$$

Then a different mutual admittance \bar{Y}_{12} is defined by (2.4) after replacing (V_1, V_2) by (\bar{V}_1, \bar{V}_2) . It can be easily shown that

$$\bar{Y}_{12} = \frac{1}{2} \left(\frac{a_1 a_2}{b_1 b_2} \right)^{1/2} Y_{12}. \quad (2.6)$$

Two remarks are in order: (i) In the limiting case that b_1 and $b_2 \rightarrow 0$, Y_{12} goes to zero as $(b_1 b_2)^{1/2}$, whereas \bar{Y}_{12} approaches a constant independent of b_1 and b_2 . (ii) For the special case $a_1 = a_2 = \lambda/2$ and

$R \rightarrow \infty$, it is \bar{Y}_{12} , not Y_{12} , that is identical to the mutual impedance Z_{12} between two corresponding dipoles calculated by the classical Carter's method [5], [8], [9]. (iii) When the slots are excited by waveguides (transmission lines), one often uses Y_{12} (\bar{Y}_{12}). From here on, we will concentrate on Y_{12} instead of \bar{Y}_{12} .

For the two slots in Figure 1, the final form of an approximate solution of Y_{12} is as follows (for $\exp +j\omega t$ time convention):

Circumferential slots

$$Y_{12} = -\frac{8}{\pi} (a_1 b_1 a_2 b_2)^{1/2} S(b_1 \sin \theta) S(b_2 \sin \theta) C(a_1 \cos \theta) C(a_2 \cos \theta) \bar{g}_\phi \quad (2.7a)$$

Axial slots

$$Y_{12} = -\frac{8}{\pi} (a_1 b_1 a_2 b_2)^{1/2} S(a_1 \cos \theta) S(a_2 \cos \theta) C(b_1 \sin \theta) C(b_2 \sin \theta) \bar{g}_z. \quad (2.7b)$$

The various factors in (2.7) are explained below. S and C are simple trigonometric functions

$$S(x) = \frac{\sin(kx/2)}{(kx/2)}, \quad C(x) = \frac{\cos(kx/2)}{1 - (kx/\pi)^2}. \quad (2.8)$$

The (simplified) Green's functions \bar{g}_ϕ and \bar{g}_z are given by

$$\begin{aligned} \bar{g}_\phi = G(s) & \left[v(\xi) \left(\sin^2 \theta + \frac{1}{ks} \cos 2\theta \right) + \frac{1}{ks} u(\xi) \cos^2 \theta \right. \\ & \left. + ju'(\xi) (\sqrt{2} kR \cos \theta)^{-2/3} \sin^4 \theta \right] \end{aligned} \quad (2.9a)$$

$$\bar{g}_z = G(s) \left[v(\xi) \left(\cos^2 \theta - \frac{1}{ks} \cos 2\theta \right) + \frac{1}{ks} u(\xi) \sin^2 \theta \right] \quad (2.9b)$$

where

$$G(s) = \frac{k^2 Y_0}{2\pi j} \frac{e^{-jks}}{ks}, \quad Y_0 = \frac{1}{120\pi} \quad (2.10)$$

$$\xi = (k \cos^4 \theta / 2R^2)^{1/3} s \quad (2.11)$$

$$s = \sqrt{z_0^2 + (R\phi_0)^2} \quad (2.12)$$

$$\theta = \tan^{-1} (z_0/R\phi_0) . \quad (2.13)$$

The Fock functions u and v are explained in the Appendix. In the limiting case $kR \rightarrow \infty$ (slots on a planar surface), (2.9) is further simplified to become

$$\begin{aligned} \bar{g}_\phi &= G(s) \left[\sin^2 \theta + \frac{1}{ks} (2 - 3 \sin^2 \theta) \right] , \\ \bar{g}_z &= G(s) \left[\cos^2 \theta + \frac{1}{ks} (2 - 3 \cos^2 \theta) \right] , \end{aligned} \quad kR \rightarrow \infty . \quad (2.14)$$

The formula in (2.4) is an approximate solution, valid under the condition

$$kR \gg 1 \quad \text{and} \quad ks \gg 1 . \quad (2.15)$$

The numerical accuracy of the formula is discussed in Section 3, and its derivation in Section 4.

3. NUMERICAL RESULTS AND DISCUSSION

For the two slots in Figure 1, the final form of the approximate solution of Y_{12} is given in (2.7). Generally speaking, its accuracy is good only if

- (i) the size of the slots is small in terms of wavelength, and/or
- (ii) the separation of the slots is large in terms of wavelength.

In this section, we will give some numerical examples to illustrate the quantitative accuracy of (2.7).

(A) Circumferential Slot - (Figures 2 and 3). The size of each slot is $0.5\lambda \times 0.2\lambda$, and the cylinder radius is 1λ . Y_{12} is presented in (dB, normalized phase) format, where $\text{dB} = 20 \log_{10} (|Y_{12}| \text{ in mho})$ and normalized phase is equal to $\text{Arg}(Y_{12} \exp jks)$. Three solutions of Y_{12} are given: the UI exact modal solution calculated from (5.2), (5.3) and (5.9); the UI asymptotic solution reported in [1]; and the approximate solution in (2.7). We note that all the three solutions are in an excellent agreement.

(B) Percentage Error vs. Slot Position - (Figures 4 and 5). In these figures, the coordinates of each point determine the center-to-center distance, in ϕ and z directions between two slots. The pairs of numbers in the parentheses are the percentage error in magnitude and the absolute error in phase of Y_{12} as calculated by the approximate formula, respectively. For the circumferential slots (Figure 4), the accuracy is generally very good. For the axial slots (Figure 5), the approximate formula gives erratic results (as high as 27 percent error in magnitude) when the two slots are very closely displaced in the ϕ -direction. The reason for this inaccuracy is that the surface field due to a magnetic dipole varies very rapidly as a function of z when the observation point is close by.

(C) Accuracy vs. Cylinder Radius (Figure 6). The accuracy of the approximate formula is not sensitive to the radius of the cylinder.

(D) Planar Slots (Tables 1 and 2). The mutual admittance Y_{12} between two identical slots of dimension ($a = 0.69\lambda$, $b = 0.3\lambda$) on an infinite conducting plane is calculated as a function of z_0 and y_0 (the center-to-center distance between two slots in z and y directions, see Figure 1b). Y_{12} is given in (dB, phase in degrees). In both E-plane and H-plane couplings, the approximate formula is accurate when the separation is at least two wavelengths (2.6"). It should be also remarked that the present slots ($0.69\lambda \times 0.3\lambda$) are relatively large. The accuracy of the approximate formula is better when the slots are smaller.

4. DERIVATION OF APPROXIMATE FORMULA

We will now give the derivation of the formula in (2.7a)[that of (2.7b) is very similar]. Consider a circumferential infinitesimal dipole located at Q' on the surface of a cylinder (Figure 7) which is described by the magnetic current density

$$\vec{K} = \hat{\phi} \frac{1}{R} \delta(r - R) \delta(\phi) \delta(z) . \quad (4.1)$$

At an observation point Q on the cylinder, the ϕ -component of the \vec{H} field, denoted by g_ϕ , is determined in Eq. (2.16b) of [1], which reads in the present notation,

$$\begin{aligned} g_\phi(t, \alpha) \sim G(t) & \left\{ v(\xi) \left[\sin^2 \alpha + \frac{1}{kt} \cos 2\alpha \right] \right. \\ & + \left(\frac{1}{kt} \right) u(\xi) \left[\cos^2 \alpha \left(1 - \frac{2j}{kt} \right) + \left(\frac{1}{kt} \right) \sin^2 \alpha \right] \\ & + j(\sqrt{2} kR / \cos^2 \alpha)^{-2/3} \\ & \cdot \left[v'(\xi) \sin^2 \alpha + \left(\tan^4 \alpha + \frac{1}{kt} \right) u'(\xi) \cos^2 \alpha \right] \Big\} \end{aligned} \quad (4.2)$$

where (t, α) are the cylindrical coordinates of Q with respect to the origin at Q' on a developed cylinder, and

$$\xi = (k \cos^4 \theta / 2R^2)^{1/3} t . \quad (4.3)$$

The formula in (4.2) is mainly based on a classical work of Fock [17], and contains a modification that introduces a field dependence on the surface curvature in the binormal direction of the surface ray (see Section 6 of [1]). This formula is asymptotically valid for $kR \rightarrow \infty$, and may be used to calculate the field at any point on the cylindrical surface.

Making use of the Green's function in (4.2), we next calculate the surface field H_ϕ due to slot 1 on a cylinder (Figure 8). The aperture distribution of slot 1 is described in (2.2a), which may be replaced by an equivalent magnetic current density (p. 108 of [18])

$$\vec{K} = \hat{\phi} \delta(r - R) \sqrt{\frac{2}{a_1 b_1}} V_1 \cos(\pi y/a_1) \quad (4.4)$$

Then, H_ϕ at an observation point Q is obtained by superposition, namely,

$$H_\phi(Q) = \sqrt{\frac{2}{ab}} V_1 \iint_{A_1} \left(\cos \frac{\pi}{a_1} y \right) g_\phi(t, \alpha) dy dz \quad (4.5)$$

The expression for calculating the mutual admittance Y_{12} between the two slots in Figure 8 is given in (2.4). Note that \vec{E}_2 is described much as (2.2a) and \vec{H}_1 in (4.5). Then (2.4) becomes

$$Y_{12} = \frac{-2}{\sqrt{a_1 b_1 a_2 b_2}} \iint_{A_1} dy dz \iint_{A_2} dy_2 dz_2 \left(\cos \frac{\pi}{a_1} y \right) \left(\cos \frac{\pi}{a_2} y_2 \right) g_\phi(t, \alpha) \quad (4.6)$$

The distance t in (4.6) is given by

$$t = [(s \cos \theta + y_2 - y)^2 + (s \sin \theta + z_2 - z)]^{1/2} \quad (4.7)$$

If s is large relative to the length of either slot, t may be approximated by

$$t \approx \begin{cases} s & (4.8a) \end{cases}$$

$$t \approx \begin{cases} s \left(1 + \cos \theta \frac{y_2 - y}{s} + \sin \theta \frac{z_2 - z}{s} \right) & (4.8b) \end{cases}$$

In evaluating the magnitude of g_ϕ in (4.6), we use the approximation in (4.8a), whereas in evaluating its progressive phase term, we use (4.8b).

Then the integrals in (4.6) can be explicitly carried out. After a further approximation by dropping the terms of order $(ks)^{-3} = (kt)^{-3}$ in (4.2), we obtain the desired solution of Y_{12} in (2.7a).

5. EXACT MODAL SOLUTION

The admittance Y_{12} defined in (2.3) may be calculated exactly by using cylindrical modes, as has been done by Stewart, Golden and Pridmore-Brown [2], [3]. Extensive numerical results of Y_{12} calculated from the SGP solution are reported in [13], [14]. As will be explained below, the SGP solution is not suitable for numerical calculations when the slot separation z_0 (Figure 1a) is large. In this section, we will derive an alternative modal solution of Y_{12} which does not have this difficulty.

Let us first consider the circumferential slots shown in Figure 1b. For the case that $a_1 = a_2 = a$ and $b_1 = b_2 = b$ (identical slots), the mutual admittance Y_{12} is given in Eq. (8) of [3]*, which reads in the present notation,

$$Y_{12} = \int_{-\infty}^{\infty} dk_z \sum_{m=-\infty}^{\infty} \psi(m, k_z) G(m, k_z) e^{-j(m\phi_0 + k_z z_0)} \quad (5.1a)$$

where

$$\psi(m, k_z) = \frac{ab}{8\pi^2 R} \frac{\sin^2(k_z b/2)}{(k_z b/2)^2} \cdot \left\{ \frac{\sin(m\phi_a + \pi/2)}{(m\phi_a + \pi/2)} + \frac{\sin(m\phi_a - \pi/2)}{(m\phi_a - \pi/2)} \right\}^2 \quad (5.1b)$$

$$\phi_a = (a/2R)$$

$$G(m, k_z) = Y_0 \left[\frac{jk}{k_t} \frac{H_m^{(2)'}(k_t R)}{H_m^{(2)}(k_t R)} + \left(\frac{mk_z}{k_t^2 R} \right)^2 \frac{k_t}{jk} \frac{H_m^{(2)}(k_t R)}{H_m^{(2)'}(k_t R)} \right] \quad (5.1c)$$

* The multiplication factor 2 in the definition of ϕ_b in [3] is a misprint and should be removed.

$$k_t = \begin{cases} \sqrt{k^2 - k_z^2} & , \text{ if } k \geq k_z \\ -j \sqrt{k_z^2 - k^2} & , \text{ if } k \leq k_z \end{cases}$$

Rewrite Y_{12} in terms of its real and imaginary parts:

$$Y_{12} = G + jB \quad (5.2)$$

It can be shown that G is given by

$$G = \int_0^k \sum_{m=0}^{\infty} \frac{\cos m\phi_0}{\epsilon_m} \cos k_z z_0 \psi(m, k_z) R(m, k_z) dk_z \quad (5.3a)$$

where

$$R(m, k_z) = \frac{2}{\pi k_t R} \cdot \frac{k}{k_t} \cdot \left[\frac{1}{M_m^2(k_t R)} + \left(\frac{mk_z}{k_t k R} \right)^2 \frac{1}{N_m^2(k_t R)} \right] \quad (5.3b)$$

$$M_m^2(\chi) = J_m^2(\chi) + Y_m^2(\chi) \quad (5.3c)$$

$$N_m^2(\chi) = J_m'^2(\chi) + Y_m'^2(\chi) \quad (5.3d)$$

$$\epsilon_m = \begin{cases} 2, & m = 0 \\ 1, & m \neq 0 \end{cases} \quad (5.3e)$$

We note that G contains a *finite* integral and can be evaluated in a straightforward manner by standard numerical integration techniques. The imaginary part of Y_{12} is given by

$$B = \int_{C_1} \sum_{m=0}^{\infty} \frac{\cos m\phi_0}{\epsilon_m} \cdot \cos k_z z_0 \cdot \psi(m, k_z) \cdot W(m, k_z) dk_z \quad (5.4a)$$

where the integration contour C_1 is shown in Figure 9 and

$$W(m, k_z) = \begin{cases} \frac{k}{k_t} (J_m J'_m + Y_m Y'_m) \left[\frac{1}{M_m^2(k_t R)} - \left(\frac{mk_z}{k_t k R} \right)^2 \frac{1}{N_m^2(k_t R)} \right], & \text{if } k > k_z \\ \frac{-k}{|k_t|} \left[\frac{K'_m(|k_t| R)}{K_m(|k_t| R)} - \left(\frac{mk_z}{|k_t| k R} \right)^2 \frac{K_m(|k_t| R)}{K'_m(|k_t| R)} \right], & \text{if } k < k_z \end{cases} \quad (5.4b)$$

The computation of B as given in (5.4a) can be quite laborious because (i) the integration with respect to k_z is of infinite range, and the factor $\cos k_z z$ is highly oscillatory for large kz_0 , (ii) $W(m, k_z)$ has nonintegrable singularities of opposite sign on both sides of $k_z = k$ (iii) $W(m, k_z)$ decays slowly with respect to m and k_z .

To circumvent the above difficulties in evaluating B, we adopt a method introduced by Duncan [19] in the study of cylindrical antenna problems.

Let us rewrite (5.4a)

$$B = \text{Im} \left\{ \sum_{m=0}^{\infty} \frac{\cos m\phi_0}{\epsilon_m} \left[-j \int_{C_1} F(m, k_z) \sin k_z z_0 dk_z + \int_{C_1} F(m, k_z) e^{jk_z z_0} dk_z \right] \right\} \quad (5.5)$$

where

$$F(m, k_z) = [R(m, k_z) + jW(m, k_z)] \psi(m, k_z) \quad (5.6)$$

The imaginary part of the first term inside the bracket of (5.5) is

$$\text{Im} \left\{ -j \int_{C_1} F(m, k_z) \sin k_z z_0 dk_z \right\} = - \int_0^k R(m, k_z) \psi(m, k_z) \sin k_z z_0 dk_z \quad (5.7)$$

In order to compute the imaginary part of the second term of (5.5), the integration contour C_1 is deformed into C_2 (Figure 9) according to the theory of complex variables. This manipulation leads to

$$\text{Im} \int_{C_1} F(m, k_z) e^{jk_z z_0} dk_z = \text{Im} \int_{C_2} F(m, k_z) e^{jk_z z_0} dk_z \quad (5.8)$$

Make the change of variable $k_z = j\eta$ in (5.8). Substitution of the resultant equation and (5.7) into (5.5) gives

$$B = \sum_{m=0}^{\infty} \frac{\cos m\phi_0}{\epsilon_m} \left\{ - \int_0^k R(m, k_z) \psi(m, k_z) \sin k_z z_0 dk_z + \int_0^{\infty} R(m, j\eta) \psi(m, j\eta) e^{-\eta z_0} d\eta \right\}. \quad (5.9)$$

Our final expression for Y_{12} is given in (5.2), with its real part G in (5.3) and its imaginary part B in (5.9). Several remarks are in order: (i) Not only G but also B is determined by $R(m, k_z)$, which is much simpler than $W(m, k_z)$ defined in (5.4b). (ii) B contains only a finite integral. (iii) The infinite integral in B , i.e., the second integral in (5.9a), contains an exponentially decaying factor $\exp[-z_0 - a]\eta$ in its integrand. The emergence of the evaluation of B is faster for larger z_0 . This is in contrast to the original expression of Y_{12} given in (5.1). (iv) There is no nonintegrable singularity in (5.3) or (5.9).

The same method applies to the derivation of an alternative expression of Y_{12} for two identical axial slots (Figure 1c with $a_1 = a_2 = a$ and $b_1 = b_2 = b$). We give below only the final result:

$$Y_{12} = - \frac{abY_0}{\pi k R^2} \sum_{m=0}^{\infty} \frac{\cos m\phi_0}{\epsilon_m} \left[\int_0^k \phi(m, k_z) e^{-jk_z z_0} \frac{dk_z}{N_m^2(k_z R)} + j \int_0^{\infty} \phi(m, j\eta) e^{-\eta z_0} \frac{d\eta}{N_m^2(R\sqrt{\eta^2 + k^2})} \right] \quad (5.10a)$$

where

$$\phi(m, k_z) = \left[\frac{\sin(m\phi_a)}{(m\phi_a)} \cdot \frac{\cos(k_z b/2)}{(k_z b/2)^2 - (\pi/2)^2} \right]^2. \quad (5.10b)$$

In summary, the alternative expression of the exact modal solutions is given in (5.2), (5.3), and (5.9) for two identical circumferential slots, and in (5.10) for two identical axial slots.

APPENDIX

FOCK FUNCTIONS

In this appendix we define and list some useful formulas of the functions: $w_1(t)$, $w_2(t)$, $v(\xi)$, $u(\xi)$, and $v_1(\xi)$. These functions are commonly known as Fock functions.

(i) Definition: For a complex t and a real ξ ,

$$w_1(t) = \frac{1}{\sqrt{\pi}} \int_{\Gamma_1} dz \exp \left(tz - \frac{1}{3} z^3 \right) \quad (\text{A-1})$$

$$w_2(t) = \frac{1}{\sqrt{\pi}} \int_{\Gamma_2} dz \exp \left(tz - \frac{1}{3} z^3 \right) = w_1^*(t) \quad (\text{A-2})$$

$$v(\xi) = \frac{1}{2} e^{j\pi/4} \xi^{1/2} \frac{1}{\sqrt{\pi}} \int_{\Gamma_1} \frac{w_2(t)}{w_2'(t)} e^{-j\xi t} dt \quad (\text{A-3})$$

$$u(\xi) = e^{j3\pi/4} \xi^{3/2} \frac{1}{\sqrt{\pi}} \int_{\Gamma_1} \frac{w_2'(t)}{w_2(t)} e^{-j\xi t} dt \quad (\text{A-4})$$

$$v_1(\xi) = e^{j3\pi/4} \xi^{3/2} \frac{1}{\sqrt{\pi}} \int_{\Gamma_1} t \frac{w_2(t)}{w_2'(t)} e^{-j\xi t} dt \quad (\text{A-5})$$

where integration contour Γ_1 (Γ_2) goes from ∞ to 0 along the line

$\text{Arg } z = -2\pi/3$ ($+2\pi/3$) and from 0 to ∞ along the real axis. Because of

different time conventions, $w_1(w_2)$ above is equal to $w_2(w_1)$ defined in [17].

(ii) Residue series representation: For real positive ξ ,

$$v(\xi) = e^{-j\pi/4} \sqrt{\pi} \xi^{1/2} \sum_{n=1}^{\infty} (t'_n)^{-1} e^{-j\xi t'_n} \quad (\text{A-6})$$

$$u(\xi) = e^{j\pi/4} 2\sqrt{\pi} \xi^{3/2} \sum_{n=1}^{\infty} e^{-j\xi t_n} \quad (\text{A-7})$$

$$v_1(\xi) = e^{j\pi/4} 2\sqrt{\pi} \xi^{3/2} \sum_{n=1}^{\infty} e^{-j\xi t'_n} \quad (\text{A-8})$$

$$v'(\xi) = \frac{1}{2} e^{-j\pi/4} \sqrt{\pi} \xi^{-1/2} \sum_{n=1}^{\infty} (1 - j2\xi t'_n) (t'_n)^{-1} e^{-j\xi t'_n} \quad (\text{A-9})$$

$$u'(\xi) = e^{j\pi/4} 3\sqrt{\pi} \xi^{1/2} \sum_{n=1}^{\infty} \left(1 - j\frac{2}{3}\xi t_n\right) e^{-j\xi t_n} \quad (\text{A-10})$$

where $\{t_n\}$ and $\{t'_n\}$ are zeros of $w_2(t)$ and $w'_2(t)$, respectively, and are tabulated in [17] and [1].

(iii) Small argument asymptotic expansion: For real positive ξ and $\xi \rightarrow 0$,

$$v(\xi) \sim 1 - \frac{\sqrt{\pi}}{4} e^{j\pi/4} \xi^{3/2} + \frac{7j}{60} \xi^3 + \frac{7\sqrt{\pi}}{512} e^{-j\pi/4} \xi^{9/2} - 4.141 \times 10^{-3} \xi^6 + \dots \quad (\text{A-11})$$

$$u(\xi) \sim 1 - \frac{\sqrt{\pi}}{2} e^{j\pi/4} \xi^{3/2} + \frac{5j}{12} \xi^3 + \frac{5\sqrt{\pi}}{64} e^{-j\pi/4} \xi^{9/2} - 3.701 \times 10^{-2} \xi^6 + \dots \quad (\text{A-12})$$

$$v_1(\xi) \sim 1 + \frac{\sqrt{\pi}}{2} e^{j\pi/4} \xi^{3/2} - \frac{7j}{12} \xi^3 - \frac{7\sqrt{\pi}}{64} e^{-j\pi/4} \xi^{9/2} + 4.555 \times 10^{-2} \xi^6 + \dots \quad (\text{A-13})$$

$$v'(\xi) \sim \frac{3\sqrt{\pi}}{8} e^{-j3\pi/4} \xi^{1/2} + \frac{7j}{20} \xi^2 + \frac{63\sqrt{\pi}}{1024} e^{-j\pi/4} \xi^{7/2} - 2.485 \times 10^{-2} \xi^5 + \dots \quad (\text{A-14})$$

$$u'(\xi) \sim \frac{3}{4} \sqrt{\pi} e^{-j3\pi/4} \xi^{1/2} + \frac{5j}{4} \xi^2 + \frac{45\sqrt{\pi}}{128} e^{-j\pi/4} \xi^{7/2} - 2.221 \times 10^{-1} \xi^5 + \dots \quad (\text{A-15})$$

(iv) Numerical evaluation: For $\xi \geq \xi_0$, the residue series representation with the first ten terms in the summation may be used. For $\xi \leq \xi_0$, the small argument asymptotic expansion with the first five terms may be used. It has been indicated in [12] that the smoothest crossover is obtained if $\xi_0 = 0.6$. In the present study, we set $\xi_0 = 0.7$, where the difference in the two representations is less than 0.1% in magnitude and 0.9° in phase [1].

REFERENCES

- [1] S. W. Lee and S. Safavi-Naini, "Asymptotic solution of surface field due to a magnetic dipole on a cylinder," University of Illinois at Urbana-Champaign, Electromagnetics Laboratory Report No. 76-11, 1976.
- [2] G. E. Stewart and K. E. Golden, "Mutual admittance for axial rectangular slots in a large conducting cylinder," IEEE Trans. Antennas Propagat., vol. AP-19, pp. 120-122, 1971.
- [3] K. E. Golden, G. E. Stewart, and D. C. Pridmore-Brown, "Approximation techniques for the mutual admittance of slot antennas on metallic cones," IEEE Trans. Antennas Propagat., vol. AP-22, pp. 43-48, 1974.
- [4] J. D. Kraus, Antennas. New York: McGraw-Hill, 1950, Chapter 10.
- [5] E. C. Jordan and K. Balmain, Electromagnetic Waves and Radiating Systems, 2nd Ed., Englewood Cliffs, New Jersey: Prentice-Hall, 1968, Chapter 14.
- [6] J. Galejs, "Self and mutual admittances of waveguides radiating into plasma layers," J. Res. Nat. Bur. Stand.-D, vol. 69D, pp. 179-189, 1965.
- [7] G. V. Borghiotti, "A novel expression for the mutual admittance of planar radiating elements," IEEE Trans. Antennas Propagat., vol. AP-16, pp. 329-333, 1968.
- [8] R. C. Hansen, "Formulation of echelon dipole mutual impedance for computer," IEEE Trans. Antennas Propagat., vol. AP-20, pp. 780-781, 1972.
- [9] R. C. Hansen, "Mutual coupling of slots on a flat ground plane," Rept. No. TR648-1 on Contract N00019-76-0276, R. C. Hansen, Inc., Tarzana, California, 1976.
- [10] Y. Hwang and R. G. Kouyoumjian, "The mutual coupling between slots on an arbitrary convex cylinder," ElectroScience Laboratory, The Ohio State University, Semi-Annual Report 2902-21, 1975; prepared under Grant NGL 36-003-138.
- [11] P. H. Pathak, "Analysis of a conformal receiving array of slots in a perfectly-conducting circular cylinder by the geometrical theory of diffraction," ElectroScience Laboratory, The Ohio State University, Technical Report ESL 3735-2, 1975; prepared under Contract N00140-74-C-6017.
- [12] Z. W. Chang, L. B. Felsen, and A. Hessel, "Surface ray methods for mutual coupling in conformal arrays on cylinder and conical surface," Polytechnic Institute of New York, Final Report (September 1975-February 1976), 1976; prepared under Contract N00123-76-C-0236.

- [13] Z. W. Chang, L. B. Felsen, A. Hessel, and J. Shmoys, "Surface ray method in the analysis of conformal arrays," in Digest of 1976 AP-S International Symposium, University of Massachusetts at Amherst, October 1976, pp. 366-369.
- [14] P. C. Bargeliotis, A. T. Villeneuve, and W. H. Kummer, "Phased array antennas scanned near endfire," Final Report (January 1975-March 1976), Contract N00019-75-0160, Hughes Aircraft Company, Culver City, California, 1976.
- [15] P. C. Bargeliotis, A. T. Villeneuve, and W. H. Kummer, "Conformal phased array breadboard," Quarterly Progress Report (May 1976-August 1976), Contract N00019-76-C-0495, Hughes Aircraft Company, Culver City, California, 1976.
- [16] J. H. Richmond, "A reaction theorem and its application to antenna impedance calculation," IEEE Trans. Antennas Propagat., vol. AP-9, pp. 515-520, 1961.
- [17] V. A. Fock, Electromagnetic Diffraction and Propagation Problems. New York: Pergamon Press, 1965.
- [18] R. F. Harrington, Time Harmonic Electromagnetic Fields. New York: McGraw-Hill, 1961.
- [19] R. H. Duncan, "Theory of the infinite cylindrical antenna including the feedpoint singularity in antenna current," Journal of Research of the National Bureau of Standards - D. Radio Propagation, vol. 66D, pp. 181-188, 1962.

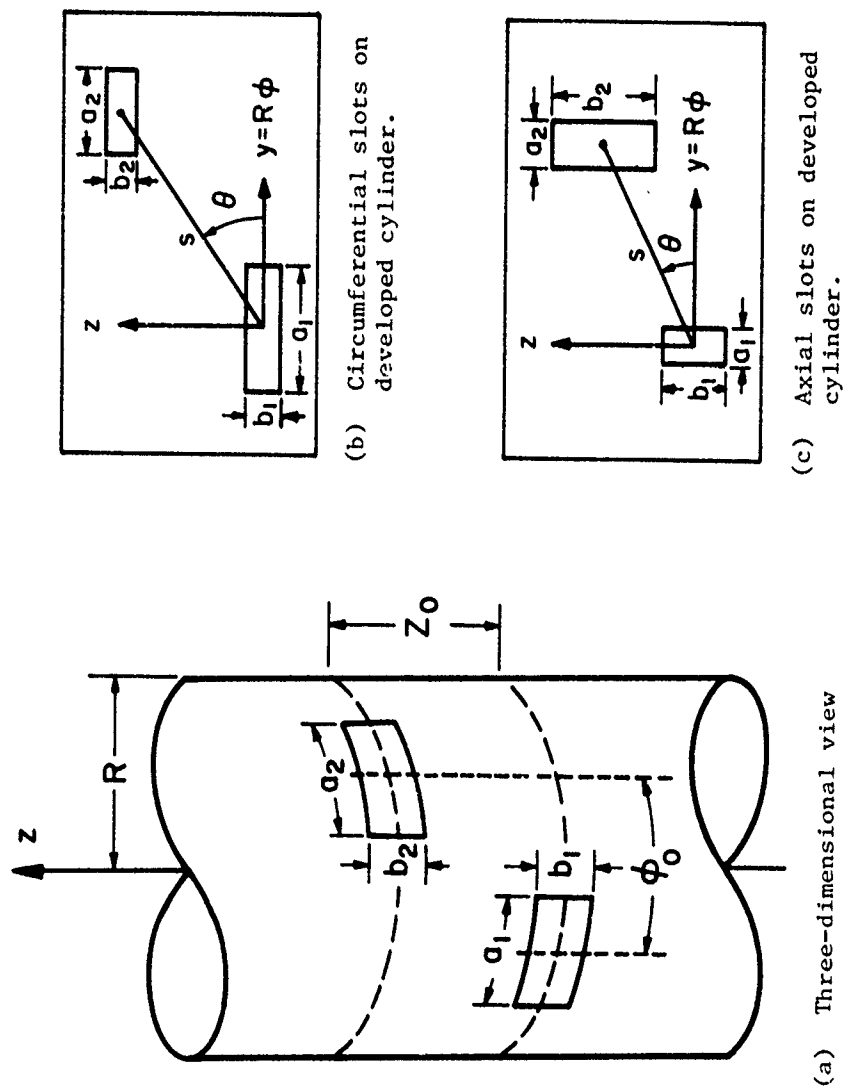


Figure 1. Two slots on the surface of a conducting cylinder.

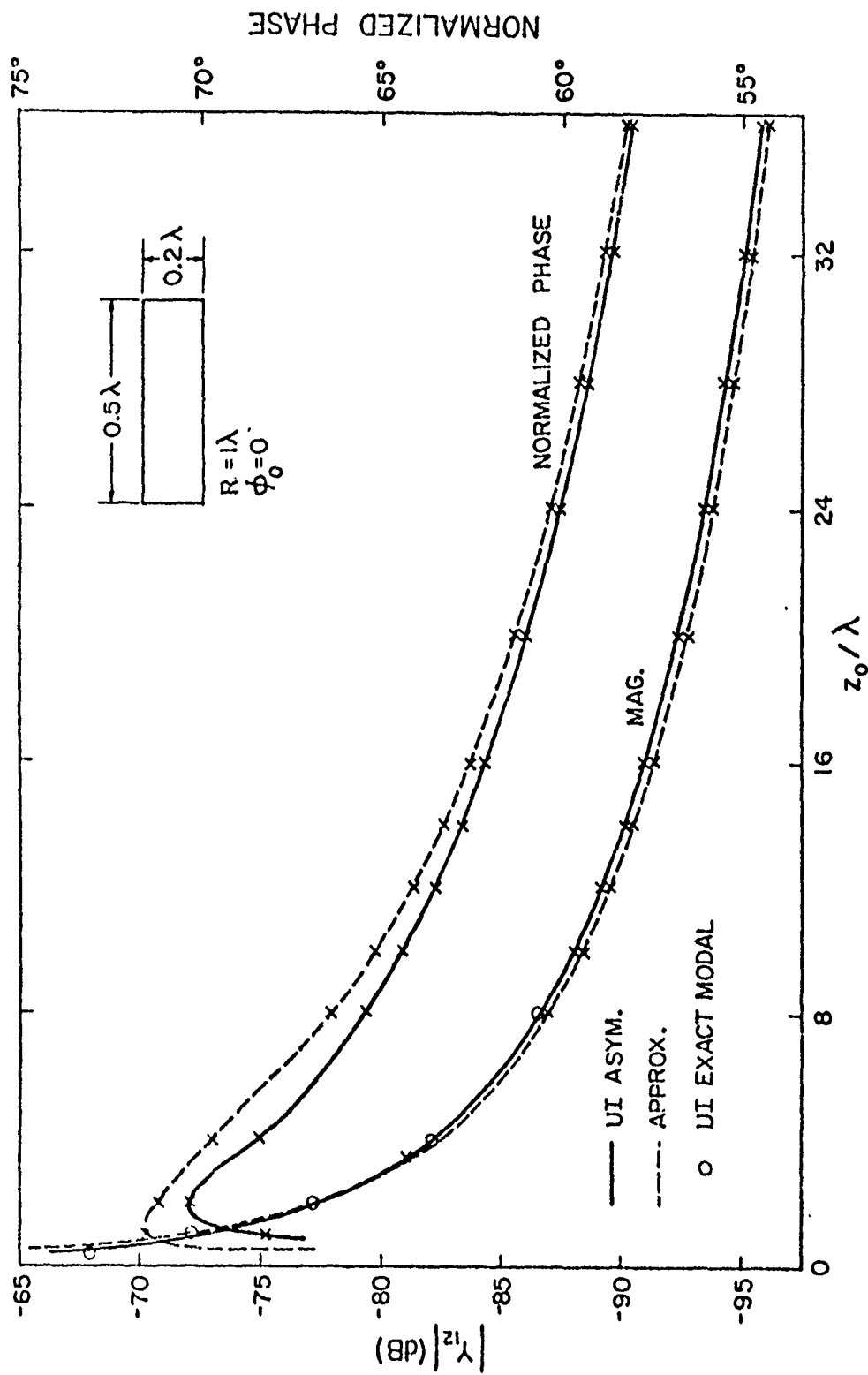


Figure 2. Mutual admittance Y_{12} between two circumferential slots as a function of z_0 .

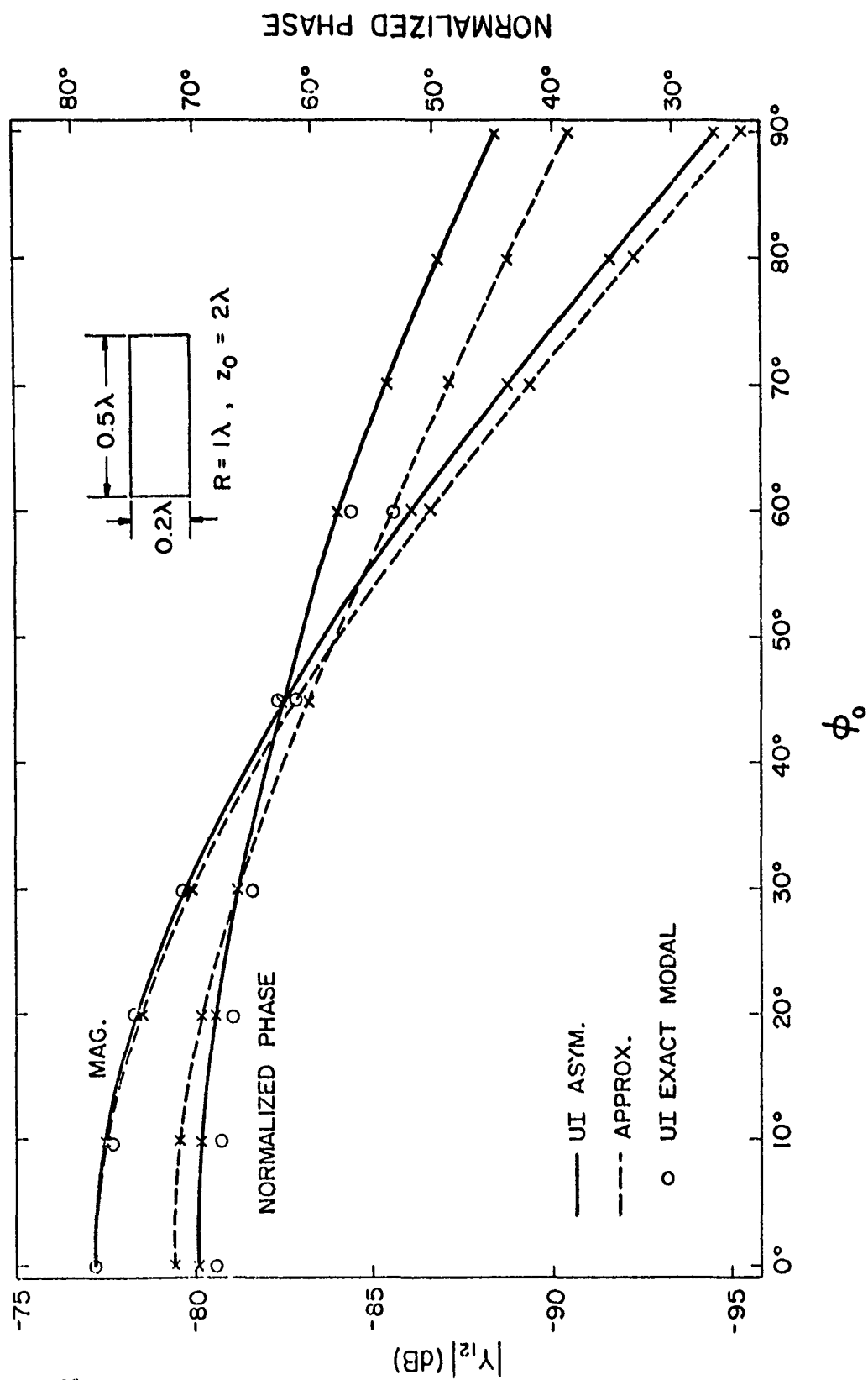


Figure 3. Mutual admittance Y_{12} between two circumferential slots as a function of ϕ_0 .

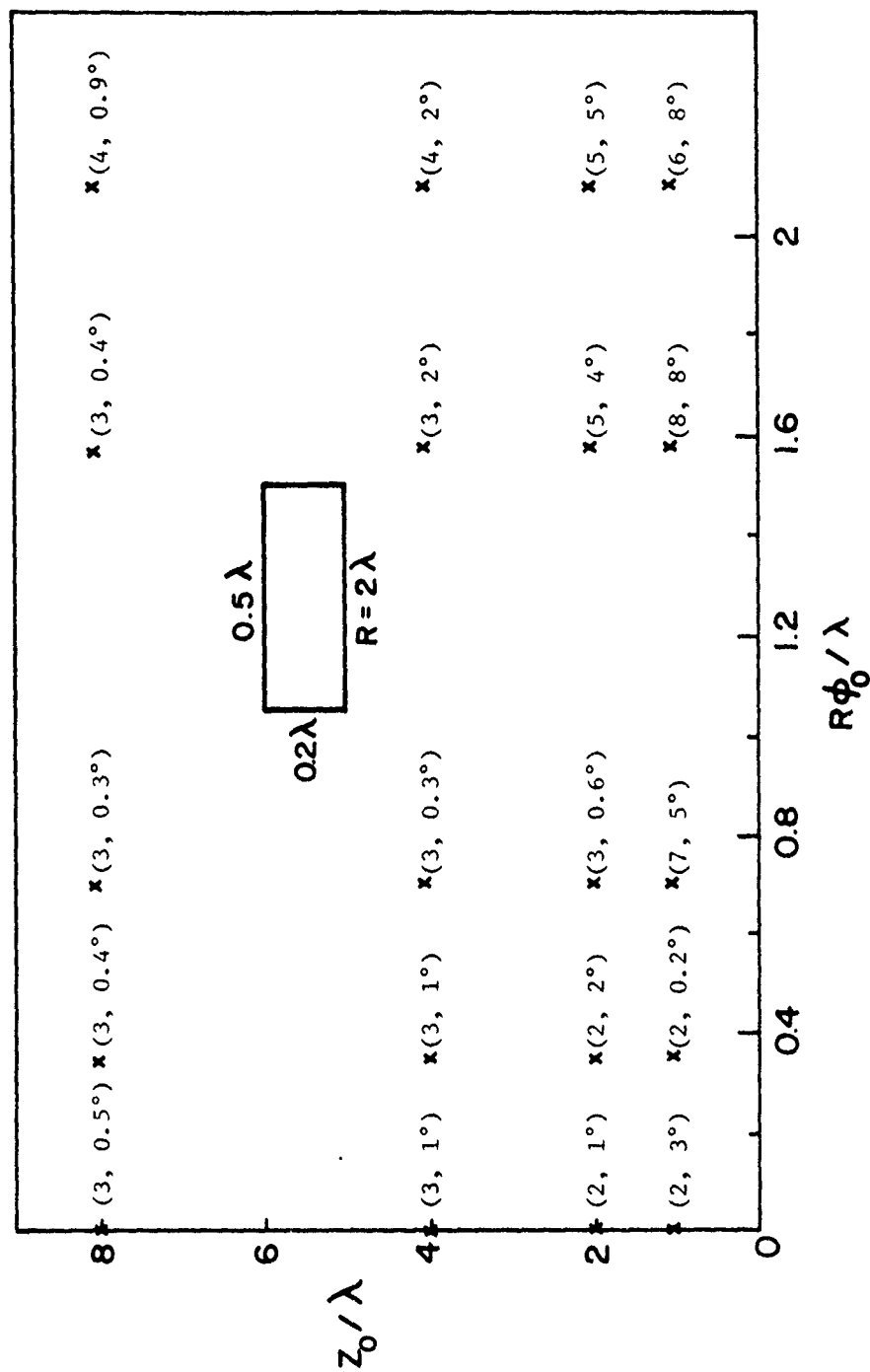


Figure 4. The percentage error in magnitude and absolute error in phase of the approximate formula of Y_{12} of circumferential slots as a function of their relative positions.

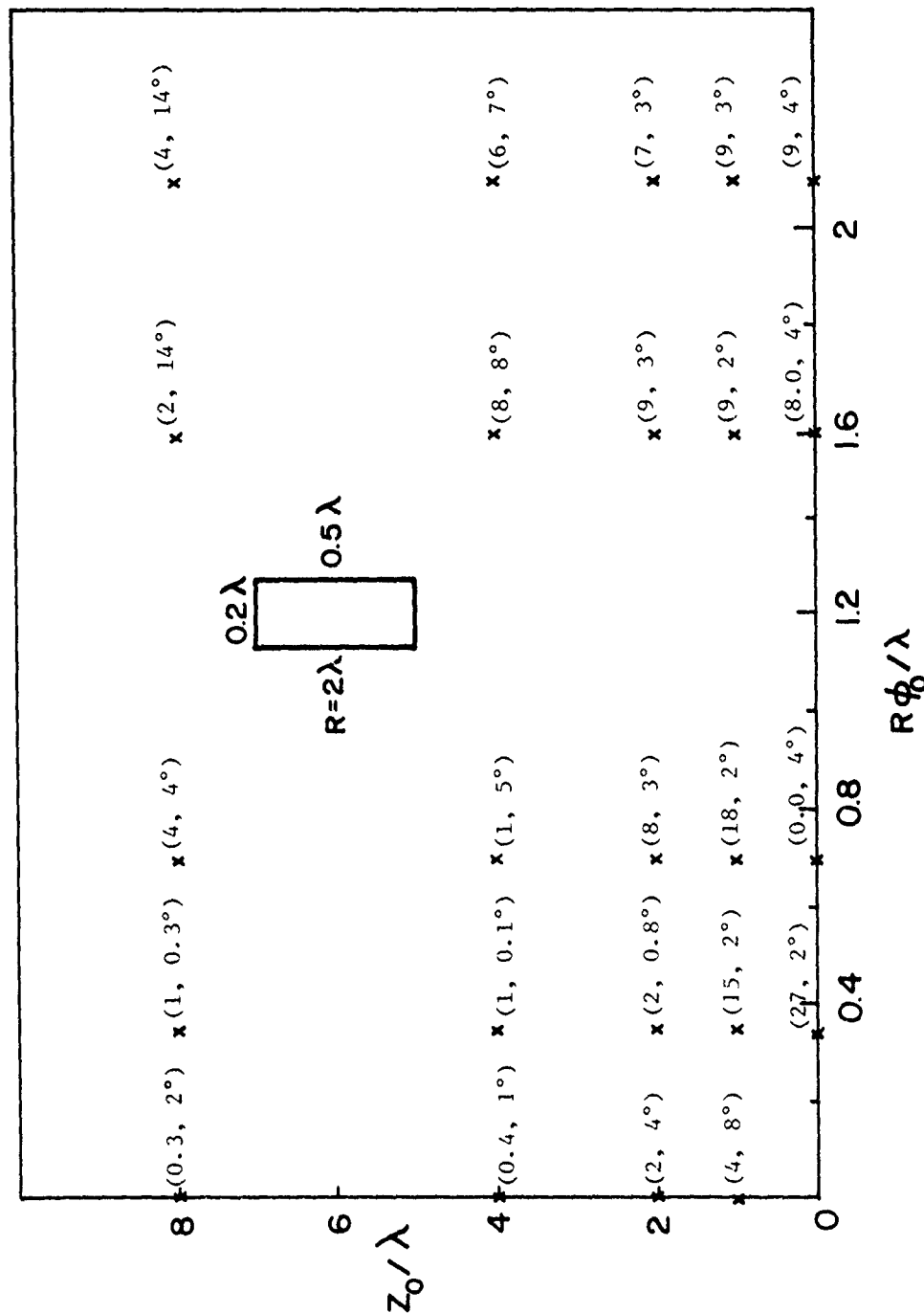


Figure 5. The percentage error in magnitude and absolute error in phase of the approximate formula of Y_{12} of axial slots as a function of their relative positions.

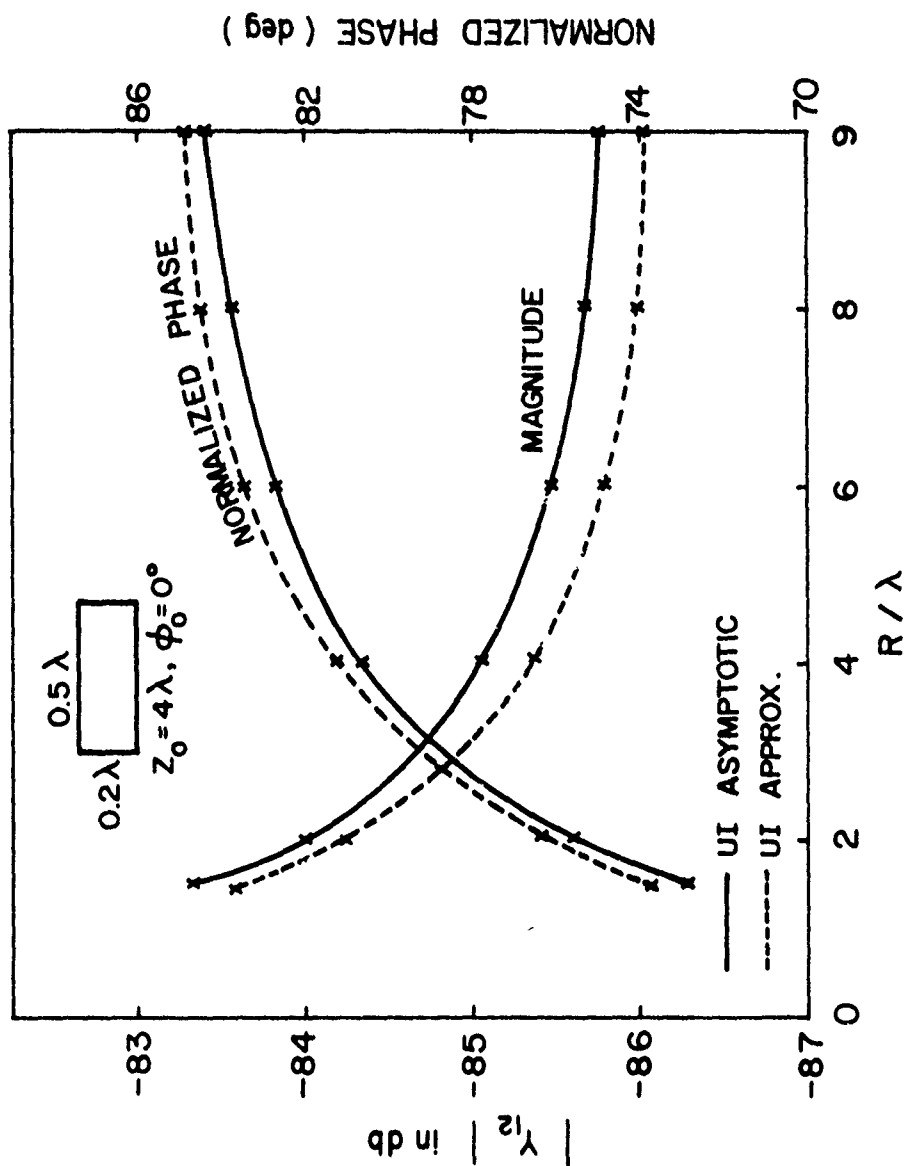


Figure 6. Mutual admittance Y_{12} between two identical circumferential slots as a function of radius R of the cylinder.

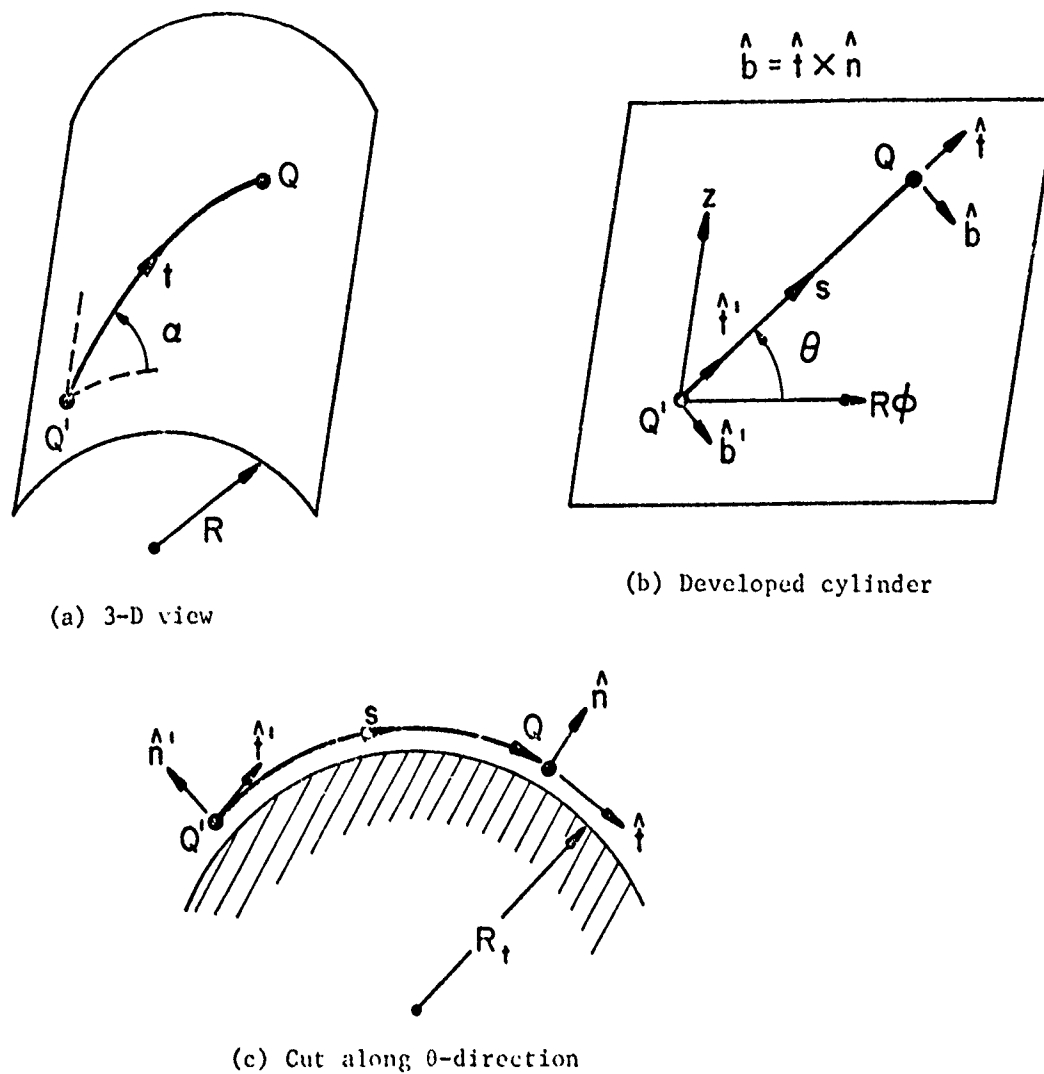


Figure 7. A surface ray from source point Q' to observation point Q on a cylinder of radius R .

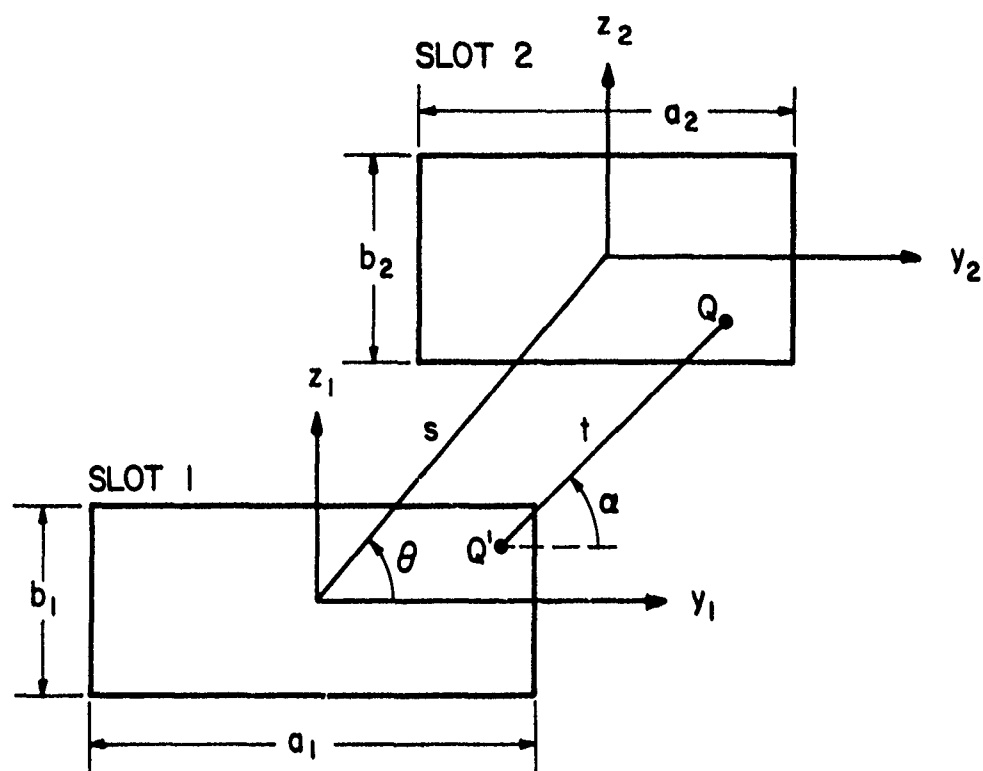


Figure 8. Two circumferential slots on a developed cylinder.

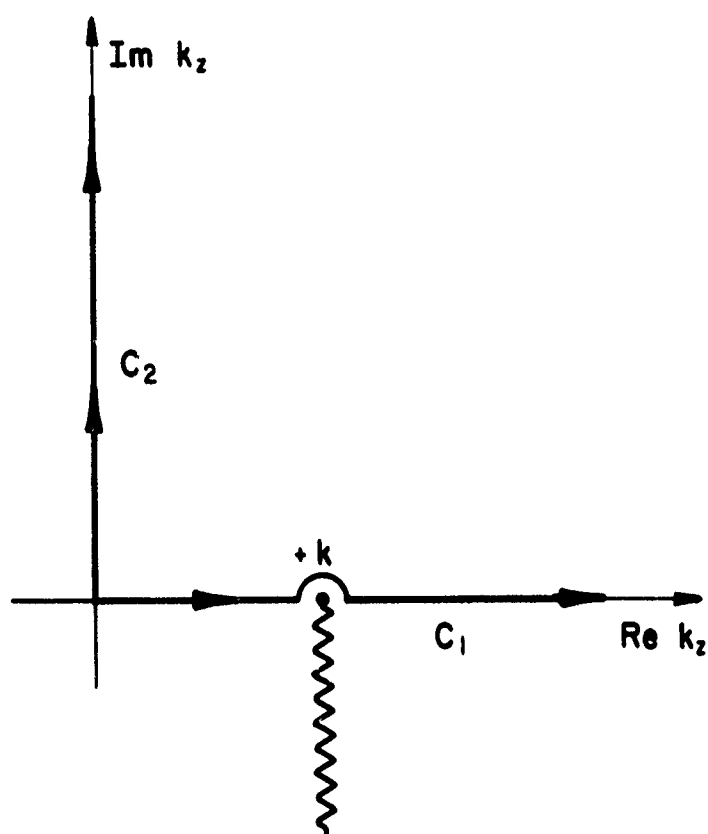


Figure 9. Contours in the complex k_z -plane for the integral in (5.4).

TABLE 1
 MUTUAL ADMITTANCE Y_{12} BETWEEN TWO SLOTS
 ON A PLANE (E-PLANE COUPLING)

z_0	Exact	Approximate
0.5λ	-64.57 dB -110°	-63.25 dB -108°
1λ	-69.48 78°	-69.58 81°
2λ	-75.13 84°	-75.68 85°
3λ	-78.58 86°	-79.22 87°
4λ	-81.06 87°	-81.72 88°
8λ	-87.05 88°	-87.75 89°

TABLE 2
 MUTUAL ADMITTANCE Y_{12} BETWEEN SLOTS ON
 A PLANE (H-PLANE COUPLING)

y_0	Exact	Approximate
1λ	-83.41 dB -53°	-85.04 dB -180°
2λ	-96.75 -168°	-97.09 -180°
3λ	-104.00 -172°	-104.13 -180°
4λ	-109.07 -174°	-109.13 -180°
8λ	-121.18 -177°	-121.17 -180°

ATTACHMENT C

MUTUAL ADMITTANCE OF SLOTS ON A CONE:
SOLUTION BY RAY TECHNIQUE*

MUTUAL ADMITTANCE OF SLOTS ON A CONE:
SOLUTION BY RAY TECHNIQUE*

S. W. Lee
Department of Electrical Engineering
University of Illinois at Urbana-Champaign
Urbana, Illinois 61801

ABSTRACT

An approximate asymptotic Green's function for the surface magnetic field due to a magnetic dipole on a general convex conducting surface is developed. Based largely on the classical work of V. A. Fock and the current GTD recipes, this solution is presented in a form that admits ray interpretations, and can be simply evaluated. We apply the Green's function to calculate the mutual admittance between two slots on a cone. The numerical results are in very good agreement with experiments.

* This work was supported by Naval Air Systems Command under Contract N00019-77-C-0127.

ACKNOWLEDGEMENT

Experimental data of mutual admittance and some theoretical values of self admittance were kindly supplied by G. E. Stewart and K. E. Golden. Valuable discussions with R. C. Hansen, W. H. Kummer, and J. Willis were appreciated.

TABLE OF CONTENTS

	Page
1. INTRODUCTION	1
2. SOLUTION OF THE GREEN'S FUNCTION	3
3. GREEN'S FUNCTION OF A CONE	7
4. MUTUAL ADMITTANCE ON A CONE.	10
5. NUMERICAL RESULTS OF MUTUAL ADMITTANCE	15
6. DERIVATION OF THE GREEN'S FUNCTION	19
REFERENCES	21
APPENDIX A. FOCK FUNCTIONS.	35
APPENDIX B. COMPUTER LISTING FOR CALCULATING MUTUAL ADMITTANCE ON A CONE BASED ON RAY TECHNIQUE	37

1. INTRODUCTION

In the past few years there has been an increasing interest in the study of conformal arrays, where the radiating elements are arranged on a curved conducting surface. A crucial as well as challenging problem in the design of a conformal array is determining the mutual coupling among elements [1], [2]. The present paper addresses itself to one such problem when

- (i) the conducting surface is an infinite cone;
- (ii) the radiating elements are slots with thin width and a length of about a half wavelength; and
- (iii) all the elements are distributed in a region which is away from the cone tip and whose radii of curvature are large in terms of wavelength.

Because of assumption (ii), the aperture field of a slot can be well-approximated by a simple cosine distribution, i.e., the so-called "one-mode approximation." Then it has been established, e.g., p. 53 of [3] or p. 8 of [4], that the calculation of the mutual coupling is reduced to that of a dyadic Green's function due to a magnetic dipole on the same curved conducting surface where the array is at.

The Green's function of a cone can be calculated in the following two ways. With normal modes involving spherical Bessel functions and associated Legendre functions, it can be expressed exactly in terms of a doubly infinite series [5], [6]. The numerical evaluation of such a series, however, is quite tedious, especially at high frequencies. Thus, up to now, no systematic numerical results have been generated from the series. An alternative way to calculate the Green's function is to employ the surface rays, which would yield a simple approximate solution valid

for high frequencies. The general concept of surface rays was introduced by J. B. Keller more than twenty years ago [7] - [9]; however, a uniformly valid formula for fields on the ray has not been developed until recently. Among the several comparable formulas [10] - [12], we chose the one reported in [12] for the present application. The reason for our choice is that, at least for the case of a cylinder, the formula in [12] gives the most accurate numerical results [13].

The organization of this paper is as follows. The formula in [12] for the Green's function applies only to a cylinder. Following the GTD recipe, we generalize it to an arbitrary convex surface with its final solution presented in Section 2, and its derivation in Section 6. In Sections 3 to 5, the Green's function is specialized to a cone and is used to calculate the mutual admittance between two slots on a cone. A conclusion is given in Section 7. The two appendices contain (A) formulas for the Fock functions, and (B) the computer listing for calculating the mutual admittance on a cone.

2. SOLUTION OF THE GREEN'S FUNCTION

Consider a perfectly conducting convex surface Σ (Fig. 1), whose radii of curvature at any point are large in terms of wavelength. At a point Q_1 , described by position vector \vec{r}_1 on Σ , there is a tangential magnetic dipole source described by a magnetic current density (for $\exp + j\omega t$ time convention)

$$\vec{K}(\vec{r}) = \vec{M}\delta(\vec{r} - \vec{r}_1) \quad (2.1)$$

when \vec{M} is the magnetic dipole moment and lies in the tangent plane of Σ . The problem is to determine a high-frequency asymptotic solution of \vec{H} at a general point Q_2 described by position vector \vec{r}_2 on Σ . In other words, the dyadic Green's function for the surface magnetic field for points \vec{r}_1 and \vec{r}_2 is to be found.

Before presenting the solution, let us introduce several definitions and parameters. According to GTD [8], [9], the dominant high-frequency contribution to $\vec{H}(\vec{r}_2)$ is the field on the surface ray from \vec{r}_1 to \vec{r}_2 . The surface ray is a geodesic of Σ . Some of its geometrical properties are described by Fig. 1)

- (i) the arc length \bar{s} which is chosen such that $\bar{s} = 0$ at the source point \vec{r}_1 and $\bar{s} = s$ at the observation point \vec{r}_2 ;
- (ii) the tangent, normal, and binormal, denoted by $(\hat{t}_n, -\hat{n}_n, -\hat{b}_n)$ at \vec{r}_n where $n = 1, 2$; and
- (iii) its two radii of curvature $R_t(\bar{s})$, and $R_b(\bar{s})$ of Σ at point \bar{s} in the directions of tangent, and binormal, respectively.

(On a general convex surface, both radii are nonnegative.)

From the above parameters, we may calculate the following quantities that are needed for the solution of the Green's function:

(i) The large parameter in our asymptotic expansion of the Green's function is

$$m(\bar{s}) = \left[\frac{1}{2} k R_t(\bar{s}) \right]^{1/3}, \quad (2.2)$$

which is a function of position along the ray from \vec{r}_1 to \vec{r}_2 .

(ii) A distance parameter from \vec{r}_1 to \vec{r}_2 is defined by

$$\xi = \int_{\vec{r}_1}^{\vec{r}_2} \frac{k}{2m^2(\bar{s})} d\bar{s}. \quad (2.3)$$

For the special case when R_t is not a function of \bar{s} (constant ray curvature), ξ is reduced to $(ks/2m^2)$, a well-known parameter introduced first by Fock [14].

(iii) The ray curvatures at the source and observation points enter in a parameter defined by

$$\tau = \left[\frac{ks}{2m(0) m(s) \xi} \right]^{1/2}, \quad (2.4)$$

which is positive real for a convex surface, and is reduced to unity for the special case of a constant ray curvature.

(iv) Consider a small pencil of surface rays originating from \vec{r}_1 and propagating toward \vec{r}_2 (Fig. 1). The angle extended by the pencil at \vec{r}_1 is $d\psi_1$, and that at \vec{r}_2 is $d\psi_2$. The divergence factor DF of the pencil is defined by

$$DF = \left(\frac{s d\psi_1}{\rho d\psi_2} \right)^{1/2} \quad (2.5)$$

where ρ is the caustic distance of the wavefront at \vec{r}_2 and is always positive. For example, if Σ is a sphere and \vec{r}_1 is the north pole, DF at

point $\vec{r}_2 = (r, \theta, \phi)$ is

$$DF = \left(\frac{\theta}{\sin \theta} \right)^{1/2}$$

which varies from one at the north pole ($\theta = 0$) to infinity at the south pole ($\theta = \pi$) as \vec{r}_2 moves along a great circle.

(v) The "mean" radii of curvature between \vec{r}_1 and \vec{r}_2 are defined by

$$\bar{R}_t = [R_t(0) R_t(s)]^{1/2} \quad (2.6a)$$

$$\bar{R}_b = [R_b(0) R_b(s)]^{1/2} \quad (2.6b)$$

Throughout this work, we always assume that Σ is a smooth surface with a slowly varying curvature. Then (\bar{R}_t, \bar{R}_b) represents a sort of average value of radii of curvature along the ray.

Return to the electromagnetic problem in Fig. 1. We assume that $m(\bar{s})$ is large and is slowly varying for all \bar{s} in the range $0 \leq \bar{s} \leq s$. Then an approximate asymptotic solution for the surface magnetic field at \vec{r}_2 due to the dipole source in (2.1) is given by

$$\vec{H}(\vec{r}_2) \approx \vec{M} \cdot (\hat{b}' \hat{b} H_b + \hat{t}' \hat{t} H_t) (DF) \quad (2.7)$$

where

$$\begin{aligned} H_b &= G(s) \left\{ \left(1 - \frac{j}{ks} \right) \tau v(\xi) - \left(\frac{1}{ks} \right)^2 \tau^3 u(\xi) + j(\sqrt{2k} \bar{R}_t)^{-2/3} \right. \\ &\quad \left. \cdot [\tau v'(\xi) + (\bar{R}_t / \bar{R}_b) \tau^3 u'(\xi)] \right\} \\ H_t &= G(s) \left(\frac{j}{ks} \right) \left[\tau v(\xi) + \left(1 - \frac{2j}{ks} \right) \tau^3 u(\xi) + j(\sqrt{2k} \bar{R}_t)^{-2/3} \tau^3 u'(\xi) \right] \\ G(s) &= \frac{k^2 Y}{2\pi j} \frac{e^{-jks}}{ks}, \quad Y = (120\pi)^{-1} \end{aligned}$$

The Fock functions u and v and their derivatives u' and v' are described in Appendix A. Several remarks about the solution in (2.7) are in order.

(i) It is derived in an approximate manner from the classical work of Fock [14] and the recipe of GTD [8], [9], as detailed in Section 6. This solution is certainly not valid when the curvature of the surface Σ is large or rapidly varying. (ii) For the special case that Σ is a planar surface ($R_t = R_b \rightarrow \infty$), (2.7) recovers the known exact solution, namely,

$$H_b = G(s) \left[1 - \frac{1}{ks} - \left(\frac{1}{ks} \right)^2 \right] \quad (2.8a)$$

$$H_t = G(s) \left(\frac{2i}{ks} \right) \left(1 - \frac{1}{ks} \right) \quad (2.8b)$$

$$DF = 1 \quad (2.8c)$$

(iii) The solution is valid for any combination of \vec{r}_1 and \vec{r}_2 . In the penumbra region (\vec{r}_2 is close to \vec{r}_1 and $\xi \ll 1$), (2.7) is nearly the planar solution in (2.8). In the deep shadow ($\xi \ll 1$), the residue series representation of the Fock functions in Appendix A may be used, and (2.7) is identified as the creeping-wave contribution. (iv) When Σ is a cylindrical surface, the formula (2.7) has been used to calculate the mutual admittance between two slots on Σ . It has been shown [12], [13] that the numerical results are in excellent agreement with a known exact solution [15] - [17]. (v) Except for the very simple surfaces such as a cylinder, cone, or sphere, no explicit parametric equations can be found for the geodesics. Thus, for a general surface, one may have to rely on numerical techniques for determining the geodesics and the divergent factor, as has been done in [18].

3. GREEN'S FUNCTION OF A CONE

Let us apply the formula (2.7) to the field on an infinite cone, described by the equations (Fig. 2a)

$$x = r \sin \theta_0 \cos \phi, \quad y = r \sin \theta_0 \sin \phi, \quad z = r \cos \theta_0 \quad (3.1)$$

where θ_0 is the half cone angle ($0 < \theta_0 < \pi/2$). Since the cone is a developable surface, the rays (geodesics) on a developed cone (Fig. 2b) are straight lines. Due to the source at $\vec{r}_1 = (r_1, \theta_0, \phi_1)$, the main contribution of the field at $\vec{r}_2 = (r_2, \theta_0, \phi_2)$ comes from the shortest ray described by

$$r_1 \sin \Omega_1 = r_2 \sin \Omega_2 \quad (3.2)$$

As the ray propagates away from the source point \vec{r}_1 , it reaches the highest altitude at M where $\Omega = \pi/2$. After M, the ray travels downward away from the cone tip. The various parameters defined in Section 2 can be simply calculated from the cone geometry [6], [19], and expressed in terms of coordinates (r_1, ϕ_1) and (r_2, ϕ_2) . The arclength is

$$s = \left(r_1^2 + r_2^2 - 2r_1r_2 \cos [(\phi_1 - \phi_2) \sin \theta_0] \right)^{1/2} \quad (3.3)$$

The angle Ω_1 at \vec{r}_1 is

$$\Omega_1 = \sin^{-1} \left\{ \frac{r_2}{s} \sin [(\phi_2 - \phi_1) \sin \theta_0] \right\} \quad (3.4)$$

We choose $|\Omega_1| < \pi/2$ if $r_2^2 < s^2 + r_1^2$, and $|\Omega_1| > \pi/2$ if otherwise. The other parameters are

$$\Omega_2 = \Omega_1 + (\phi_2 - \phi_1) \sin \theta_0 \quad (3.5)$$

$$\bar{R}_t = \frac{\sqrt{r_1 r_2} \tan \theta_0}{\sin \Omega_1 \sin \Omega_2}, \quad \bar{R}_b = \frac{\sqrt{r_1 r_2} \tan \theta_0}{\cos \Omega_1 \cos \Omega_2} \quad (3.6)$$

$$\xi = \left(\frac{1}{2} k r_1 \sin \Omega_1 \sin \theta_0 \right)^{1/3} |\phi_2 - \phi_1| \cos^{2/3} \theta_0 \quad (3.7)$$

$$\tau = (ks/\xi)^{1/2} (2k^2 r_1 r_2)^{-1/6} (\sin \Omega_1 \sin \Omega_2 \cot \theta_0)^{1/3} \quad (3.8)$$

$$DF = 1 \quad (3.9)$$

When the above parameters in (3.3) through (3.9) are substituted into (2.7), we obtain an approximate solution for the surface field on a cone due to a direct surface ray contribution. Let us consider a special observation point \vec{r}_2 such that

$$ks \gg 1, \Omega_1 \text{ and } \Omega_2 \text{ are not close to } \pi/2 \quad (3.10)$$

Then the two components of the field in (2.7) are reduced to, after making use of the residue series representations for the Fock functions (Appendix A) and keeping only the leading terms,

$$H_b \sim \frac{k^2 (\sin \Omega_1 \sin \Omega_2 \cot \theta_0)^{1/3}}{1528 (k^2 r_1 r_2)^{1/6} (ks)^{1/2}} \exp \left[-0.88\xi - j \left(\frac{5\pi}{12} + 0.51\xi + ks \right) \right] \quad (3.11a)$$

$$H_t \sim O[(ks)^{-3/2}] \quad (3.11b)$$

which agrees with the rigorous asymptotic solution given in Eqs. (50) and (53) of [6]. (In making the comparison, note the corresponding notations used in [6] and here: $-1 \rightarrow j$, $\theta_c \rightarrow \theta_0$, $L_1 \rightarrow s$, $r_+ \rightarrow r_1$, $r_- \rightarrow r_2$, $\beta_{s+} \rightarrow \pi/2 - \Omega_1$, and $\bar{q}_1 \rightarrow |t_1|$.) We emphasize that the result in (3.11) or that in [6] is valid only under the conditions in (3.10). For an arbitrarily located observation point, (2.7) should be used.

Two final remarks about the formula in (2.7) are in order. (i) For a given source and observation point, there are infinitely many rays (geodesics) passing through them. The contribution from each ray may be calculated from (2.7), and the final field solution is the superposition of all ray contributions. In most practical problems (all the numerical computations presented in this paper), only the ray with the shortest arclength gives the significant contribution to the field solution, whereas all other rays may be ignored. (ii) Depending on the polarization and the distances of the source and observation points from the cone tip, there may be another significant contribution to the field from the diffraction at the tip. In such a case, the total field at any point contains two dominant contributions: one from the direct ray according to formula (2.7), and one from the tip-diffracted ray. More about the latter will be given in Section 4.

4. MUTUAL ADMITTANCE ON A CONE

On the surface of a cone, let us consider two arbitrarily oriented slots. Under the assumption that the dimensions of the slots are relatively small compared with the radii of curvature of the cone surface, the shapes of slots are taken to be rectangular on a developed cone. Note that, depending on the exact manner in which the feeding waveguide is fitted into the cone surface, the shape of a slot mapped on a developed cone may be quite irregular. Our assumption of rectangular shapes represents a good approximation for practical cases; at the same time, it simplifies the subsequent calculations.

Referring to Fig. 3, we describe the dimensions and the positions of the two slots by

$$(a_n, b_n) \text{ and } [c_n, (n-1)\phi_0, \omega_n], \quad n = 1, 2$$

Thus, the radial separation of the two slots is $(c_2 - c_1)$ and the angular separation is ϕ_0 . The angle ω_n measures the deviation of the longitudinal direction of slot n from the radial direction of the cone. If $\omega_n = 0$, slot n is radial; if $\omega_n = \pi/2$, slot n is circumferential. The mutual admittance Y_{12} between the two slots is defined as follows. Throughout this work we always assume that

$$(i) \text{ the slots are thin, and} \quad (4.1a)$$

$$(ii) \text{ their length is roughly a half-wavelength.} \quad (4.1b)$$

Then the aperture field in each slot can be adequately approximated by a simple cosine distribution, which is the so-called "one-mode" approximation. The aperture field of slot 1 under the "one-mode" approximation is given by

$$\vec{E} = V_1 \vec{e}_1, \quad \vec{H} = I_1 \vec{h}_1 \quad (4.2a)$$

where

$$\vec{e}_1 = \hat{z}_1 \sqrt{\frac{2}{a_1 b_1}} \cos \frac{\pi}{a_1} y_1, \quad \vec{h}_1 = \hat{x}_1 \vec{e}_1. \quad (4.2b)$$

Here (y_1, z_1) are the local rectangular coordinates, with the origin at the center of slot 1 and y_1 -axis parallel to the longer dimension of the slot.

(V_1, I_1) are respectively the modal (voltage, current) of slot 1. The mutual admittance Y_{12} is defined by

$$Y_{12} = Y_{21} = \frac{I_{21}}{V_1} \quad (4.3)$$

where I_{21} is the induced current in slot 2 when slot 1 is excited by a voltage V_1 and slot 2 is short-circuited. An alternative expression for Y_{12} is

$$Y_{12} = \frac{1}{V_1 V_2} \iint_{A_2} \vec{E}_2 \cdot \vec{H}_1 \cdot d\vec{s}_2 = \frac{-1}{V_1 V_2} \iint_{A_2} (\vec{E}_2 \cdot \hat{z}_2) (\vec{H}_1 \cdot \hat{y}_2) dy_2 dz_2 \quad (4.4)$$

where

A_2 = aperture of slot 2,

\vec{H}_1 = magnetic field when slot 1 is excited with voltage V_1 , and slot 2 is covered by a perfect conductor,

\vec{E}_2 = electric field when slot 2 is excited with voltage V_2 , and slot 1 is covered by a perfect conductor.

Because $\vec{H}_1 = I_{21} \vec{h}_2$ and $\vec{E}_2 = V_2 \vec{e}_2$, it is a simple matter to verify that (4.3) and (4.4) are equivalent.

At high frequencies, \vec{H}_1 in (4.4) has two dominant contributions: one from the direct rays going from slot 1 to slot 2, and the other from the rays diffracted at the tip of the cone, namely,

$$\vec{H}_1 \sim \vec{H}_1^d + \vec{H}_1^t \quad (4.5)$$

Accordingly, Y_{12} also has two parts

$$Y_{12} \sim Y_{12}^d + Y_{12}^t \quad (4.6)$$

Let us concentrate on Y_{12}^d first. Making use of the Green's function in (2.7) and the aperture distribution in (4.2), Y_{12}^d may be explicitly written as

$$Y_{12}^d = \frac{-2k^2}{(a_1 b_1 a_2 b_2)^{1/2}} \int_{-a_1/2}^{a_1/2} dy_1 \int_{-b_1/2}^{b_1/2} dz_1 \int_{-a_2/2}^{a_2/2} dy_2 \int_{-b_2/2}^{b_2/2} dz_2 \times \left(\cos \frac{\pi}{a_1} y_1 \right) \left(\cos \frac{\pi}{a_2} y_2 \right) g(y_1 z_1; y_2 z_2) \quad (4.7a)$$

where

$$g(y_1 z_1; y_2 z_2) = H_b \cos \omega_3 \cos \omega_4 + H_t \sin \omega_3 \sin \omega_4 \quad (4.7b)$$

The Green's function components (H_b, H_t) are given in (2.7), and angles (ω_3, ω_4) are shown in Fig. 3. In evaluating the integrals in (4.7a), for two given points (y_1, z_1) and (y_2, z_2) , we must calculate some geometrical parameters appearing in H_b and H_t . Those calculations lead to the following results

$$r_n = \left[c_n^2 + y_n^2 + z_n^2 - 2c_n \sqrt{y_n^2 + z_n^2} \cos (\omega_n - \omega_{n+4}) \right]^{1/2} \quad (4.8a)$$

$$\phi_n = (\sin \theta_0)^{-1} \sin^{-1} \left[\sqrt{y_n^2 + z_n^2} r_n^{-1} \sin (\omega_n - \omega_{n+4}) \right] \quad (4.8b)$$

$$\omega_{n+4} = \tan^{-1} (z_n / y_n) \quad (4.8c)$$

$$\omega_{n+2} = \Omega_n + (\pi/2) - \omega_n - \phi_n \sin \theta_0 + (n-1) \phi_0 \sin \theta_0 \quad (4.8d)$$

where $n = 1$ and 2 . We evaluate the integrals in (4.7a) numerically with the aid of a computer.

Next let us consider Y_{12}^t , the part of mutual admittance due to the rays diffracted at the cone tip. For the special case of circumferential slots, an approximate expression of Y_{12}^t is given in [16], which reads

$$Y_{12}^t \approx T, \text{ if } \omega_1 = \omega_2 = \pi/2, \quad (4.9a)$$

where

$$T = \sigma_0 \frac{(a_1 b_1 a_2 b_2)^{1/2}}{30\pi^4 c_1 c_2 \sin \theta_0} \left(\frac{\tan \theta_0}{2\pi} \right)^{1/2} \frac{\sin(kb_1/2) \sin(kb_2/2)}{(kb_1/2)(kb_2/2)} \cdot \exp j \left(\frac{\pi}{4} - kc_1 - kc_2 \right). \quad (4.9b)$$

Here σ_0 is the zeroth-order tip diffraction coefficient and is a function of the half cone angle θ_0 . A numerical table of σ_0 for several typical values of θ_0 is given in [16]. We have fitted those values by a simple expression, viz.,

$$\sigma_0 = A \exp jB, \quad (4.10)$$

where

$$A = 1.3057\theta_0^{-1} - 1.755 + 2.772\theta_0 - 1.459\theta_0^2$$

$$B = 2.7195 + 1.4608\theta_0 - 1.1295\theta_0^2 + 0.6566\theta_0^3$$

Both θ and B are in radians.

As may be seen from Fig. 4, the numerical values of σ_0 calculated from (4.10) are in excellent agreement with those tabulated in [16]. For the special case of axial slots, Y_{12}^t according to [16] is approximately

$$Y_{12}^t \approx 0, \text{ if } \omega_1 = \omega_2 = 0. \quad (4.11)$$

In the present paper, we are interested in the general case that the two slots have arbitrary orientations. Before a more exact solution can be

found, we will use the following formula

$$Y_{12}^t \approx T \sin \omega_1 \sin \omega_2 \quad (4.12)$$

which matches the two extreme cases in (4.9) and (4.11), and interpolates the in-between cases by regarding each slot as a thin magnetic dipole.

5. NUMERICAL RESULTS OF MUTUAL ADMITTANCE

The final solutions for Y_{12} (total mutual admittance) and Y_{12}^d (partial mutual admittance) are given in (4.6), (4.7), (4.12), and (4.9b). For a given geometry of the slots and cone, the two surface integrals in (4.7a) are evaluated numerically by choosing an integration grid roughly equal to $0.05\lambda \times 0.05\lambda$. Thus, for two typical $0.5\lambda \times 0.2\lambda$ slots, the integrals are replaced by a summation of 1600 terms. Fortunately, the integrand is simple enough that each Y_{12} calculation takes about one second on the CDC Cyber 170 Series Computer Systems. We have analyzed a large number of cases for Y_{12} . Typical results are summarized below.

Unless specified otherwise, all numerical computations are based on two identical slots with

$$\text{slot length} = 0.5\lambda, \text{ width} = 0.2\lambda. \quad (5.1)$$

The other parameters are the half cone angle θ_0 , the slot orientations (ω_1, ω_2) , the distances from slot centers to the cone tip (c_1, c_2) , and the slot angular separation $\phi_0 = \phi_2 - \phi_1$ (Fig. 3).

(A) "Equivalent" cylinder. It has been conjectured in [16] that, in calculating Y_{12}^d (the contribution from the direct rays) approximately, the cone may be replaced by an "equivalent" cylinder with parameters (Fig. 5)

$$z_0 = c_1 - c_2, \phi_0 = \phi_0, R = \frac{1}{2}(c_1 + c_2) \sin \theta_0. \quad (5.2)$$

This conjecture can be now quantitatively checked out. In Table I we compare Y_{12}^d on a cone with $\theta_0 = 15^\circ$ or 30° calculated from (4.7), and Y_{12} on a cylinder calculated by a similar GTD solution reported in [12]. All values of Y_{12} (or Y_{12}^d) are listed in $(\text{DB} = 20 \log_{10} |Y_{12}|, \text{phase in degree})$ format. For the cone with the smaller angle ($\theta_0 = 15^\circ$), the

"equivalent" cylinder method gives a good approximation for Y_{12}^d . For the cases listed in Table I, the magnitude error of Y_{12}^d is within 0.5 dB (6 percent) and phase error within 15° . For the cone with the larger angle ($\theta_0 = 30^\circ$), however, the "equivalent" cylinder method is not very accurate with magnitude, and phase errors as large as 2.5 dB (33 percent), and 56° , respectively.

(B) Comparison with experiments. A set of experimental data on the mutual coupling between two X-band open-ended waveguides ($0.9'' \times 0.4''$) on a cone was reported in [16]. As a function of frequency, measurements were done on the coupling coefficient S_{12} , which is related to Y_{12} through the relation

$$S_{12} = \frac{-Y_g Y_{11}}{(Y_g + Y_{11})^2 - Y_{12}^2} \quad (5.3)$$

Here $Y_g = (120\pi)^{-1} [k^2 - (\pi/a)^2]^{1/2}$ is the admittance of the TE_{10} mode in the feed waveguide. Y_{11} is the self-admittance of a slot on the cone.

In the present calculations, we use, instead, the Y_{11} on an "equivalent" cylinder which is calculated by the exact modal solution described in [16] (for example, $Y_{11}/Y_g = 0.8178 + j0.3886$ at 8.5 GHz, and $0.8591 + j0.3828$ at 9 GHz). Since Y_{11} is least sensitive to the geometry, the approximation of a cone by a cylinder should not introduce any significant error in S_{12} . In Figs. 6 and 7, three sets of data are presented: (i) the experimental data; (ii) the theoretical results from the present analysis in which the calculation of Y_{12}^d is based on a cone, e.g., Equation (4.7); (iii) the theoretical results from [16] in which Y_{12}^d is calculated from the exact modal solution of an "equivalent" cylinder. Several observations can be made. (a) Both theoretical results are in good agreement with the

experimental data (with the present result being slightly better). As explained in (A), the "equivalent" cylinder method works because the cone angles ($\theta_0 \sim 10^\circ$) are small. (b) The peaks and valleys are caused by the interference between Y_{12}^d and Y_{12}^t , which are of comparable magnitudes due to the large angular separations (60.8° and 80°). (c) There exists a slight shift in frequency ($\Delta f/f \approx 3$ percent) between the theoretical and experimental valleys in Fig. 6. We speculate that this may be due to a slight phase inaccuracy in Y_{12}^t . As a final remark, it has been found experimentally (private communication from G. E. Stewart and K. E. Golden of Aerospace Corporation) that the Y_{12}^t contribution is sensitive to the exact shape of the cone tip. When the tip is not extremely sharp, the peaks and valleys in Figs. 6 and 7 become much less predominant.

(C) Mutual admittances of circumferential slots. In Figs. 8 to 10, Y_{12} and Y_{12}^d for two circumferential slots are displayed as functions of angular separation ϕ_0 and the radial separation ($c_1 - c_2$). We note that the effect of Y_{12}^t can modify the curves of Y_{12} in several different ways. When the slots are at the same latitude (Fig. 8), the direct coupling is weak. Thus, tip contribution is noticeable even at a small angular separation. As the radial separation is increased (Fig. 9), the tip contribution is almost negligible for $\phi_0 < 65^\circ$. When the two slots are widely separated in the radial direction with one slot near the tip (Fig. 10), the tip contribution gets stronger, and the direct contribution becomes insensitive to ϕ_0 . Hence, the oscillation on the Y_{12} curve has a much larger period. In fact, there is only a half "cycle" in the range $0 < \phi_0 < 90^\circ$, and Y_{12} appears to be shifted from Y_{12}^d by a fixed amount.

(D) Effect of slot orientation on mutual admittance. Consider two slots separated by 1λ along the radial direction. The magnitude of Y_{12} as functions of the slot orientation angles ω_1 and ω_2 is plotted in Fig. 11. As expected, the maximum value (-73 dB) occurs when both slots are circumferential ($\omega_1 = \omega_2 = 90^\circ$). This value is above 14 dB higher than that when both slots are radial ($\omega_1 = \omega_2 = 0$). The minimum value (-113 dB) of Y_{12} occurs when the top slot is radial and the bottom one is circumferential. This result confirms a common belief that the mutual coupling between two orthogonal slots is generally negligible.

6. DERIVATION OF THE GREEN'S FUNCTION

We will now describe briefly the derivation for the Green's function for the general convex surface given in (2.7).

Our starting point is the corresponding Green's function for a cylinder. For the latter problem, several versions of the asymptotic solutions [10] - [12] exist. All the versions are of similar nature, and contain some approximations that have not yet been fully justified. For the cylinder problem, both [11] and [12] give excellent numerical results (with [12] being slightly better as demonstrated in [13]). We quote below the Green's function for a cylinder reported in [12], which again can be written in the form of (2.7) with $DF = 1$ and

$$H_b = G(s) \left\{ \left(1 - \frac{1}{ks} \right) v(\xi) - \left(\frac{1}{ks} \right)^2 u(\xi) + j(\sqrt{2} k R_t)^{-2/3} \cdot [v'(\xi) + (R_t/R_b) u'(\xi)] \right\} \quad (6.1a)$$

$$H_t = G(s) \left(\frac{1}{ks} \right) \left[v(\xi) + \left(1 - \frac{21}{ks} \right) u(\xi) + j(\sqrt{2} k R_t) u'(\xi) \right] \quad (6.1b)$$

where

$$R_t = R/\cos^2 \theta, \quad R_b = R/\sin^2 \theta$$

$$\xi = ks(\cos^4 \theta / 2k^2 R^2)^{1/3}$$

R = radius of cylinder

θ = angle between the ray and the ϕ -direction.

Since θ is a constant along a ray (geodesic), so are the three parameters R_t , R_b , and ξ appearing in (6.1). The formula (6.1) is basically derived from Fock's classical solution for vector potentials of a sphere [14], but contains a modification, namely, the last term in (6.1a)

$$G(s) j(\sqrt{2} k R_t)^{-2/3} (R_t/R_b) u'(\xi) \quad (6.2)$$

was added to the Fock's solution in an arbitrary manner. Note that this

additional term introduces a very small contribution for a sphere, or for a cylinder as long as θ is not close to $\pi/2$. For $\theta = \pi/2$ on a cylinder, H_b in (6.1a) becomes (see Eq. (2.10) of [12])

$$H_b = [H_b]_{pl} + \frac{3}{8} \sqrt{\frac{1}{2\pi}} k^2 y e^{-j3\pi/4} \frac{1}{kR} \frac{e^{-jks}}{\sqrt{ks}}. \quad (6.3)$$

Here $[H_b]_{pl}$ is the corresponding solution on an infinite plane and it decays as $(ks)^{-1}$ for large ks . The second term in (6.3) comes from the additional term in (6.2), and is the dominant contribution at large ks because it decays as $(ks)^{-1/2}$. Recently, J. Boersma (private communication) has shown that (6.3) is in exact agreement with a rigorous asymptotic solution for the cylinder. Thus, the additional term in (6.3) is justified for $\theta = \pi/2$ where its contribution is most significant.

Now, let us generalize (6.1) to a general convex surface sketched in Fig. 1 following the GTD recipe [8], [9], [18]: (i) The divergence factor in (2.5) is introduced from the consideration of energy conservation. (ii) The generalized ξ in (2.3) and τ in (2.4) are based on the rigorous solutions of two-dimensional canonical problems. The only remaining problem is the generalization of R_t and R_b in (6.1). We note that the above GTD recipe is valid only if R_t and R_b are slowly varying along a ray. Thus, any sort of average values of R_t and R_b should give approximately the same result. We choose the geometrical mean in (2.6) for its simplicity and symmetry between the source and observation points. From these considerations, we obtain the generalized solution (2.7) from (6.1).

REFERENCES

- [1] W. H. Kummer, ed., Special issue on conformal arrays, IEEE Trans. Antennas Propagat., vol. AP-22, no. 1, January 1974.
- [2] J. Willis, ed., Conformal Antennas (research program review and workshop). Washington, D.C.: Naval Air Systems Command, April 1975, AIR-310B.
- [3] J. Shapira, L. B. Felsen, and A. Hessel, "Ray analysis of conformal antenna arrays," IEEE Trans. Antennas Propagat., vol. AP-22, pp. 49-63, 1974.
- [4] P. H. Pathak, "Analysis of a conformal receiving array of slots in a perfectly-conducting circular by the geometrical theory of diffraction," ElectroScience Laboratory, The Ohio State University, Technical Report ESL 3735-2, 1975; prepared under Contract N00140-74-C-6017.
- [5] L. B. Felsen and N. Marcuvitz, Radiation and Scattering of Waves. Englewood Cliffs, New Jersey: Prentice-Hall, 1973, p. 703.
- [6] K. K. Chan, L. B. Felsen, A. Hessel, and J. Shmoys, "Creeping waves on a perfectly conducting cone," to appear in IEEE Trans. Antennas Propagat., 1977.
- [7] J. B. Keller, "Diffraction by a convex cylinder," IRE Trans. Antennas Propagat., vol. AP-4, pp. 312-321, 1956.
- [8] B. R. Levy and J. B. Keller, "Diffraction by a smooth object," Comm. Pure Appl. Math., vol. XII, pp. 159-209, 1959.
- [9] R. G. Kouyoumjian, "The geometrical theory of diffraction and its application," in Topics in Applied Physics, R. Mittra, ed. New York: Springer-Verlag, 1975.
- [10] Y. Hwang and R. G. Kouyoumjian, "The mutual coupling between slots on an arbitrary convex cylinder," ElectroScience Laboratory, Department of Electrical Engineering, The Ohio State University, Semi-Annual Report 2902-21, 1975; prepared under Grant NGL 36-003-138.
- [11] Z. W. Chang, L. B. Felsen, and A. Hessel, "Surface ray methods for mutual coupling in conformal arrays on cylinder and conical surface," Polytechnic Institute of New York, Final Report (September 1975-February 1976), 1976; prepared under Contract N00123-76-C-0236.
- [12] S. W. Lee and S. Safavi-Naini, "Asymptotic solution of surface field due to a magnetic dipole on a cylinder," University of Illinois at Urbana-Champaign, Electromagnetics Laboratory Report no. 76-11, 1976.
- [13] S. W. Lee, S. Safavi-Naini, and R. Mittra, "Mutual admittance between slots on a cylinder," University of Illinois at Urbana-Champaign, Electromagnetics Laboratory Report no. 77-8, 1977.

- [14] V. A. Fock, Electromagnetic Diffraction and Propagation Problems. New York: Pergamon Press, 1965.
- [15] G. E. Stewart and K. E. Golden, "Mutual admittance for axial rectangular slots in a large conducting cylinder," IEEE Trans. Antennas Propagat., vol. AP-19, pp. 120-122, 1971.
- [16] K. E. Golden, G. E. Stewart, and D. C. Pridmore-Brown, "Approximation techniques for the mutual admittance of slot antennas on metallic cones," IEEE Trans. Antennas Propagat., vol. AP-22, pp. 43-48, 1974.
- [17] P. C. Bargeliotis, A. F. Seaton, A. T. Villeneuve, and W. H. Kummer, "Conformal phased array breadboard," Hughes Aircraft Company, Culver City, California, Final Report for Contract N00019-76-C-0495, January 1977.
- [18] W. D. Burnside, M. C. Gilreath, R. J. Marhefka, and C. L. Yu, "A study of KC-135 aircraft antenna patterns," IEEE Trans. Antennas Propagat., vol. AP-23, pp. 551-558, 1975.
- [19] L. B. Felsen, A. Hessel, J. Shapira, and J. Shmoys, "Ray analysis of mutual coupling in conformal arrays," Polytechnic Institute of New York, Final Report (April 1973 - March 1974), 1974; prepared under Contract N00123-73-C-1481.
- [20] M. Abramowitz and I. A. Stegun, Handbook of Mathematical Functions. New York: Dover, 1965.

TABLE I.
 Y_{12}^d ON CONE AND Y_{12} ON CYLINDER*

ϕ_0	z_0/λ	Cone $\theta_0 = 15^\circ$	Cylinder	Cone $\theta_0 = 30^\circ$
30°	0	- 91.35dB 155°	- 91.47 153°	- 90.99 160°
60°	0	-110.97 116°	-111.28 101°	-108.78 151°
0	1	- 73.35 73°	- 73.64 73°	- 73.49 74°
0	4	- 83.89 77°	- 84.30 75°	- 84.06 75°
30°	1	- 86.52 - 74°	- 86.59 - 76°	- 86.60 -70°
30°	4	- 86.95 24°	- 87.14 20°	- 86.83 35°
60°	1	-104.64 -35°	-104.17 -42°	-106.28 -13°
60°	4	- 94.41 -118°	- 94.64 -133°	- 94.12 -77°

* The parameters are $\omega_1 = \omega_2 = 90^\circ$, $R = 2\lambda$, $a = 0.5\lambda$, and $b = 0.2\lambda$.

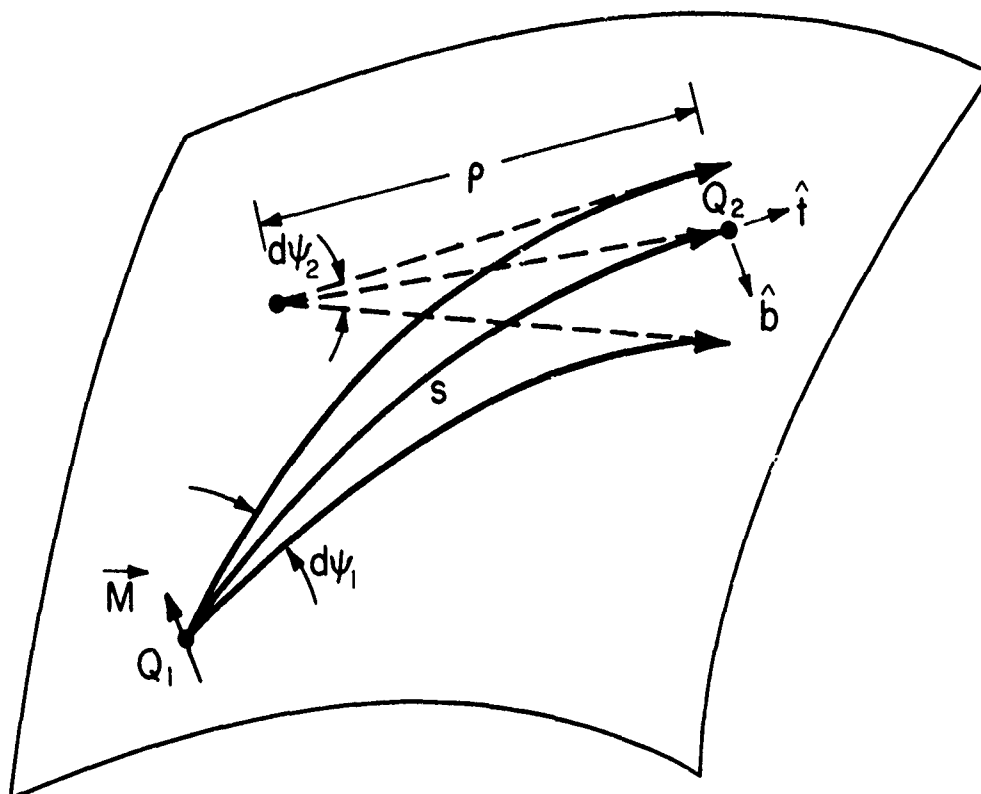


Fig. 1. A surface ray pencil originating from the magnetic dipole source at Q_1 . The central ray of the pencil passes through the observation point Q_2 . The angle extended by the pencil is $d\psi_1$ at Q_1 and $d\psi_2$ at Q_2 .

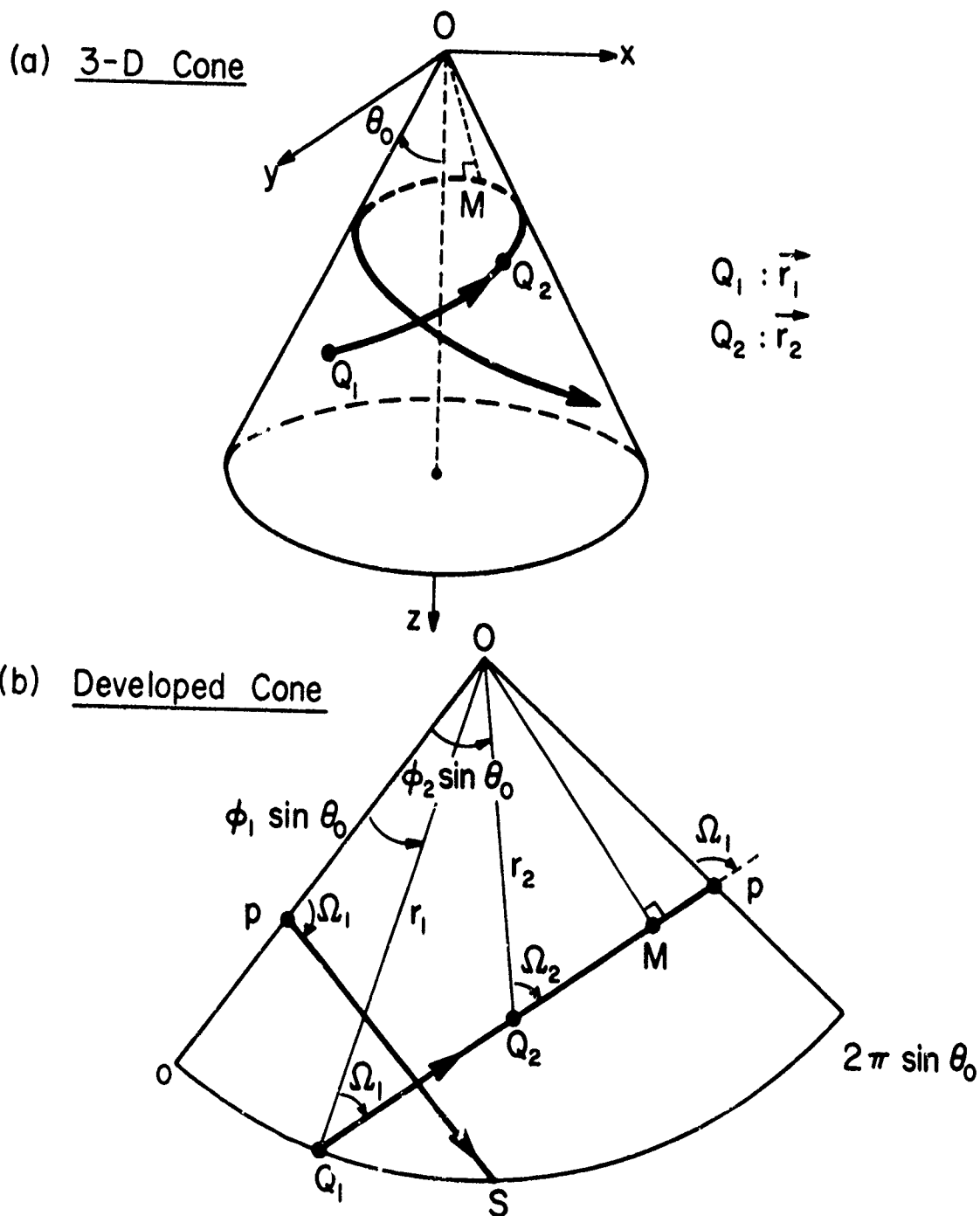


Fig. 2. A surface ray from source point Q_1 to observation point Q_2 on a cone with half cone angle θ_0 .

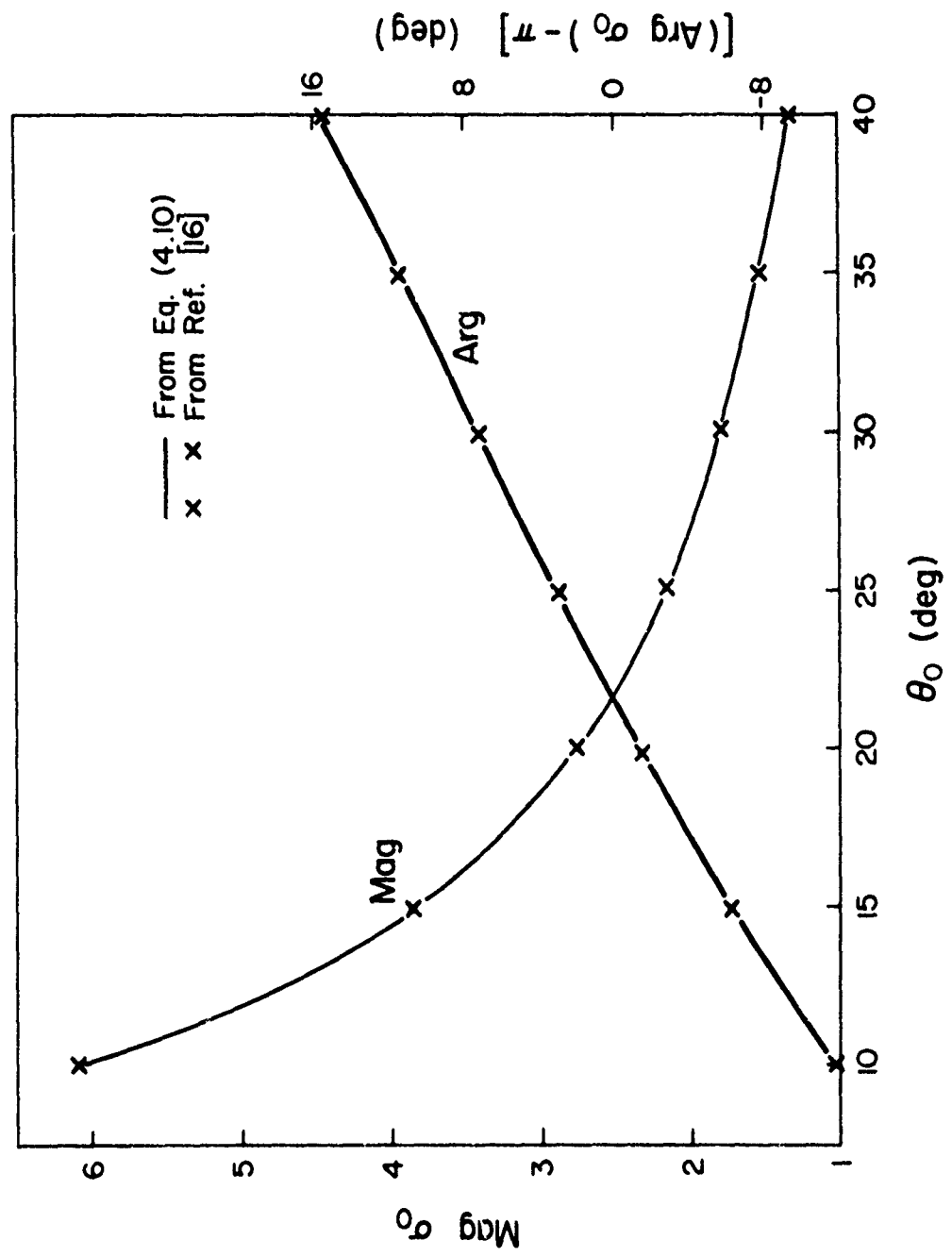


Fig. 4. Tip diffraction coefficient σ_0 of a cone which appeared in (4.9b).

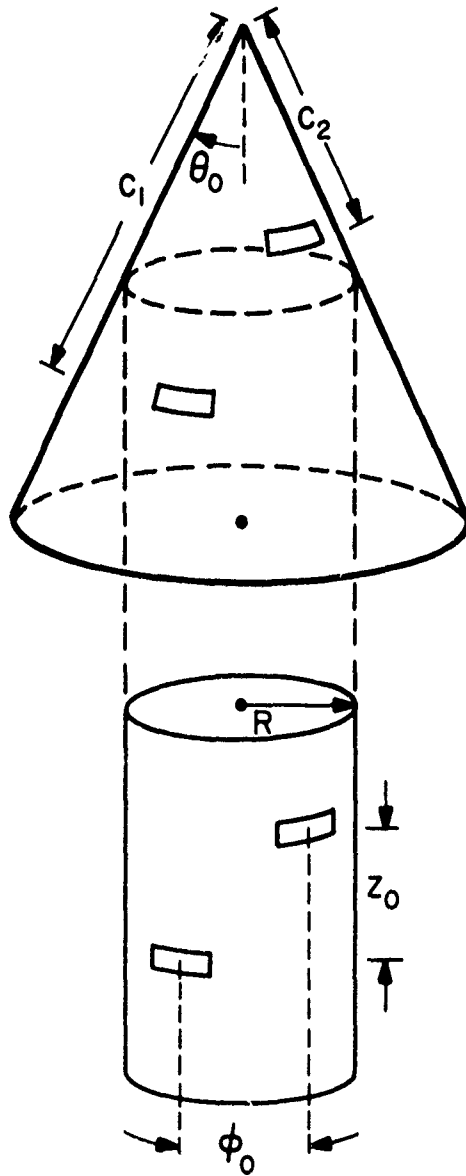


Fig. 5. To calculate Y_{12}^d of a cone approximately, the cone may be locally replaced by an "equivalent" cylinder.

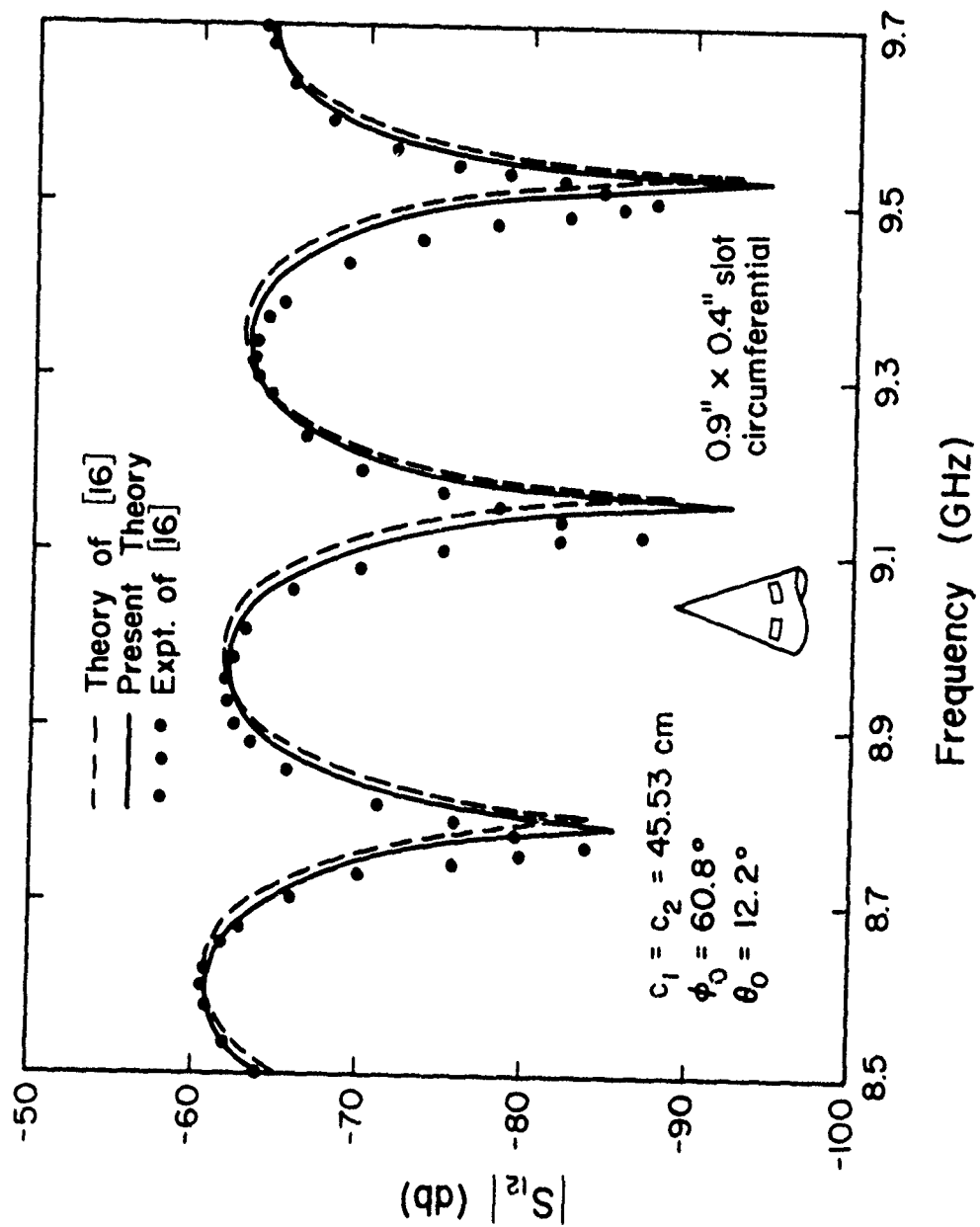


Fig. 6. Coupling coefficient S_{12} between two circumferential slots on a cone as a function of frequency.

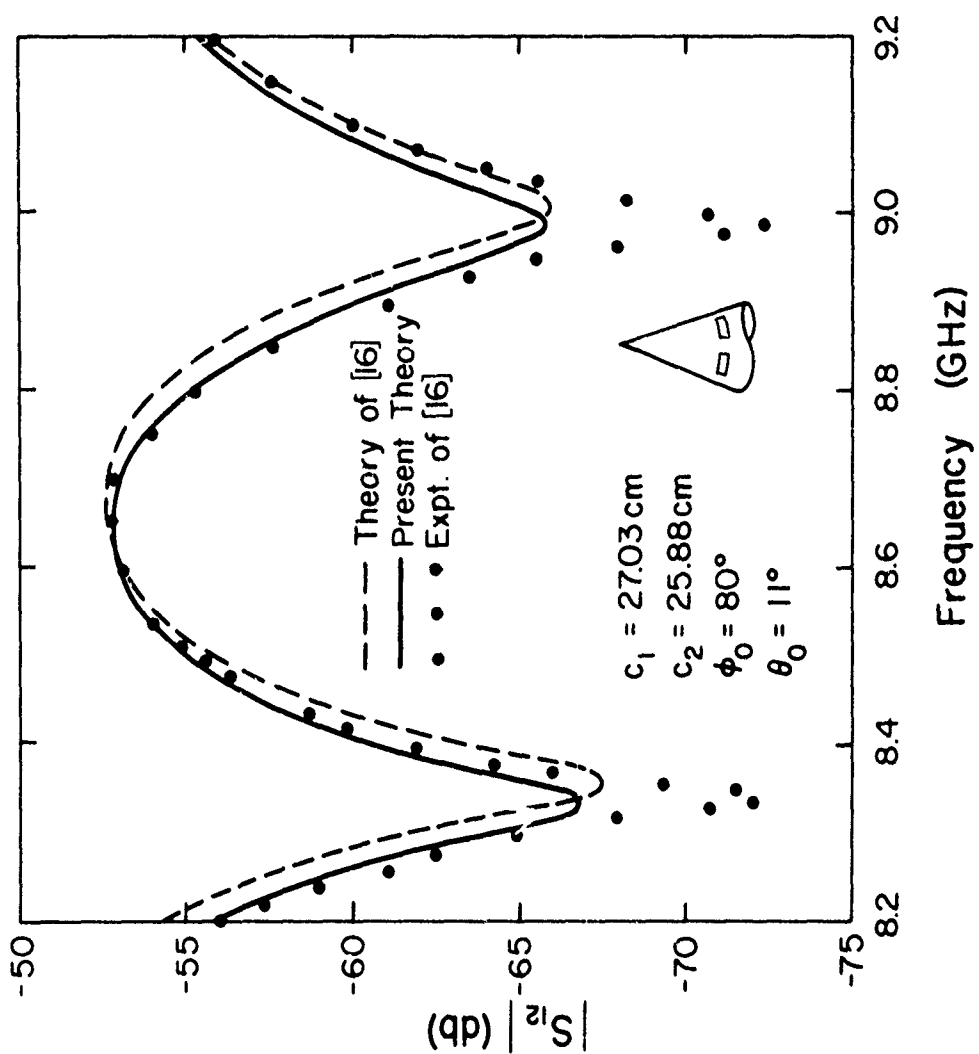


Fig. 7. Coupling coefficient S_{12} between two circumferential slots on a cone as function of frequency.

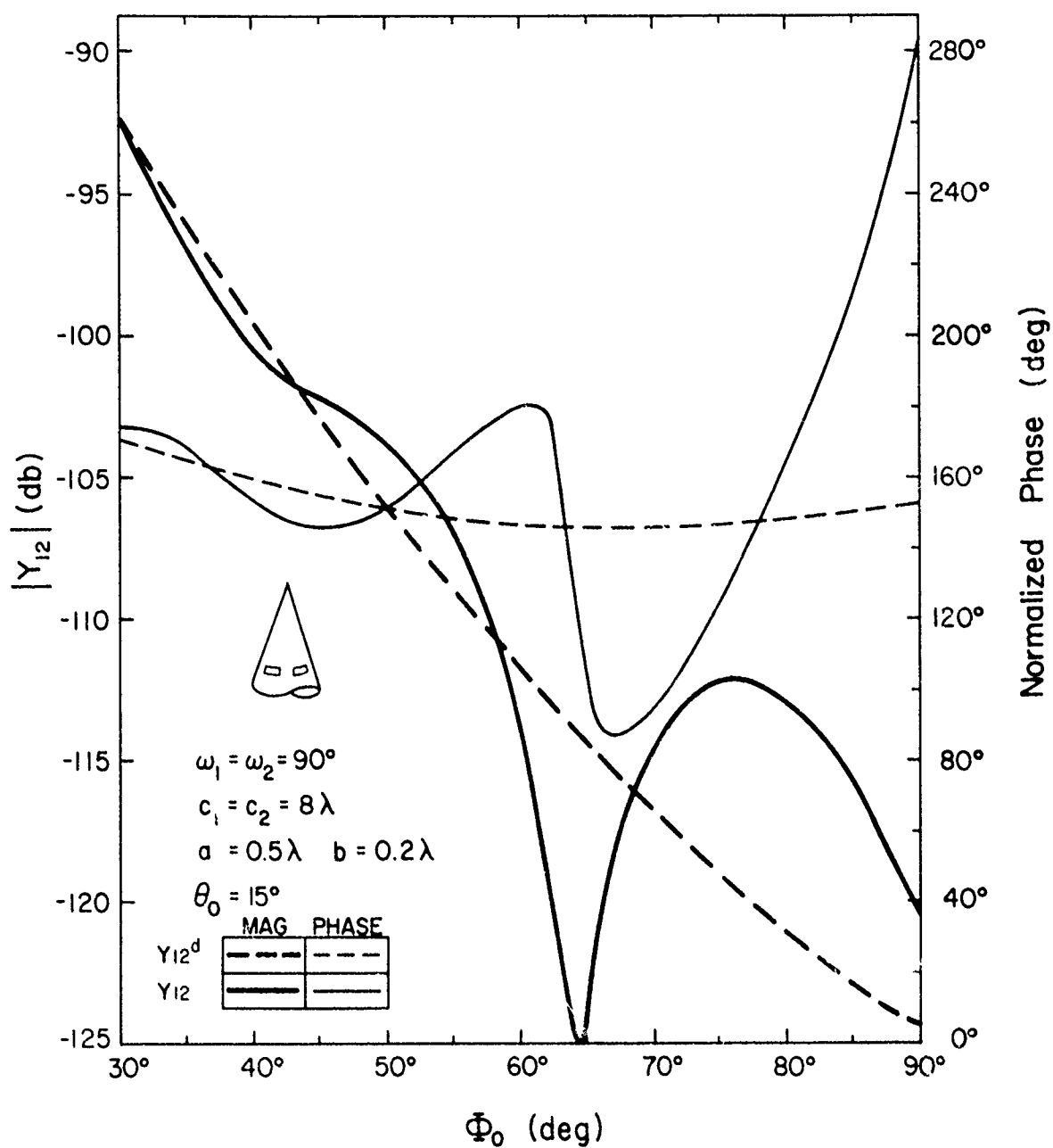


Fig. 8. Mutual admittances on a cone calculated from GTD described in Section 4.

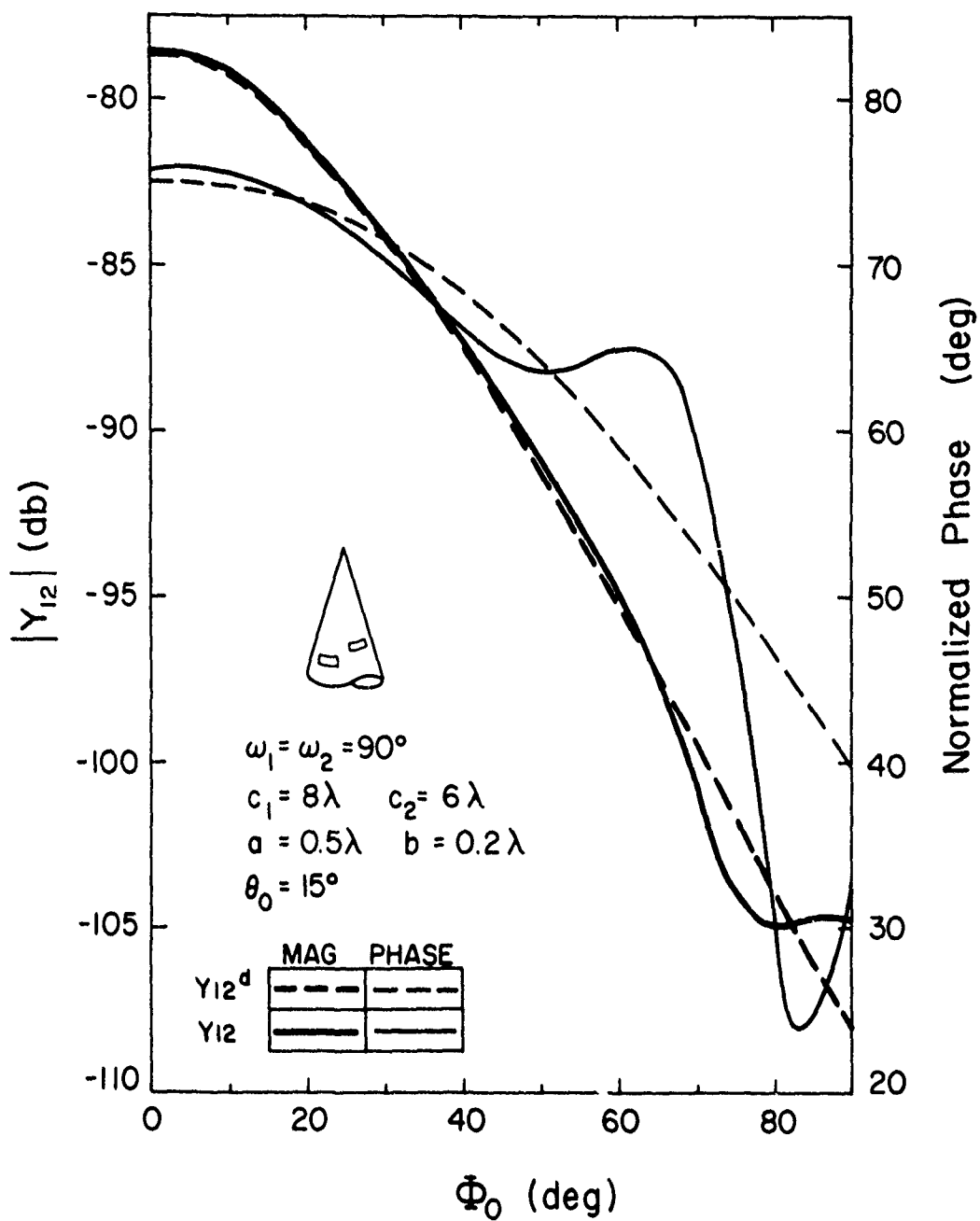


Fig. 9. Mutual admittances on a cone calculated from GTD described in Section 4.

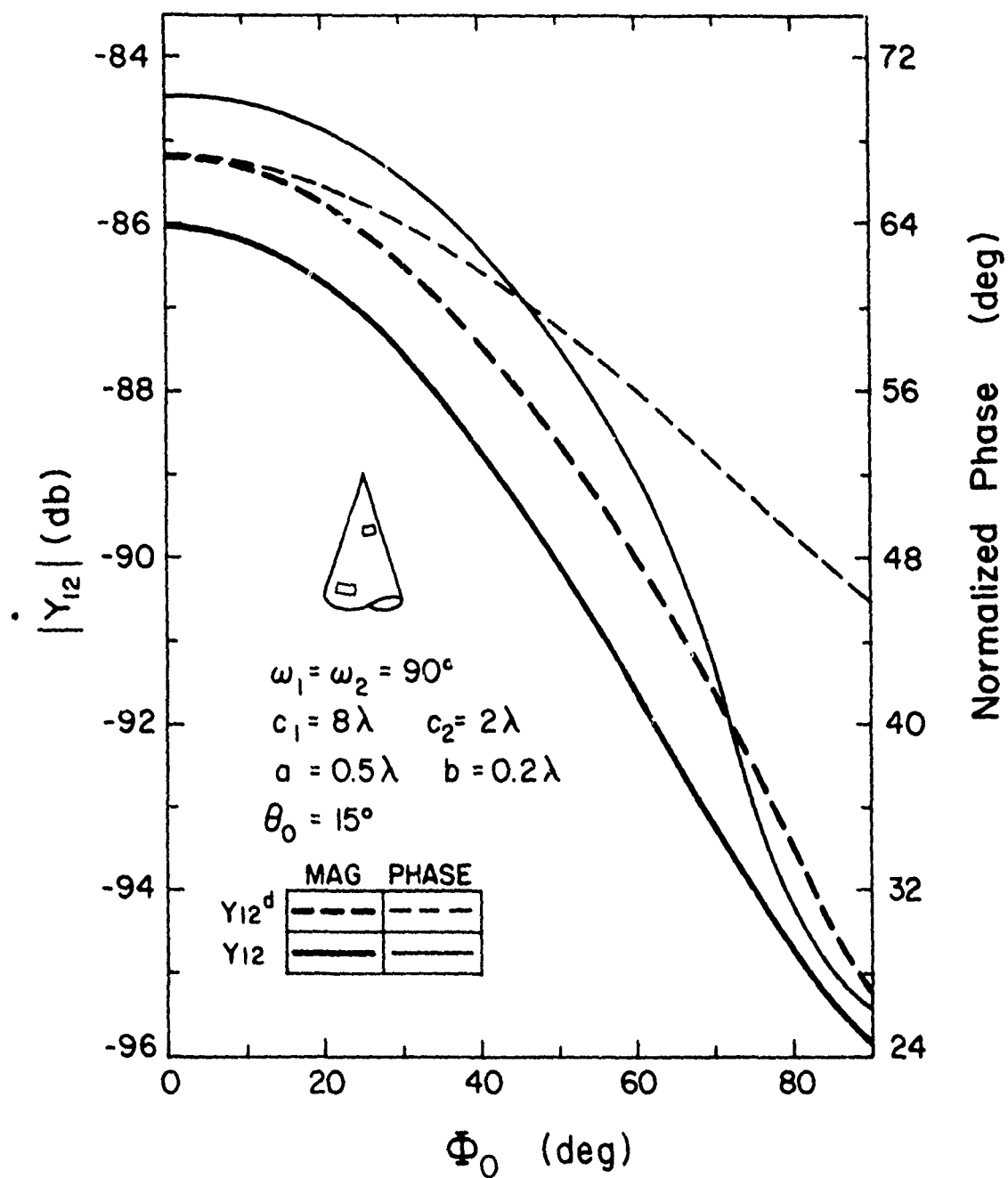


Fig. 10. Mutual admittance on a cone calculated from GTD described in Section 4.

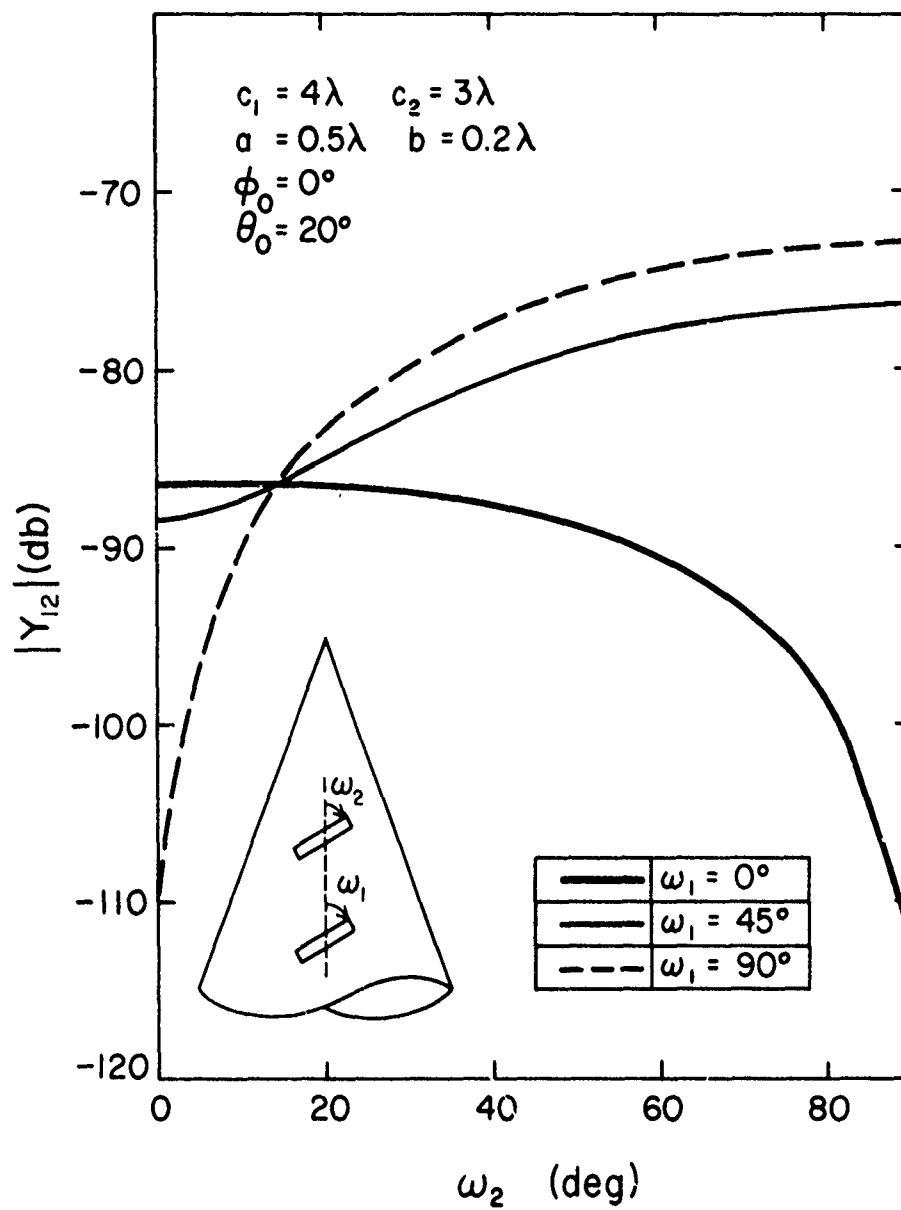


Fig. 11. Mutual admittance Y_{12} between two arbitrarily oriented slots on a cone.

APPENDIX A
FOCK FUNCTIONS

In this appendix we define and list some useful formulas of the functions $w_1(t)$, $w_2(t)$, $v(\xi)$, $u(\xi)$, and $v_1(\xi)$. These functions are commonly known as Fock functions.

(i) Definition: For a complex t and a real ξ ,

$$w_1(t) = \frac{1}{\sqrt{\pi}} \int_{\Gamma_1} dz \exp \left(tz - \frac{1}{3} z^3 \right) \quad (A-1)$$

$$w_2(t) = \frac{1}{\sqrt{\pi}} \int_{\Gamma_2} dz \exp \left(tz - \frac{1}{3} z^3 \right) = w_1^*(t) \quad (A-2)$$

$$v(\xi) = \frac{1}{2} e^{j\pi/4} \xi^{1/2} \frac{1}{\sqrt{\pi}} \int_{\Gamma_1} \frac{w_2(t)}{w_2'(t)} e^{-j\xi t} dt \quad (A-3)$$

$$u(\xi) = e^{j3\pi/4} \xi^{3/2} \frac{1}{\sqrt{\pi}} \int_{\Gamma_1} \frac{w_2'(t)}{w_2(t)} e^{-j\xi t} dt \quad (A-4)$$

$$v_1(\xi) = e^{j3\pi/4} \xi^{3/2} \frac{1}{\sqrt{\pi}} \int_{\Gamma_1} t \frac{w_2(t)}{w_2'(t)} e^{-j\xi t} dt \quad (A-5)$$

where integration contour $\Gamma_1(\Gamma_2)$ goes from ∞ to 0 along the line $\text{Arg } z = -2\pi/3 (+2\pi/3)$ and from 0 to ∞ along the real axis. Because of different time conventions, $w_1(w_2)$ above is equal to $w_2(w_1)$ defined in [14].

(ii) Residue series representation: For real positive ξ ,

$$v(\xi) = e^{-j\pi/4} \sqrt{\pi} \xi^{1/2} \sum_{n=1}^{\infty} (t'_n)^{-1} e^{-j\xi t'_n} \quad (\text{A-6})$$

$$u(\xi) = e^{j\pi/4} 2\sqrt{\pi} \xi^{3/2} \sum_{n=1}^{\infty} e^{-j\xi t_n} \quad (\text{A-7})$$

$$v_1(\xi) = e^{j\pi/4} 2\sqrt{\pi} \xi^{3/2} \sum_{n=1}^{\infty} e^{-j\xi t'_n} \quad (\text{A-8})$$

$$v'(\xi) = \frac{1}{2} e^{-j\pi/4} \sqrt{\pi} \xi^{-1/2} \sum_{n=1}^{\infty} (1 - j2\xi t'_n) (t'_n)^{-1} e^{-j\xi t'_n} \quad (\text{A-9})$$

$$u'(\xi) = e^{j\pi/4} 3\sqrt{\pi} \xi^{1/2} \sum_{n=1}^{\infty} \left(1 - j \frac{2}{3} \xi t_n\right) e^{-j\xi t_n} \quad (\text{A-10})$$

where $\{t_n\}$ and $\{t'_n\}$ are zeros of $w_2(t)$ and $w'_2(t)$, respectively, and they are tabulated in [12], [14] and p. 478 of [20].

(iii) Small argument asymptotic expansion: For real positive ξ and $\xi \rightarrow 0$,

$$v(\xi) \sim 1 - \frac{\sqrt{\pi}}{4} e^{j\pi/4} \xi^{3/2} + \frac{7j}{60} \xi^3 + \frac{7\sqrt{\pi}}{512} e^{-j\pi/4} \xi^{9/2} - 4.141 \times 10^{-3} \xi^6 + \dots \quad (\text{A-11})$$

$$u(\xi) \sim 1 - \frac{\sqrt{\pi}}{2} e^{j\pi/4} \xi^{3/2} + \frac{5j}{12} \xi^3 + \frac{5\sqrt{\pi}}{64} e^{-j\pi/4} \xi^{9/2} - 3.701 \times 10^{-2} \xi^6 + \dots \quad (\text{A-12})$$

$$v_1(\xi) \sim 1 + \frac{\sqrt{\pi}}{2} e^{j\pi/4} \xi^{3/2} - \frac{7j}{12} \xi^3 - \frac{7\sqrt{\pi}}{64} e^{-j\pi/4} \xi^{9/2} + 4.555 \times 10^{-2} \xi^6 + \dots \quad (\text{A-13})$$

$$v'(\xi) \sim \frac{3\sqrt{\pi}}{8} e^{-j3\pi/4} \xi^{1/2} + \frac{7j}{20} \xi^2 + \frac{63\sqrt{\pi}}{1024} e^{-j\pi/4} \xi^{7/2} - 2.485 \times 10^{-2} \xi^5 + \dots \quad (\text{A-14})$$

$$u'(\xi) \sim \frac{3}{4} \sqrt{\pi} e^{-j3\pi/4} \xi^{1/2} + \frac{5j}{4} \xi^2 + \frac{45\sqrt{\pi}}{128} e^{-j\pi/4} \xi^{7/2} - 2.221 \times 10^{-1} \xi^5 + \dots \quad (\text{A-15})$$

(iv) Numerical evaluation: For $\xi \geq \xi_0$, the residue series representation with the first ten terms in the summation may be used. For $\xi \leq \xi_0$, the small argument asymptotic expansion with the first five terms may be used. It has been indicated in [11] that the smoothest crossover is obtained if $\xi_0 = 0.6$. In the present study, we set $\xi_0 = 0.7$, where the difference in the two representations is less than 0.1% in magnitude and 0.9° in phase.

APPENDIX B

COMPUTER LISTING FOR CALCULATING MUTUAL ADMITTANCE ON A CONE BASED ON RAY TECHNIQUE

37

PROGRAM
↓ SCONE (INPUT,TAPE6,OUTPUT,TAPES=INPUT)

```

C
C
C
C *****
C *
C *      MUTUAL ADMITTANCE OF SLOTS ON A CONE
C *      =====
C *
C *
C *      BY:      S. W. LEE
C *              C. L. LAW
C *              P. CHANG
C *
C *
C *      DATE:    10/18/77
C *
C *      UNIVERSITY OF ILLINOIS
C *
C *****
C
C
C C#1111 PRECISION : SINGLE
C C#1111 LANGUAGE   : FORTRAN
C C#1111 MACHINE    : CDC CYBER 170 SERIES COMPUTER SYSTEM.
C
C C#1111 SUBROUTINE NEEDED : FOCK.
C
C C#1111 INPUT FORMAT : FREE.
C
C
C LATEST REVISIN : 10/18/77
C
C
C IMPLICIT COMPLEX (C,H,Z),REAL (A-B,D-G,K,O-Y)
C REAL ANGLE(20),R11(20),R22(20)
C DIMENSION TITLE(13)
C REAL TN(10),TNPI(10)
C REAL W(7)
C COMMON /DATA1/ TN,TNPI,RHO,C1,C2,F2,IOP,CC,RAIN,DEG
C COMMON /CF/ CVF,CUF,CVIF,CVFF,CUPF
C DATA TN/2.33811,4.0875,5.52156,6.78671,7.99417,
C ↓      9.02265,10.04017,11.00852,11.93602,12.82878/
C DATA TITLE/13(' ')/
C DATA TNPI/1.01879,3.24820,4.82010,6.16331,7.37218,

```

187

BEST AVAILABLE COPY

\$ 8.48849,9.53545,10.52766,11.47506,12.38479/

C
C

```

PI=4.*ATAN(1.E0)
PI02=2.*PI $ SORT2=SQRT(2.)
DEG=180./PI $ ACON1=2./3.
RADN=PI/180.
PRINT*, " INPUT A LINE OF MESSAGE ABOUT THE CURRENT JOB"
911 READ(5,911)TITLE
FORMAT(13A10)
PRINT*, " HALF CONE ANGLE=",
READ*,THATHE
PRINT*, " A1,B1,A2,B2=",
READ*,A1,B1,A2,B2
PRINT*, " W11,W22=",
READ*,W11,W22
PRINT*, " # OF PHI=",
READ*,NP
PRINT*, " INPUT PHI(N), ONE ON EACH LINE"
DO 913 INF=1,NP
913 READ*,ANGLE(INF)
PRINT*, " # OF SETS OF C",
READ*,NSC
PRINT*, " INPUT C, ONE SET ON EACH LINE"
DO 916 INSC=1,NSC
916 READ*,R11(INSC),R22(INSC)
PRINT*, " INPUT THE INTEGRATION GRIDS"
PRINT*, " WHICH ARE CORRESPONDED TO (A1,B1,A2,B2)"
READ*,IP2,IP1,IP4,IP3
PRINT*, " THANK YOU FOR YOUR ACCURATE INPUT!!!"
WRITE(6,515)TITLE
WRITE(6,111)
111 FORMAT(" ",14X,46(" ") /,15X,"*",44X,"*"/,15X
$, "*" MUTUAL ADMITTANCE OF SLOTS ON A CONE */,15X,"*",44X,"*"
$/ ,15X,46(" ")////)
WRITE(6,1111)
1111 FORMAT(/,20(" ") /, "*" /, "*" FREQUENCY : K=0.6238D 01 <1/WAVELENGT
$H>"/ "*" /,20(" "))
C
CCCCCCCCCCCCCCCC
C
C
THETHA=THATHE*RADN
SN=SIN(THETHA)
ATN=TAN(THETHA)
ACD=COS(THETHA)
WRITE(6,222)THATHE
222 FORMAT(/,20(" ") /, "*" /, "*" GEOMETRY : HALF CONE ANGLE=",F7.2,
$ " <DEG>"/, "*" /,20(" "))
515 FORMAT("1",10X,8A10/10X,8A10///)
W1=W11*RADN
W2=W22*RADN

```

```

WRITE(6,333)A1,B1,A2,B2
333  FORMAT(/,20(" "),/,,""/,," SLOT DIMENSION <WAVELENGTH> :  A1=",
      $F7.3,5X,"B1=",F7.3," ; ",5X,"A2=",F7.3,5X,"B2=",F7.3/,,""/,
      $20(" "))
WRITE(6,444)W1,W2
444  FORMAT(/,20(" ")/,,""/,," SLOT ORIENTATION :  W1=",F7.2,
      $" <DEG>",5X,"W2=",F7.2," <DEG>" /,,""/,20(" "))
WRITE(6,555)IP2,IP1
555  FORMAT(/,20(" ")/,,""/,," INTERGRATION GRID :  ",I2," X ",I2/
      $,,""/,20(" "))
C1=CEXP(CMPLX(0.E0,-PI/3.))
C2=CEXP(CMPLX(0.E0,PI/4.))
CC=C2**3
ANSR=1.3057/THETHA-1.755+2.772*THETHA-1.459*THETHA**2
ANSL=2.7195+1.4608*THETHA-1.1295*THETHA**2+0.6566*THETHA**3
K=2.*PI
KA1=K*A1
KB1=K*B1
KA2=K*A2
KB2=K*B2
E2=SQRT(PI)
WIDTH1=KB2/IP1
WIDTH2=KA2/IP2
WIDTH3=KB1/IP3
WIDTH4=KA1/IP4
XL1=-KB2/2.-WIDTH1/2.
XL2=-KA2/2.-WIDTH2/2.
XL3=-KB1/2.-WIDTH3/2.
XL4=-KA1/2.-WIDTH4/2.
DO 100 II=1,NSC
WRITE(6,666)
666  FORMAT(///,10X,"$$$$$ DATA OUTPUT  $$$$$$")
KR1=K*R11(II)
KR2=K*R22(II)
TERM1=KA1*((KR1+KB1/2.):**2-(KR1-KB1/2.):**2)/(2.*KR1)
TERM2=KA2*((KR2+KB2/2.):**2-(KR2-KB2/2.):**2)/(2.*KR2)
PART1=KA1*KB1*KA2*KB2*SQRT(ATN/(PI*2*TERM1*TERM2))
PART2=1./(30.*PI**4*KR1*KR2*SN)
PART3=SIN(KB1/2.)*SIN(KB2/2.)/(KB1*KB2/4.)
DDD1=ANSR*COS(ANSL)
DDD2=ANSR*SIN(ANSL)
ZYTIP=CMPLX(DDD1,DDD2)
$      *CEXP(CMPLX(0.E0,PI/4.-KR1-KR2))*PART1*PART2*PART3
$      *SIN(W1)*SIN(W2)
TMAG=CABS(ZYTIP)
IF(TMAG.EQ.0.)GOTO 37
TDB=20.*ALOG10(TMAG)
TPHASE=ATAN2(AIMAG(ZYTIP),REAL(ZYTIP))*DEG
37  CONTINUE
DO 100 I=1,NP
777  FORMAT(/,," PHI=",F7.2," <DEG> ;",3X,"C1=",E12.7," <WAVELENGTH>;",
      $,2X,"C2=",E12.7," <WAVELENGTH> ;",3X,"SLOT DIST=",E12.7,

```

```

$* <WAVELENGTH>*//)
PHI=ANGLE(I)*RADN
IF(ABS(PHI).LT..01)PHI=.01
ZSUM=0.
DO 10 N1=1,IP4
TKY1=XL4+WIDTH4*N1
DO 20 N2=1,IP3
TKZ1=XL3+WIDTH3*N2
W5=ATAN2(TKZ1,TKY1)
IF(W5)1000,2000,2000
1000 W5=W5+PI/2
2000 CONTINUE
TKY1Z1=TKY1**2+TKZ1**2
TKR1=ABS(SQRT(KR1**2+TKY1Z1-2.*KR1*SQRT(TKY1Z1)*COS(W1-W5)))
TPHI1=1./SN*ASIN(SQRT(TKY1Z1)/TKR1*SIN(W1-W5))
DO 30 N3=1,IP2
TKY2=XL2+WIDTH2*N3
DO 40 N4=1,IP1
TKZ2=XL1+WIDTH1*N4
W6=ATAN2(TKZ2,TKY2)
IF(W6)3000,4000,4000
3000 W6=W6+PI/2
4000 CONTINUE
TKY2Z2=TKY2**2+TKZ2**2
TKR2=ABS(SQRT(KR2**2+TKY2Z2-2.*KR2*SQRT(TKY2Z2)*COS(W2-W6)))
TPHI2=PHI+1./SN*ASIN(SQRT(TKY2Z2)/TKR2*SIN(W2-W6))
KS=SQRT(TKR1**2+TKR2**2-2.*TKR1*TKR2*COS((TPHI2-TPHI1)
$ *SN))
OMEGA1=ASIN(TKR2*SIN((TPHI2-TPHI1)*SN)/KS)
IF(TKR2**2.GT.TKR1**2+KS**2) OMEGA1=PI-OMEGA1
OMEGA2=OMEGA1+(TPHI2-TPHI1)*SN
OM1SIN=SIN(OMEGA1)
OM2SIN=SIN(OMEGA2)
OM1COS=COS(OMEGA1)
OM2COS=COS(OMEGA2)
OM12S=ABS(OM1SIN*OM2SIN)
OM12C=ABS(OM1COS*OM2COS)
IF(OM12C.LT.3.E-6)OM12C=3.E-6
IF(OM12S.LT.3.E-6)OM12S=3.E-6
UPPER=SQRT(TKR1*TKR2)*ATN
KRT2=UPPER/OM12S
KRC2=UPPER/OM12C
KA=ABS(TKR1*OM1SIN*SN*ACO**2/2.)
$ *(1./3.)*ABS(TPHI2-TPHI1)
TAU=((OM1SIN*OM2SIN/ATN)**2/(2.*TKR1*TKR2))
$ *(1./3.)*KS/KA
IF(KA.LT.0.7) GO TO 1
CALL FOCK(KA)
GO TO 2
1 CALL FOCK1(KA)
2 ZC=(0.,-1.)*CEXP(CMPLX(0,E0,-KS))/(240.*KS*PI**2)
SRTAU=SQRT(TAU) $ TAU15=TAU**1.5

```

```

HB=ZG*(CMPLX(1.E0,-1./KS)*SQTAU*CVF-CUF/KS**2*TAU15
$  I(0.,1.)*(1./(SQRT2*KRT2))*ACON1*SQTAU*CVF
$  +(0.,1.)/(SQRT2*KRT2))*ACON1*KRT2/KRB2*TAU15*CUF)
HT=ZG*(0.,1.)/KS*(SQTAU*CVF+CMPLX(1.E0,-2./KS)*TAU15
$  *CUF+(0.,1.)/(SQRT2*KRT2))*ACON1*TAU15
$  *CUF)
W3=OMEGA1-TPHI1*SN+PI/2.-W1
W4=OMEGA2-(TPHI2-PHI)*SN+PI/2.-W2
ZGREEN=COS(W3)*COS(W4)*HI+SIN(W3)*SIN(W4)*HT
ZSUM=ZSUM+COS(PI/KA1*TKY1)*COS(PI/KA2*TKY2)*ZGREEN
40 CONTINUE
30 CONTINUE
20 CONTINUE
10 CONTINUE
ZY12D=ZSUM*WIDTH1*WIDTH2*WIDTH3*WIDTH4
$  *(-2.)/SQRT(KA1*KB1*KA2*KB2)
XMAG=CABS(ZY12D)
PHASE=ATAN2(AIMAG(ZY12D),REAL(ZY12D))*DEG
DB=20*XALOG10(XMAG)
DIST=K*SQRT(R11(II)**2+R22(II)**2-2*R11(II)*R22(II)
$ *COS(PHI*SN))
SDIST=DIST/K
WRITE(6,777)ANGLE(I),R11(II),R22(II),SDIST
ZZZP=ZY12D*CEXP(CMPLX(0.E0,DIST))
PHASEN=ATAN2(AIMAG(ZZZP),REAL(ZZZP))
PHASEN=PHASEN*DEG
WRITE(6,888)XMAG,PHASE,DB,PHASEN
888 FORMAT(2X,"Y12D=",E13.4," <MHO> ",F7.2," <DEG> ",5X,"DB= ",E12.5,
1 " ",NORM PHASE= ",F7.2," <DEG>"/)
WRITE(6,999)TMAG,TPHASE,TDB
999 FORMAT(2X,"Y12T=",E13.4," <MHO> ",F7.2," <DEG> ",5X,"DB= ",E12.5/)
ZY12=ZY12D+ZY12TIP
XMAG=CABS(ZY12)
PHASE=ATAN2(AIMAG(ZY12),REAL(ZY12))*DEG
DB=20*XALOG10(XMAG)
ZZZP=ZY12*CEXP(CMPLX(0.E0,DIST))
PHASEN=ATAN2(AIMAG(ZZZP),REAL(ZZZP))
PHASEN=PHASEN*DEG
WRITE(6,889)XMAG,PHASE,DB,PHASEN
889 FORMAT(2X,"Y12 =",E13.4," <MHO> ",F7.2," <DEG> ",5X,"DB= ",E12.5,
1 " ",NORM PHASE= ",F7.2," <DEG>"/)
100 CONTINUE
WRITE(6,1919)DDD1,DDD2
1919 FORMAT(5X,////5X,"REAL=",G10.2,"IMAG=",G10.2)
STOP
END

```

C THIS SUBROUTINE IS USED TO CALCULATE THE FUNCTIONS CVF,CUF,CV1F,CVFF,CUPF
C

```

SUBROUTINE FOCK(X)
IMPLICIT REAL(A-B,D-H,F-Y),COMPLEX (C,Z)
REAL TN(10),TNPI(10)
COMMON/CF/CVF,CUF,CV1F,CVFF,CUPF
COMMON/DATA1/TN,TNPI,RHO,C1,C2,F2,IOP,CC,RADN,DEG
F1=SQRT(X)
F3=X**1.5
CVF=0.
CUF=0.
CV1F=0.
CVFF=0.
CUPF=0.
DO 20 N=1,10
  ZTN=TN(N)*C1
  ZTNPI=TNPI(N)*C1
  C3=CEXP(CMPLX(0.0,-X)*ZTNPI)
  C4=CEXP(CMPLX(0.0,-X)*ZTN)
  CVF=CVF+C3/ZTNPI
  CUF=CUF+C4
  CV1F=CV1F+C3
  CVFF=(1.0-CMPLX(0.0,2*X)*ZTNPI)*C3/ZTNPI+CVFF
  CUPF=(1.0-CMPLX(0.0,2*X/3.)*ZTN)*C4+CUPF
20 CONTINUE
CVF=F2*F1*CVF/C2
CUF=2.*F2*F3*C2*CUF
CV1F=2.*F2*F3*C2*CV1F
CVFF=F2*CVFF/(2.*F1*C2)
CUPF=3.*F2*F1*C2*CUPF
RETURN
ENTRY FOCK1
XTHREE=X**3
F1=SQRT(X)
F3=XTHREE
Z1=F2*C2*SQRT(F3)
Z2=CMPLX(0.0,1.0/60.)*XTHREE
Z3=F2*X**4.5/(C2*64.)
F4=F3**2
CVF=1.0-Z1/4.+7*Z2+7.*Z3/8.-4.141E-3*F4
CUF=1.0-Z1/2.+25.*Z2+5.*Z3-3.701E-2*F4
CV1F=1.0+Z1/2.-35.*Z2-7.*Z3+4.555E-2*F4
CVFF=.375*F1*F2/CC+21.*Z2/X+63.*Z3/(16.*X)-2.485E-2*F4/X
CUPF=.75*F1*F2/CC+CMPLX(0.0,1.25*X**2)+22.5*Z3/X
1 -2.221E-1*F4/X
RETURN
END

```